Heat waves in South Africa: Observed variability, structure and trends

Innocent Lifa Mbokodo (15012570)

A Master's dissertation submitted to the
Department of Geography and Geo-Information Sciences
School of Environmental Sciences,
University of Venda

In fulfilment of the requirements for Master of Environmental Sciences degree
In the field of Climatology

Supervisor: Dr NS Nethengwe
Co-Supervisor: Dr H Chikoore
Co-Supervisor: Dr MM Bopape

February 2017

DECLARATION

I, Innocent Lifa Mbokodo hereby declare that the dissertation for the Master of Environmental Science degree at the University of Venda hereby submitted by me has not previously been submitted for a degree at this or any other university, and that it is my own work in design and in execution and that all referenced material contained therein has been duly acknowledged.

Signature: _____ Date: _____

ACKNOWLEDGEMENTS

This study was supervised by Dr NS Nethengwe and co-supervised by Dr H Chikoore and Dr MM Bopape from the Council for Scientific and Industrial Research (CSIR). Their guidance, recommendations, interest, encouragement and thorough supervision of the research will always be appreciated. I also appreciate the assistance from a colleague, Mr MAT Mpanza, from the South African Weather Service (SAWS) with the use of Grids Analysis and Display Systems (GrADS).

Several data sources are recognized for making this study possible. SAWS provided temperature data while other climatological data was obtained from the National Center for Environmental Prediction (NCEP). The Southern Oscillation Index (SOI) and Niño 3.4 sea surface temperature (SST) from National Oceanic-Atmospheric Administration (NOAA) Climate Prediction Center (CPC) was obtained via Royal Netherlands Meteorological Institute (KNMI) Climate Explorer.

The International Research Institute (IRI) for climate and society application helped in mapping Normalized Difference Vegetation Index (NDVI) and elevation from the United States Geological Survey (USGS) data portal. CSIR is also acknowledged for providing resources of modelling future heat waves using the Conformal Cubic Atmospheric Model (CCAM). Climate service department of SAWS provided RClimDex (1.0) software package to conduct trend analysis of temperature indices. This study was supported by a generous funding from the National Research Foundation (NRF) and the Applied Centre for Climate and Earth System Sciences (ACCESS).

ABSTRACT

Heat waves are warm extreme temperature events that have environmental and socio-economic impacts in many regions across the world. Negative impacts of warm extreme temperatures over South Africa necessitate the need to study the nature of heat waves. Observations and satellite datasets are analysed in the investigation of the nature and trends of heat waves over South Africa in the present (1983-2012) and future (2010-2039, 2040-2069, 2070-2099) climates. Case study and composite analysis of National Centers for Environmental Prediction datasets were done using the Grids Analysis and Display Systems to get an in-depth understanding of the structure of heat waves in South Africa. Future climate model output obtained from the Conformal Cubic Atmospheric Model was used for future heat wave trends in South Africa**.** The simulations were made using the Representative Concentration Pathways 4.5 and 8.5. Heat waves are unusual events in the present climate (1983-2012) over much of the country, with 20 of the selected 24 stations experiencing an average of less than one heat wave per season. Heat waves are also more frequent and last longer during warm phase of El Niño-Southern Oscillation (ENSO) than in cool phase of ENSO with the north-east being the most prone region. Composite analysis of 500 hPa omega indicates subsidence over the interior of South Africa in both phases of ENSO. Heat waves in South Africa are localized and associated with a middle level high pressure system that persists over the interior inducing anticyclonic flow and subsidence. The anticyclonic circulation over a region experiencing heat wave weakens with decreasing height over land areas which may be due to frictional forces at the surface and the high is placed further south-east at the surface. Advection of dry continental northerly winds also contributes to high maximum temperatures during heat waves in the interior. Maximum temperatures are expected to increase drastically from the present-day climate to the 2070 – 2099 period, with an average increment of about 8°C during DJF in much of the central interior. As a result, heat wave occurrences are expected to be higher in the future warmer climates when climate change signal is higher. Most increases are expected for heat waves lasting for a week than those lasting for over 2 weeks. CCAM outputs also indicated that heat waves in South Africa are expected to last longer and become more intense during the future warmer climates. Longer lasting and more intense heat waves are expected over the Karoo than in other parts of the country.

Key words: Heat wave variability; Thermal discomfort; Atmospheric structure; CCAM; RCP.

To my late parents, Saraphinah Zulu and Simon Mbokodo

“There will be booth for shade by day from the heat, and for a refuge and a shelter from the storm and the rain”.

- Isaiah 4:6 (The Holy Bible, English Standard version)

TABLE OF CONTENTS

LIST OF FIGURES

LIST OF TABLES

LIST OF ACRONYMS

CCAM	Conformal Cubic Atmospheric Model
CSIR	Council for Scientific and Industrial Research
CSIRO	Commonwealth Scientific and Industrial Research Organisation
DJF	December-January-February
DTR	Diurnal temperature range
EA	Enumeration area
ENSO	El Niño-Southern Oscillation
GHG	Greenhouse-gas
GIS	Geographical information system
GPCP	Global Precipitation Climatology Project
GrADS	Grids Analysis and Display System
HI	Heat index
HWDI	Heat wave duration index
JJA	June-July-August
KNMI	Royal Netherlands Meteorological Institute
LST	Land surface temperature
MAM	March-April-May
MSD	Monthly Standard Deviation
NASA	National Aeronautics and Space Administration
NCEP/NCAR	National Centers for Environmental Prediction-National Center for Atmospheric Research
NDVI	Normalized Difference Vegetation Index
NH	Northern hemisphere
NMC	National Metrological Center
NOAA	National Oceanic-Atmospheric Administration
NWP	Numerical weather prediction
OLR	Outgoing longwave radiation
RCM	Regional climate model
RCP	Representative Concentration Pathway
RH	Relative Humidity

SAWS	South African Weather Service
SH	Southern hemisphere
SOI	Southern Oscillation Index
SON	September-October-November
SST	Sea surface temperature
UHI	Urban heat islands
USGS	United States Geological Survey
WMO	World Meteorological Organization

CHAPTER 1

INTRODUCTION AND BACKGROUND

1.1 General introduction

Weather and climate extremes have adverse effects on society. Climate change has resulted in frequent occurrence of extreme weather events in recent decades (Shongwe *et al*. 2009). Several studies also indicated that extreme weather events are not only occurring more frequently, but they are becoming more intense and more severe (e.g. Clark *et al*. 2006; Fischer and Schär 2010). Vulnerability to extreme weather events is highly variable across the world, depending on economic status. The poorest are likely to be hit the hardest (IPCC 2012).

There is no single definition of an extreme weather event as they may be quantified in terms of their intensity and impact on both the natural environment and the economy (Beniston and Stephenson 2004; Stephenson 2008). Stephenson (2008) also indicated that occurrences of extreme events are rare. Climate extremes such as floods, droughts and heat waves have become topical issues since they triggered most natural disasters over the past decades (Shongwe *et al*. 2009), that can potentially affect humans and the natural environment.

Floods and strong winds can cause damage to property and lead to fatalities. Droughts and heat waves can drastically increase death rate of a particular region (Stefanon *et al*. 2012). Characteristics of extreme events are thought to be changing, and expected to change because of global warming. Global warming can simply be defined as increasing atmospheric temperatures (Crichton 2003) and it is caused by an increase in anthropogenic greenhouse gases (GHGs) such as carbon dioxide, Chlorofluorocarbon and methane.

Global emissions of GHGs are observed to be increasing in different parts of the world (Houghton *et al.* 2001), with anthropogenic activities being the main driver for this increase resulting in warming of the atmosphere (Le Quéré *et al*. 2009; Cook *et al*. 2013). Over southern Africa, greatest warming is observed in South Africa (Figure 1.1). Anthropogenic activities have a bigger role in altering global probabilities of the occurrence and intensity of both weather and climate extremes (Peterson *et al*. 2013). However, these changes may not necessarily be the same on regional basis, as different regions are characterized by varying weather and climate features.

South Africa is a country characterised by a variety of weather conditions with floods and droughts being regular features of the summer climate (Rouault and Richard 2005). The country experiences strong austral summer rainfall gradient (Figure 1.2), where the eastern part is relatively wetter compared to the western part. Strong vegetation gradient is also observed over the study area (Figure 1.3), which is consistent with mean rainfall. There is significant rainfall variability over South Africa on a range of spatial and temporal scales and the country is also subjected to serious drought and flood events (Tyson 1986).

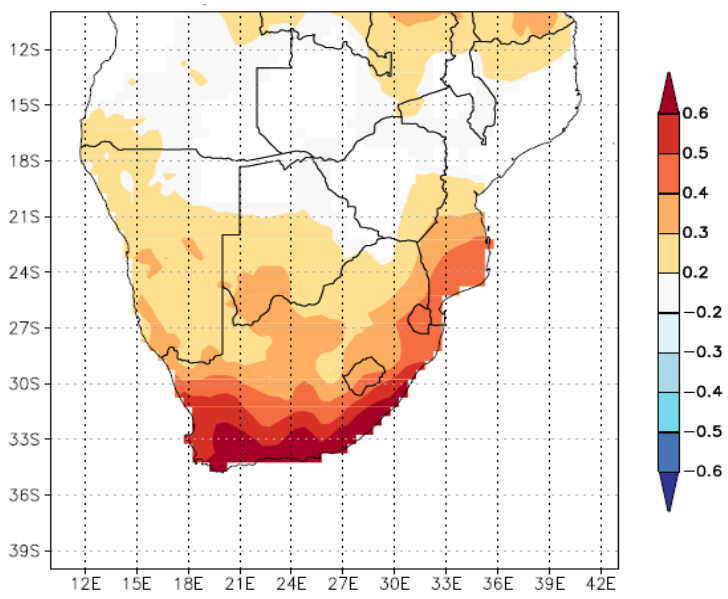

Figure 1.1: University of East Anglia's Climate Research Unit DJF maximum temperature trends over southern Africa from 1901 to 2012.

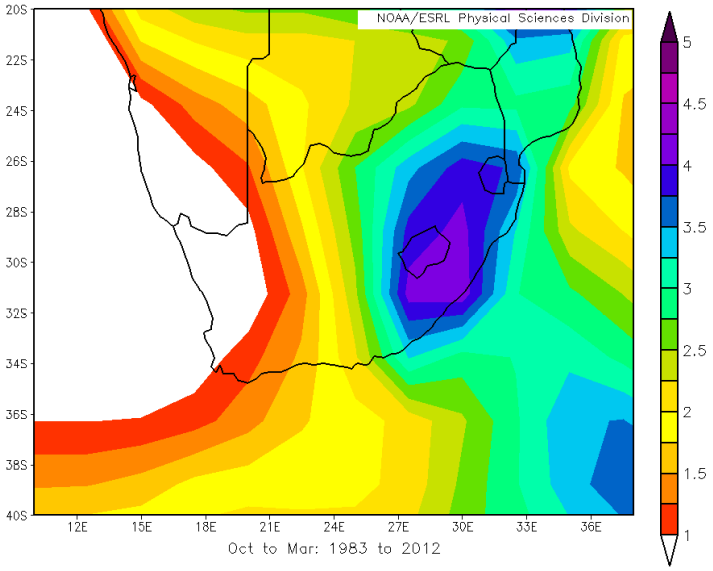

Figure 1.2: October-March mean Global Precipitation Climatology Project precipitation (mm/day) over South Africa from 1983-2012.

The country also experiences little north-south temperature variation, but vary considerably from east to west resulting from the Agulhas current bringing warm and moist air on the eastern part of the country, and Benguela current bringing cold air in the western part (Benhin 2006). South Africa is also characterised by warm climate and average annual temperature >17°C in most regions across the country (Archer *et al*. 2010). Much of the country shows positive temperature trends (Kruger and Shongwe 2004; New *et al*. 2006; Kruger and Sekele 2013), in response to an increase in GHGs concentration.

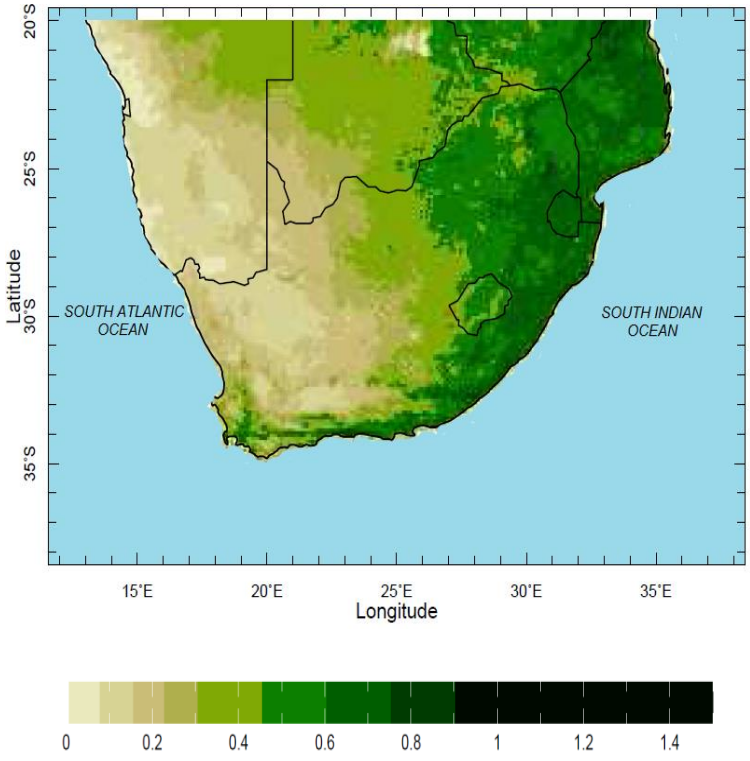

Figure 1.3: Oct-Mar mean NDVI over South Africa from 1983-2012.

Subtropical high pressure systems play a crucial role in weather and climate of subtropical regions (Sinclair 1996). South Africa is located in the subtropics between two semi-permanent subtropical high pressure systems, the South Atlantic high on its adjacent western part and the South Indian high on the eastern part. Several studies have suggested that there is a strong connection between heat waves over land areas and persistent blocking high pressure systems (e.g. Palecki *et al*. 2001; Galarnean *et al*. 2012).

In addition to floods and droughts, South Africa is also prone to heat waves. Floods and droughts have received rigorous research in South Africa, with less attention to heat waves. Meehl and Tebaldi (2004) determined an increase in global heat wave frequency, intensity and duration but also argued that projections of most extreme events are not evenly distributed across the world and are characterised by changes in large scale circulations.

Other studies (e.g. Karl and Knight 1997; Unkaševica and Tošic 2009) also have noted a high possibility of heat waves becoming more frequent, intense and also lasting for longer durations as a result of increasing mean temperatures in most regions. A heat wave event occurs when there is hot weather for several days (Robinson 2001).

There is also a link between sea surface temperature (SST) and the occurrence and intensity of heat waves over a region (Feudale and Shukla 2007). During the 2003 boreal summer, Europe was affected by an intense heat wave and the Mediterranean SSTs were above normal with anomalies ranging from 2°C to 4°C. Feadale (2006) indicated that the persistent anticyclonic circulation which led to the occurrence of heat wave during this period was linked to warm SSTs of the Mediterranean Sea. Feudale and Shukla (2010) suggested that mechanisms at the surface (land surface and sea surface) play a crucial role in the variability of both precipitation and temperature, and can result in favourable condition for heat wave occurrences.

There are several causes of heat waves, which include warming of the lower troposphere (Unkaševica and Tošic 2009). Other factors such as lack of convective rainfall together with summer temperature lead to soil moisture deficits and can results in the occurrence of heat waves in a certain region (Brabson *et al.* 2005). Soil moisture deficits are observed during heat waves since there is usually a joint occurrence of heat waves and droughts (Lyon 2009). Higher atmospheric temperatures are favourable to tropical diseases such as malaria. Frequent cold front passages can terminate heat waves over a region (Kysely 2010) because of the decline in temperature behind a cold front.

Heat waves are strongly connected with large scale anticyclonic patterns, which cause subsidence and produce very warm and dry environmental conditions over a region (Patulikof *et al.* 1996). This can result in prolonged drought that may lead to desertification (Palutikof *et al.* 1996). Dryness and high temperatures are ideal conditions conducive for the occurrence of forest fires that can rage out of control over large areas. Fires destroy crops, both forestry and agricultural, and can also destroy the ecological balance within vegetation and fauna. Impacts of heat waves to ecosystems and human society are severe when the hotness over a region prevails for extended periods (Unkaševica and Tošic 2009). But understanding of heat waves in the present climate can enhance forecasting ability which may reduce negative impacts arising from these events.

Several studies have indicated that there is a strong linkage between heat waves and droughts (e.g. Chang and Wallace 1987; Lyon 2009; Albright *et al*. 2010: Williams 2014; Mazdiyasni and AghaKouchak 2015). Heat waves usually tend to be more frequent during the positive phase of El Niño-Southern Oscillation (Lyon 2009), and eastern part of southern

Africa experience negative rainfall anomalies during this period (Davis 2011). While rainfall deficits can be a contributor to extreme temperatures, heat waves also result in a decrease in convective precipitation ((Mazdiyasni and AghaKouchak 2015) because of the subsiding nature of air during heat waves (Palutikof *et al.* 1996).

1.2 Problem statement

Temperature trends over South Africa have been investigated in several studies (e.g. Muhlenbruch 1992; Karl *et al.* 1993; Kruger and Shongwe, 2004; New *et al*. 2006; Tshiala *et al.* 2011); however, other studies had contrasting findings. New *et al.* (2006) suggested an increase in both minimum and maximum temperatures, however with steeper increase of maximum temperatures than minimum temperatures. Karl *et al.* (1993) suggested an increase in daily maximum and minimum temperatures, with decreases of diurnal temperature range in South Africa. These findings were in contrast to earlier findings of the study of Muhlenbruch (1992), which reported an increase in minimum temperature but decrease in maximum temperature. In this research, heat wave occurrences are analysed, providing trends of diurnal temperature range, minimum and maximum temperatures in the process, improving findings on temperature trends.

The occurrence of heat waves may lead to illnesses, particularly on children and the elderly (Vandentorren *et al*. 2006) which may result in an increased mortality rate. Heat waves can impact on water supplies through increased evaporation rates, can also damage crops and vegetation in general. Thus, understanding climatological features of heat waves can help in predicting its future characteristics as well. Inasmuch as heat waves have been extensively studied in areas such as Europe (e.g. Beniston 2004; Cassou *et al.* 2005) and Australia (e.g. Perkins *et al*. 2013; Nairn and Fawcett 2013; Boschat *et al*. 2014), the study of heat waves has not received rigorous research attention in South Africa even though they have devastating impacts on society and livelihoods. Hence this study provides a better understanding of heat waves in the context of South Africa. It has been noted that there is a considerable variation of heat wave impacts from region to region (Hunt 2007). Studying heat waves is also important because the probability and vulnerability changes over time.

Heat waves also have negative impacts ranging from agricultural yields to health problems. Heat waves may minimize crop production since it is known that environmental factors such as temperature and soil moisture are determinants factors of yields (Waggoner 1983). Heat waves can also affect the economy of a region through extensive usage of air conditioners as a mitigation strategy to heat stress (Maller and Strengers 2011). Several studies have indicated that heat waves can cause health problems that may lead to death (e.g. Larsen

2003; Fischer 2007). The impacts of heat waves to agriculture, economy and on human beings highlight the necessity to study the occurrence and nature of these events.

Duration, frequency and intensity of extreme events are subjected to increase according to dynamical model projections for the 21st century (Perkins *et al.* 2013). South Africa experiences severe weather events such as floods, droughts and heat waves. However, more research has been done on floods and droughts with less focus on heat waves, especially in the southern hemisphere. The impacts of heat waves to agriculture, wildlife, economy and on human beings highlight the necessity to study the occurrence and nature of these events. In depth knowledge about the occurrence of heat wave will assist different stakeholders in decision making which seek to prepare appropriate mitigation and/or adaptation strategies which can minimize negative impacts of heat waves.

Several studies focussed on seasonal heat waves (e.g. Kunkel *et al*. 1996; Karl and Knight 1997; Beniston 2004; Fink *et al*. 2004), with limited research done on short lived heat waves. Short lived heat waves can result in wildfires, since it is known that these heat waves usually occur during droughts, when the vegetation is dry. In 1995, a heat wave which only lasted 3 days killed about 700 people in Chicago (Karl and Knight 1997), so it is evident that short lived heat waves can negatively impact on human livelihoods by increasing atmospheric temperatures which may result in illnesses or even deaths, and also through inducing wildfire that can damage property.

1.3 Aim

The aim of this study is to analyse the variability, meteorological structure and trends of heat waves over South Africa in the present (1983 to 2012) and future climate (2010-2039, 2040-2069, 2070-2099).

1.4 Specific objectives

a) To identify and examine characteristics of heat waves over South Africa from 1983 to 2012.
b) To analyse the spatial and temporal heat wave variability from 1983 to 2012.
c) To determine large scale circulation patterns and meteorological structure associated with heat waves.
d) To model heat waves in warmer future climate (2010-2039, 2040-2069, 2070-2099).

1.5 Research questions

a) What are the characteristics of heat waves in South Africa?
b) Which large-scale climate features are associated with heat waves?
c) Which regions in South Africa are more prone to heat waves?

d) Will heat waves become more frequent, intense and longer in the projected warmer future climate?

1.6 Study area

The study area of this work is South Africa (Figure 1.4), which is the southern tip of the southern African subcontinent, found in the subtropics between 22°- 34°S and 16°- 32°E. South Africa is the area of interest because of its high degree of climate variability on different time scales. Owing to its latitudinal location, weather and climate of the country is affected by temperate and tropical latitude circulation systems and also by the high pressure systems in the subtropics which are semi-permanent (Mukheibir and Sparks 2006).

Figure 1.4: South Africa, which is the area of interest and the adjacent oceans.

South Africa is characterized by spatial variation in temperature, warmer in the interior but relatively cooler in coastal regions (Kruger and Sekele 2013). The country is characterized by extreme events such as heat waves, droughts and floods on different time scales (Mukheibir and Sparks 2006). Because of the rising mean temperatures on a global scale (Orssengo 2010), heat waves are also expected to be more frequent over the country (Engelbrecht *et al*. 2015) and that might pose an increased threat on human health. Other sectors such as water sector may also be in intense stress because of the known relationship between heat waves and droughts (e.g. Lyon 2009; Williams 2014).

The country is made up of nine provinces, namely Gauteng, Eastern Cape, North West, Northern Cape, KwaZulu-Natal, Limpopo, Mpumalanga, Free State, and Western Cape. South Africa is between oceans, the South Indian Ocean on the east adjacent side and

South Atlantic Ocean on the west adjacent side. The country lies well above 850 m, with an exception of the low-altitude coastal areas. The country is also characterised by a central plateau which is moderately elevated (Figure 1.5).

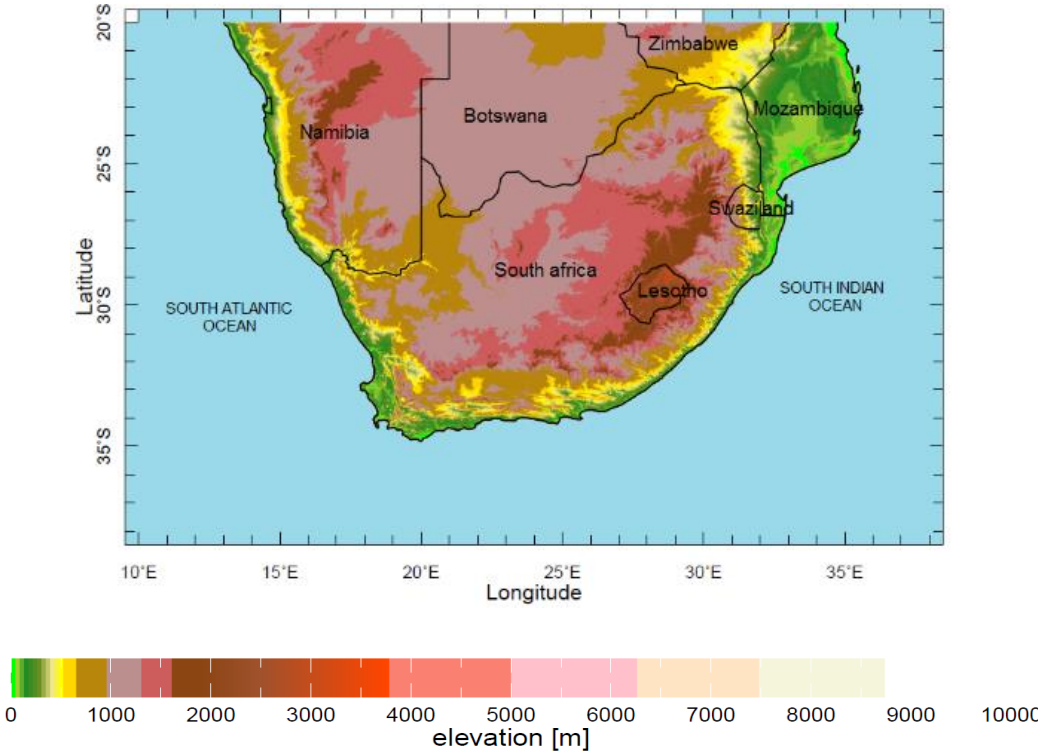

Figure 1.5: Elevation (m) of South Africa, showing that much of the region lies well above 800 m, with an exception of the low-altitude coastal plains.

The topographical variation and the adjacent oceans also influence weather and climate of South Africa. The elevated central part experiences continental temperatures, while SSTs play a major role in influencing temperatures in coastal regions, which experience moderate temperatures throughout the year (Kruger 2008). The escarpment which is about 1 200 m above sea level, experiences cold winters while summer seasons are relatively hot (Archer *et al.* 2010). The escarpment reaches about 3 500 m in the eastern part of the country and act as a boundary between the interior and coastal regions (Kruger 2008).

Ocean currents play a huge role in South African weather: the warm Agulhas advects warm water from the subtropics to coastal regions in the mid-latitudes, often causing rainfall to increase over the adjacent lands in the eastern parts of the country (Jury *et al.* 1992). The cold Benguela current along the west coast and the warm Agulhas current, which retroflect near Cape Agulhas, have contrasting influence on the weather conditions of the adjacent coast and interior areas. Kruger (2008) suggested that the Benguela current causes cause dry and cold weather condition along the western coast, while the Agulhas current cause moist and warm condition along the eastern coast.

1.7 Definition of key terms

a) Heat waves: There is no standard definition of heat waves. This study define heat wave as an event when for at least 3 consecutive days maximum temperature (T_X) of a certain region is 5°C higher than the daily mean of the hottest month.

b) Heat wave occurrence: Definition of heat wave occurrences in this work includes two components; heat waves frequency and duration. It is defined as the number of heat waves events that has occurred in a given summer season, and the number of days in each event.

c) Diurnal temperature range (DTR): It is defined as the difference between T_X and minimum temperature (T_N). DTR can be calculated for daily, monthly and annual time scales. DTR equation (1.1) is given below.

$$DTR = T_X - T_N \qquad (1.1)$$

d) ENSO: El Niño-Southern Oscillation (ENSO) phenomenon is an irregular equatorial Pacific Ocean SST variation which affects weather and climate across the world (Davis 2011). There is a joint occurrence of droughts and heat wave occurrences (Chang and Wallace 1987; Lyon 2009), and warm phase of ENSO is associated with droughts over southern Africa.

e) Thermal comfort: It is the condition of mind that expresses satisfaction with the thermal environment and is assessed by subjective evaluation (Yousif and Tahir 2013).

1.8 Dissertation outline

This dissertation has 7 chapters and the chapter outline is as follows: -

- Chapter 1: The first chapter provides the general introduction of the whole study and background on the occurrence and nature of heat waves. The chapter also provided the description of the study area. The main aim, specific objectives, key research questions and problem statement of this dissertation were presented here.
- Chapter 2: The second chapter provided literature review which is relevant to this study, and the literature reviewed present different methods of analysis used to understand the occurrence of heat waves, meteorological systems and large scale patterns associated with heat waves. It has also provide impacts of heat waves on society and livelihoods. Present-day climate temperature trends are also presented here.

- Chapter 3: Description of datasets used in this study to analyse conditions conducive for heat wave occurrence is presented in this chapter. The chapter also present different sources of the data used and methods of analysis applied to achieve the objectives outlined in the first chapter. Temperature which is a major dataset of this study was obtained from South African Weather Service station observations while most data sets used will be secondary data; this chapter further indicate procedures involved in obtaining the data.
- Chapter 4: Trends of diurnal temperature range, maximum and minimum temperatures will be presented in this chapter. Seasonal variability in the number of hot days will be discussed here. Trends of heat wave occurrences in the present climate, both inter-annual variability of heat wave frequency and duration are discussed here.
- Chapter 5: Detailed large scale circulation patterns associated with heat waves of different severity are discussed in this chapter. The chapter also provides meteorological parameters such as outgoing longwave radiation, wind vector and relative humidity anomalies to understand the meteorological structure of heat waves in the perspective of South Africa. Monthly soil moisture and land surface temperature were also mapped to observe their relationship with heat wave occurrences. Thermal discomfort index of the selected heat waves will be calculated in this chapter.
- Chapter 6: This chapter provided characteristics of future heat waves over South Africa. Frequency, duration and intensity of heat waves in the future warming climate is discussed here. Comparison between present and future heat waves is also provided here.
- Chapter 7: Discussions and general conclusions are presented in this chapter, which is the last chapter of the dissertation. Summary of key findings are presented here. This chapter also provides recommendations on what can be done on future studies to further analyse heat waves, to improve the quality of the results and save more lives.

CHAPTER 2

LITERATURE REVIEW

2.1 Introduction

Heat wave occurrences can lead to negative impacts in different sectors across the country, from water resources to energy sector (Zuo *et al*. 2015). Heat waves can also increase illnesses or even mortality and morbidity rates (Bi *et al*. 2011) as some population group are more vulnerable to heat stress (Peng *et al.* 2011). Several studies (e.g. Meehl and Tebaldi 2004; Cowan *et al*. 2014) suggest that heat waves are projected to last longer, become more frequent and more intense on a global scale. Understanding historical nature of heat waves over South Africa can assist in formulating mitigation strategies which seek to minimize the negative impacts resulting from these events in the country.

The aim of this chapter is to provide a literature review about temperature trends and the nature of heat wave over South Africa. This chapter also seeks to provide an understanding of heat wave variability, trends, meteorological structure and impacts. There are different definitions of a heat wave based on the methodology and local conditions of the area of interest in different studies. Different heat wave definitions are investigated so as to adopt the one suitable for this study. A detailed relationship between heat waves and droughts is also provided here.

2.2 Temperature trends in South Africa

It is evident that global warming has a significant effect on in temperature trends in many regions across the world. Trends include maximum, minimum and difference between the two temperatures which is termed diurnal temperature range (DTR). The latest Intergovernmental Panel on Climate Change *(*IPCC 2013*)* also stated that over the last century, there is an increasing trend of global mean temperature and it is largely due to anthropogenic activities involving enhanced GHG emissions (Trenberth *et al*. 2007). Changes in South African temperatures have resulted in an increased (decreased) number of warm (cold) days and nights (Kruger and Shongwe 2004).

Several studies investigated temperature trends over South Africa (e.g. Muhlenbruch 1992; Kruger and Shongwe 2004; New *et al*. 2006; Tshiala *et al.* 2011; Kruger and Sekele 2012; MacKellar *et al*., 2014). Surface temperatures in most of these studies have trends which are consistent with the general positive trends in recent decades (Donat *et al*., 2013). However, the warming in South Africa is not evenly distributed across different seasons. Strongest

positive trends of surface temperatures are observed in autumn and smallest around spring (Kruger and Shongwe 2004; MacKellar *et al.* 2014). The subsequent section provide trends in DTR, maximum and minimum temperatures.

2.2.1 Maximum and minimum temperature trends

Temperature trends over South Africa are strongly related to anthropogenic greenhouse gas emissions (Solomon *et al*. 2007). Temperature trends over South Africa have been changing between negative and positive over the past century. Jones (1994) suggested that from 1885 to 1915, the country was cooling but an increasing temperature trend was observed for a 30-year period between 1915 and 1945 (Figure 2.1). Cooling of the atmosphere was observed again until 1970, where a rapid warming occurred after that. Easterling (1997) also found a positive trend of mean daily maximum and minimum temperature between 1950 and 1993. However, other studies (e.g. Hulme *et al*. 2001) found negative trends over South Africa's coastal regions, with warming occurring in the central interior of the country, particularly from 1901 to 1995.

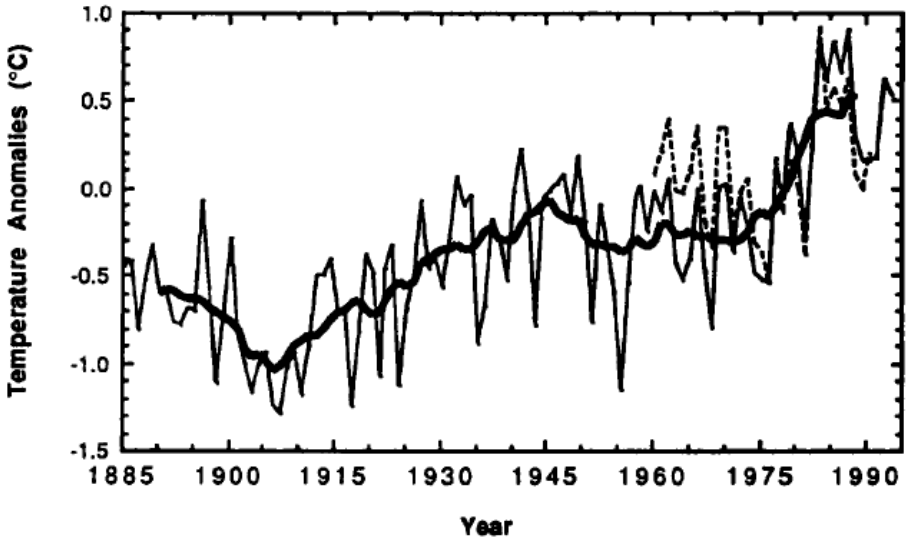

Figure 2.1: Atmospheric temperature anomalies over South Africa from 1885 to 1993, with 10-year running mean and 1960 to 1990 non-urban sites temperature anomalies (Dashed line) (Source: Jones 1994).

Global temperature trends are not necessarily the same with regional temperature trends. Temperature trends across South Africa. New *et al.* (2006) suggested an increase in both maximum and minimum temperatures in South Africa, however with steeper increase of maximum temperatures than minimum temperatures. Karl *et al.* (1993) also suggested an increase in daily maximum and minimum temperatures, with decreases DTR in South Africa, suggesting the increased rates of minimum and maximum temperatures are not the same. These findings were a contrast to earlier findings of the study of Muhlenbruch (1992), which

reported an increase in minimum temperature but decrease in maximum temperature. Studies by Kruger and Shongwe (2004) and Kruger and Sekele (2013) also showed increases in maximum and minimum temperatures over most of South Africa, which also increases chances of warm extreme temperature events such as heat waves.

2.2.2 Diurnal temperature range trends

Days Local factors such as soil moisture, ground heat capacity and albedo largely influence variations in DTR trends (Tshiala *et al*. 2011). DTR has been narrowing since 1950 in a global scale due to slow increasing rate of minimum temperature, relative to maximum temperature (Easterling *et al.* 2000; Hartmann *et al.* 2013). Regional behaviour of DTR is different to that of global DTR trends. While DTR has been decreasing globally, Makowski *et al.* (2008) suggested that in Western Europe DTR changed from negative to positive trends between 1950 and 2005. And this was also the case in Eastern Europe in the 1980s.

DTR trends in regions such as eastern Africa correspond with the global behaviour of DTR (Christy *et al*. 2009), while regions such as the main land of China experienced decreasing DTR in recent decades (Zhuo and Ren 2011). Despite DTR narrowing globally, Easterling *et al*. (1997) found increasing trends. South African regions experience variations in DTR trends. It was also stated that DTR trends across South Africa are equally divided between negative and positive trends (Kruger and Shongwe 2004). However, about 80% of the country's northern parts experiences positive DTR trends (Tshiala *et al*. 2011).

2.3 Defining heat wave

There is no universal definition of a heat wave because threshold conditions vary across the world. Heat wave can simply be defined as a period of excessively hot weather (Robinson 2001; Meehl and Tebaldi 2004; Nairn and Fawcett 2013). A constant fixed temperature threshold for all locations would not be meaningful because the climatology of a given region may vary to that of other regions. According to Robinson (2001), there are two theoretical aspects involved in setting threshold for identifying heat waves. The first aspect involves identifying values exceeding particular fixed values of a given local area. The second aspect is based on deviation away from normal conditions, such as a fixed percentile threshold of all observed values. Hunt (2007) defined heat wave as an event consisting of several days or more with temperatures significantly above normal. Heat waves can also be defined as a period of at least 48 hours during which neither the overnight low nor the daytime heat index falls below the United States (US) National Weather Service (NWS) heat stress thresholds of 27°C and 41°C respectively in the United States of America (Robinson 2001; Son *et al.* 2010).

Heat waves were also defined as days or nights with both maximum and minimum temperatures above certain percentiles (usually between the 90th and 99th) of a day temperature distribution (e.g. Hajat *et al.* 2006; Anderson and Bell 2009). Lyon (2009) defined heat waves as events occurring between December and February (DJF) with 3 consecutive days of daily maximum temperatures exceeding the 90th percentile. Lyon (2009) further suggested that longer periods only identify fewer cases when defining a heat wave. A definition similar to the one from SAWS, in terms of the threshold of 5°C above maximum temperature of the hottest month, was also used by Unkaševica and Tošic (2009), but applied heat wave duration index (HWDI) for period of more than five consecutive days. Most past studies have illustrated that even though heat waves are defined in terms of days, their duration can exceed a month (e.g. Kysely 2010). However, other studies defined heat wave in a more seasonal sense, while temporal variations are of most importance (e.g. Fischer *et al.* 2007).

Huth *et al.* (2000) used three criteria for defining heat waves: (a) daily maximum temperature exceeding the 97.5th percentile for at least three consecutive days, (b) average daily minimum temperature above the 97.5th percentile for at least three consecutive days, and lastly (c) daily maximum temperature above the 81st percentile for the entire duration.

The generally accepted standard is the heat index (HI), which a model resulting from extensive bio-meteorological studies (Rothfusz 2009). The HI was primarily used by NWS in the US to issue guidance when heat stress conditions are expected. It uses 20 physical and atmospheric parameters to calculate the apparent temperature one feels in an open space (equation 2.1) (Myron 2011). After certain manipulations, the equation tends to require only two variables as inputs to calculate HI; where T represents the ambient dry bulb temperature and R represent RH.

$$HI = -42.379 + 2.04901523T + 10.14333127R - 0.22475541TR - 6.83783x10^{-3}T^2 - 5.481717x10^{-2}R^2 + 1.22874x10^{-3}T^2R + 8.5282x10^{-4}TR^2 - 1.99x10^{-6}T^2R^2 \quad (2.1)$$

2.4 Structure of heat waves

Heat waves usually result from large scale persistent high pressure systems (Kunkel *et al.* 1996; Palecki *et al.* 2001) that produce positive temporal atmospheric temperature anomalies over a certain region. This also increases land surface temperature of that region, because of the warming nature of the descending air from the center of high pressure systems (Palutikof *et al.* 1996). Positive 500 hPa geopotential height anomalies are a favourable condition for the occurrence of heat waves (Kysely 2000). This is because of the

warm airflow towards an area due to experience heat wave, or ridge or anticyclone over that particular area. Kysely (2000) also suggested that cyclonic air circulations are not favourable for Heat wave occurrences. It is mainly because cyclonic circulations are associated with rising air, hence can be linked to cloud cover or even rainfall that can suppress atmospheric temperature of the area of interest.

It is well known that most heat waves are characterised by dry atmospheric conditions (e.g. Kysely 2010). However, this is not always the case in other parts of the world. Summer heat waves over regions such as the north-eastern parts of Australia can be accompanied by heavy rainfall (Parker *et al.* 2014), even though this is rare. Reeder and Smith (1987) previously suggested that this may be as a result of cold fronts following a ridging high pressure system during heat waves and the rainfall result from the ridging high.

Such rare occurrences can be accompanied by high moisture content in the atmosphere (Cerne *et al*. 2006). High humidity during hot weather conditions can make the situation far more dangerous to human health (Cerne *et al*. 2006) and can result in respiratory problems, especially to younger children (< 3 years old) and older people (> 65 years old), both which are population groups that can easily be affected by heat stress (Bolund and Hunhammar 1999).

The persistent high pressure system, which influenced the occurrence of heat waves over land areas, occurs through the atmosphere-ocean interactions on intra-seasonal time scale (Cowan *et al.* 2013). Hence it can be said that the oceans play a significant role in the occurrence of heat wave events through the persistent high pressure system. Remote and more local oceanic conditions contribute to heat wave development (Purichat *et al.* 2014). Increasing SST of the subtropical Indian Ocean increases baroclinicity, and aids Rossby wave trains development which feed the atmospheric blocking system (Pezza *et al.* 2012). Positive SST anomalies have been found to largely contribute to summer heat wave onset in other region across the world, such as Southeast Australia (e.g. Boschat *et al.* 2014).

2.5 Heat waves and droughts

There is usually a joint occurrence between heat waves and summer droughts in most cases (Chang and Wallace 1987; Lyon 2009). Meteorological drought can be defined as an event where there is scarcity or lack of precipitation for prolonged episodes (MacKee *et al.* 1993), and the effect of this event to human beings relies on the severity and duration (Rouault and Richard 2003). Severe and longer droughts tend to have more negative impacts to human health and livelihoods.

The relationship between droughts and heat waves is such that there is little or no rain during heat waves, and high surface temperatures usually characterise droughts during the summer (Change and Wallace 1987). Dry atmospheric conditions are usually experienced, resulting from soil moisture deficits which induce heat wave occurrences. However, droughts and heat waves are treated as two distinct phenomena because both duration and spatial extent differ (Chang and Wallace 1987).

Several studies have investigated droughts (e.g. Rouault and Richard 2003; Rouault and Richard 2005) and heat waves (e.g. Beniston 2003; Basara *et al*. 2010; Albright *et al*. 2011) in isolation. Individually, these events may cause environmental and socioeconomic impacts (Mazdiyasni and AghaKouchak 2015); however studies by Lyon (2009) and Albright *et al*. (2010) suggested that their co-occurrence have even adverse impacts. While droughts usually persist for longer periods, heat waves are usually defined in shorter time scales (i.e. days).

Drought is a phenomenon that is not easily defined or measured (Thomas 2013), but best represented by quantitative parameters which indicates the imbalance between water demand and supply or the total environmental moisture status of a particular region (Zwiers *et al*. 2011). Soil moisture is a key contributor to the relationship between heat wave occurrences and droughts (Albright *et al.* 2010), because negative soil moisture anomalies are associated with droughts (Trenberth and Shea 2005). The negative soil moisture anomalies increase Bowen ratio, resulting in hotter land surfaces which then increase atmospheric temperatures (Fischer *et al*. 2007).

More than one short lasting heat wave can occur in a given summer season (Khaliq *et al.* 2005). The intensity of daily heat wave is higher compared to the intensity of seasonal Heat wave, given their short duration (Hunt 2007). As a direct result of the joint occurrence between heat waves and droughts, there are negative anomalies of soil moisture, reducing surface evaporation (Hunt 2007), but increases the atmospheric demand.

However, there are cases where droughts and heat waves do not coincide. Heat waves can also be observed during either normal or above-normal rainfall (Gershunov *et al*. 2009). Trenberth and Shea (2005) also indicated that droughts can also occur during extremely cold periods, even though it is not usual.

2.6 Heat waves and the urban heat island

Urban heat island (UHI) is an urban area which experiences warmer atmospheric temperature than the surrounding areas (Basara *et al.* 2010). Unlike heat waves, the effect of UHI is always more localized (Li and Bou-Zeid 2013) and results from the gradual land

surface modification, higher anthropogenic heat releases and limited plants (Oke 1982). HIG (2005) suggested that urban areas have darker surfaces compared to rural areas which are usually dominated by more vegetation. Dark surfaces tends to heat up faster, and has lower albedo, which can be due to radiative effects (Li and Bou-Zeid 2013), and results in higher air temperatures. Li and Bou-Zeid (2013) illustrated an interaction mechanism between heat waves and UHI (Figure 2.2) and emphasized that there is a positive atmospheric temperature anomaly over cities during UHIs. The strength of this anomaly is measured by a UHI Index, which is defined as surface or air temperature difference between urban and rural areas.

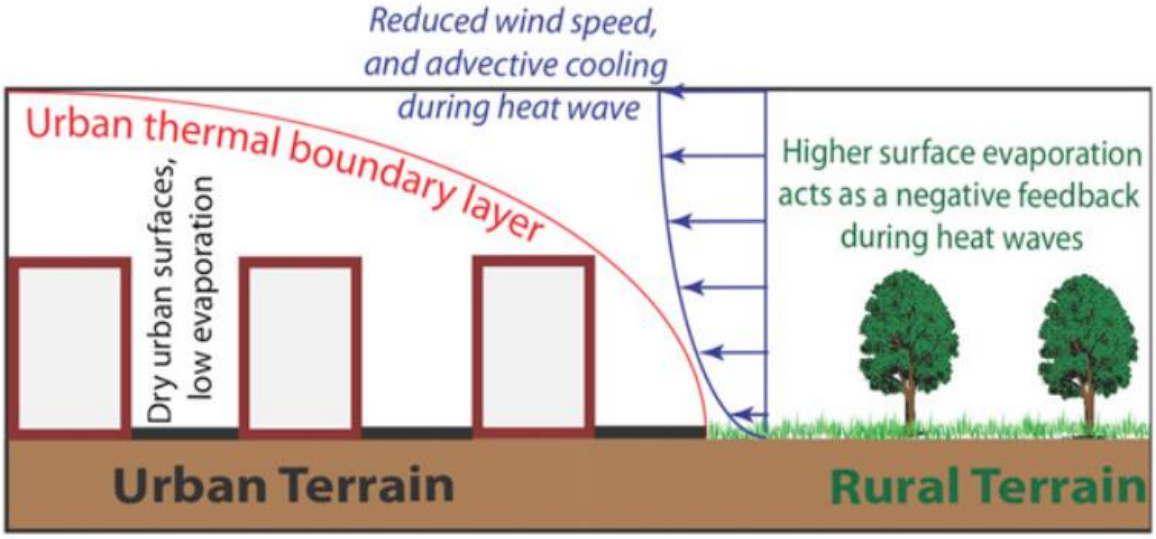

Figure 2.2: Interactions between urban heat islands and heat waves (Source Li and Bou-Zeid 2013)

Five factors were identified which contribute to the occurrence and intensity of UHIs: (1) geographical location, (2) weather, (3) city form, (4) city function, (5) time of the day and season (Voogt 2004). High lying Inland areas tend to experience intense UHI during the summer season than coastal cities, because of the oceans cooling effect in coastal areas. Dry climate in tropical climate tend to favour large heat island magnitudes. Areas constituting of dense building materials, where most industries are located may also lead to high air temperatures and intense UHIs (Voogt 2004).

Interaction of heat waves and UHIs has been discussed in previous studies (e.g. Tan *et al.* 2010; Li and Bou-Zeid 2013). heat waves are associated with low wind speed, because they are link with a persistent high pressure system, and it is widely known that low wind speeds are experienced at the center of a high (Ackerman and Knox 2012). However, occurrences of heat waves may strengthen secondary wind circulations (Li and Bou-Zeid 2013). Hotter air over cities rise because of its low density compared to air of the surrounding rural areas,

which is drawn to the cities and acts as a negative feedback on the strength of UHIs (Hidalgo *et al.* 2010). But a different case is observed in coastal cities because temperature is also influenced by the steady sea surface temperatures. Secondary circulations intensify during heat waves because of the higher land surface temperatures in urban areas, which later cool because of sea breeze in coastal areas (Lebassi *et al.* 2009). Intense heat waves can have negative impacts on health of human beings, agriculture and also stagnate the economy of a particular region.

2.7 Impacts of heat waves

Heat waves link to different issues related to human livelihood. They have significant negative impacts on health, water quality, energy demand, infrastructure performance, agriculture and economy (Zuo *et al.* 2015). One heat wave event can affect a considerable number of people, as it was the case in Australia where about one million people were affected in some way by one heat wave event in 2009 (Kiem *et al.* 2010). The negative impact from this heat wave include casualties due to high heat stress, and power cuts resulting in huge amount of financial losses, and public transport (Kiem *et al.* 2010). Factors which may play a crucial role in the mitigation of heat waves related impact include policies and plans, building design, and cultural change (Kiem *et al.* 2010). However, an understanding of heat wave characteristics is required first. The subsections provide an insight of heat waves impacts on human health, agriculture, veld fires and economy.

2.7.1 Human health

The health of human beings is endangered by heat wave occurrences across the world. It has been noted that high temperatures during heat waves threaten human health directly and indirectly. Heat waves affect human health through air pollution (Fischer 2007). Ordonez *et al.* (2005) noted that heat waves are associated with high solar radiation which then lead to elevated concentration of air pollutants, and may result in air-borne diseases. Several studies (e.g. Larsen 2003; Koppe and Jendritzky 2004; Fisher *et al.* 2007) suggest that heat waves largely increases mortality. Typical example will be the 1995 heat wave in Chicago which lasted for 3 days and killed 700 people more than the expected number (Karl and Knight 1997). Zacharias *et al*. (2014) also illustrated the response of mortality rate to high temperatures.

In addition to people with mental disorder (Cusack *et al.* 2011), the elderly and young people, poor and homeless people are also most vulnerable to heat waves (Vandentorren *et al.* 2006; Peng *et al.* 2011). The increasing mortality caused by heat wave results from a range of health impacts such as kidney failure, heart attacks, heat exhaustion, sunburn and heat stress (WHO 2004). In areas such as the Australia and United States, heat waves are

even the major cause of fatalities (Robinson 2001; BoM 2013). It is widely reported that most heat waves are characterised by dry atmospheric conditions, with fewer heat waves accompanied by high humidity (Cerne *et al.* 2006). Zanobetti *et al.* (2014) stated that the high humidity experienced in some heat waves results in declining mental capacity and stress of human being.

2.7.2 Agriculture

The vast majority of African countries depend on subsistence agriculture for survival (Ruth and Ruth 2013). Agriculture is a backbone for most African countries (Hussein *et al.* 2008), and between 70 and 90% of Africa people are employed in this sector (FAO 2007). The agricultural sector is highly affected by climate extremes and climate variability (Thornton *et al*. 2007; Easterling *et al*. 2007). But inasmuch as agriculture proves to be vulnerable to climate change, it also contributes to climate change (Aydinalp and Cresser 2008). The contribution is mainly via the agricultural production of GHGs such as carbon dioxide, nitrous oxide and methane (IPCC 2007).

Agricultural productivity largely depends on weather and climate (Adams *et al.* 1998; Gornall *et al.* 2010). Owing to the observed warming climate in South Africa over recent decades (Figure 1.1), functioning of most agricultural components may be disturbed. Livestock and crop production, input supplies and hydrological balances are some of the components that can be influenced by climate change (Adams *et al.* 1998). Heat waves are projected to increase in the warming climate (Cubasch *et al.* 2013), and this can minimize crop production since it is known that environmental factors such as temperature and soil moisture are determinant factors of yields (Waggoner 1983).

A recent study by Fontana *et al*. (2015) suggested that regions affected by heat waves usually experience negative wheat yield anomalies, and they suggested that the adoption of new wheat varieties over time also plays a crucial role. Heat waves are characterised by high temperature and soil moisture deficits. For the germination of the most important crop grown in South Africa, maize, require soil moisture of about 60% and temperature should range from 20 to 30°C (Du Plessis 2003).

High temperatures during heat waves also affect livestock direct and indirect. Just like human beings, animal health is directly affected by hot and moist atmospheric conditions in the form of thermal discomfort (Semenza and Menne 2009; Gale *et al*. 2010) and also disturb growth of livestock, production (Smith 1996) and their performance. McDowell (1972) indicated that most livestock tends to have best performance in temperatures with threshold of 4 to 24°C. Temperatures above this threshold then reduces food intake as animals do not graze in extremely hot conditions (Scholtz *et al*. 2010).

High temperatures affect livestock indirectly by affecting their physical environment (Rust and Rust 2013). High temperatures alters the nutritional environment (Rust and Rust 2013), hence affecting the quantity and quality of pasturage (Topp and Doyle 1996). This can drastically reduce agricultural production and lead to starvation in other regions.

Changes of short term temperature extremes, such as heat waves, can be critical and can drastically reduce agricultural production in most regions across the country (Wheeler *et al.* 2000). However, establishing a relationship between agricultural production and climate change is very complicated because there are other non-climate factors such as change in livestock, overgrazing and migration (Rust and Rust 2013) which also influence agricultural changes. Heat waves usually occur during drought events, and soil moisture deficit together with high temperatures associated with these events lead to crop losses (Lyon 2009).

2.7.3 Spontaneous combustion and veld fires

It has been noted in section 2.5 that that there is a joint occurrence of heat wave and droughts where hot conditions usually coincide with dry seasons. This is the period where veld fires caused by combustion or lighting can be expected (Mudekwe 2007). This is also where anthropogenic veld fires usually occur can be expected because of dry vegetation and forests. Nyamadzawo *et al*. (2013) defined veld fires as blazes that usually get out of control, destroying extensive tracts of forests and grasslands and may result in the loss of life and have economic and environmental impacts. Weather conditions during heat waves have been discussed in section 2.4 and are conducive for the occurrences of veld fires.

Veld fires in South Africa usually occur after a long period with no precipitation and are associated with dry and strong northerly to westerly winds (Rowles 2012). The impacts of veld fires include social, economic and environmental consequences (e.g. Forsyth *et al*. 2010; Rowles 2012; Nyamadzawo *et al*. 2013). Veld fires lead to reduced food availability because it damages agricultural equipment, hence resulting in a reduction of agricultural yields (WWF 2001). Trauma (Fowler 2003) and disturbing memories (Maida *et al*. 1989) to victims of veld fires are some of the known psychological impacts.

Veld fires can affect the economy of a region by affecting plantation forests, homesteads, infrastructure, and industrial facilities such as sawmills and fodder that have an economic value (Forsyth *et al*. 2010). However, veld fires do not always have negative impacts. Nyamadzawo *et al*. (2013) stated that fires has the ability to serve as an important function in maintaining health of certain ecosystems and also on improving the growth of green grass which provides grazing for animals during dry seasons.

2.7.4 Economy

Owing to global warming, studies suggest that countries are experiencing rising electricity demand (e.g. Miller *et al*. 2008). This is because hot days are becoming more frequent and the population is growing (Tebaldi *et al*. 2006; Alley *et al*. 2007), hence increasing usage of air-conditioners which is seen by most as a mitigation strategy to heat stress.

There are direct and indirect impacts of heat waves to the economy (Zuo *et al.* 2015). Heat waves can affect the economy of a region through extensive usage of air conditioners as a mitigation strategy to avoid heat related diseases resulting from high atmospheric temperatures (Maller and Strengers 2011). This impact is difficult to estimate, unless for areas with high insurance density (Munich re 1999). Heat waves can directly affect the economy through reducing agricultural yields as discussed in section 2.7.2.

2.8 Summary

This chapter discussed the nature of temperature trends over South Africa compare to global temperature trends and provided different definitions of heat waves previously used in different studies. This chapter has provided a general background on the structure of heat waves in the different regions across the world. It also discussed how these events are associated with other phenomena such as droughts and urban heat islands and also discussed the negative impacts associated with the heat waves.

From the literature, it is noted that:

a) South African temperature trends are not well understood as there are contradictions from different studies [e.g. Muhlenbruch (1992) and Karl *et al*. (1993)].
b) There is no universal definition of a heat wave because threshold conditions vary across the world. A heat wave definition may depend on the methodology followed, but it is generally a period of hot weather.
c) Positive 500 hPa geopotential height anomalies are a favourable condition for the occurrence of heat waves (Kysely 2000).
d) Heat waves in most parts of the world are characterised by dry atmospheric weather conditions.
e) The northern hemisphere (NH) experiences more heat waves compared to the southern Hemisphere (SH), as a results of the continentality effect. The NH has more land areas than SH.
f) There is a joint occurrence between heat waves and drought events in most cases.
g) Heat waves negatively impact human livelihoods through impacts such reducing agricultural productions and human health such as respiratory problems.

h) SST are associated with both warm and cold extreme temperature events, hence play a role in the occurrence of heat waves.

The next chapter provides a description of all datasets used in this study. Methods of analysis adopted to analyse the datasets in order to achieve the aim and objectives outlined in chapter 1 are also detailed in the next chapter.

CHAPTER 3

RESEARCH METHODOLOGY

3.1 Introduction

South Africa's weather and climate is strongly influenced by regional topography and ocean currents (Bhavika 2007; Davis 2011). Owing to its latitudinal location, the country is dominated by subtropical high pressure systems (Tyson and Preston-Whyte 2010). When these high pressure systems persist over land areas they induce anticyclonic circulation which is linked to heat wave occurrences (Kunkel *et al.* 1996; Palecki *et al.* 2001) in the country. Heat waves have indirect impacts to human beings via reducing agricultural yields (Aydinalp and Cresser 2008) and direct impacts such as respiratory problems to patients with asthma (D'Amato *et al*. 2014) and even deaths (Kovats *et al*. 2004) if they do not receive medical attention.

Regional temperature characteristics, trends of heat waves and large scale circulation patterns and meteorological structure they are associated with was studied. Different datasets ranging from South African Weather Service (SAWS) climate station distributed across South Africa, high temporal and spatial resolution satellite data to model reanalysis were used. The aim of this chapter is to present and describe data used in this study and their sources. It also present the methods adopted and applied to analyse the data in order to achieve the specific objectives of the study outlined in chapter 1. The subsequent sections detail the datasets used in this study and methods used to analyse the data.

3.2 Data sources and description

3.2.1 Daily temperatures

Daily maximum temperature (T_X) and minimum temperature (T_N) were obtained from SAWS for the 30 year period (i.e. 1983 to 2012). This study period assist in analysing more recent heat waves where there is high resolution data availability needed for the analyses of this study. Anthropogenic influences to global warming is expected to be smaller during this period than during the future climate. Data is collected using temperature point stations distributed across South Africa. The data is recorded at a uniform time in all stations as per the World Meteorological Organization (WMO) standard. This study selected stations of different altitudes (Table 3.1) that have at least 95% data available from 1983 to 2012 across South Africa (Figure 3.1). SAWS also provided Relative humidity (RH) from point stations.

Table 3.1: SAWS weather stations utilized in this study

Station Name	Climate Number	Latitude	Longitude	Altitude (m)	Data availability
Bethlehem	0331585 9	28.25°S	28.33°E	1 689	1983 – 2012
Bothaville	0399894 4	27.41°S	26.5°E	1 267	1983 – 2012
Cape Agulhas	0003020 4	34.83°S	20.01°E	11	1983 – 2012
Cape Columbine	0060620 9	32.83°S	17.86°E	62	1983 – 2012
Cape St. Francis	0017582 7	34.2°S	24.83°E	7	1983 – 2012
Escourt	0300690 1	29.02°S	29.87°E	1 144	1983 – 2012
Fraserburg	0113025A2	31.92°S	21.51°E	1 264	1983 – 2012
Lephalale	0674341 8	23.68°S	27.7°E	839	1983 – 2012
Lydenburg	0554816A7	25.11°S	30.48°E	1 439	1983 – 2012
Mara	0722099 1	23.15°S	29.57°E	894	1983 – 2012
Marico	0546630 3	25.47°S	26.38°E	1 082	1983 – 2012
Mount Edgecombe	0241072 9	29.71°S	31.05°E	94	1983 – 2012
Pofadder	0247668A4	29.12°S	19.39°E	984	1983 – 2012
Port Nolloth	0242644 6	29.25°S	16.87°E	8	1983 - 2012
Pretoria	0513284 8	25.74°S	28.18°E	1 286	1983 – 2011
Punda Maria	0768011A8	22.68°S	31.02°E	457	1983 – 2012
Queenstown	0123685 X	31.91°S	26.87°E	1108	1983 – 2012
Richards bay	0305168 5	28.77°S	32.08°E	47	1983 – 2012
Skukuza	0596179 3	24.99°S	31.59°E	276	1983 – 2012
Twee Rivieren	0461208 4	26.47°S	20.61°E	882	1983 – 2012
Vanwyksvlei	0193561A8	30.35°S	21.82°E	965	1983- 2012
Vryburg	0432237 3	26.95°S	24.65°E	1 245	1983- 2012
Wepener	0172877 1	29.92°S	26.85°E	1212	1983 – 2012
Willowmore	0050887 2	33.3°S	23.48°E	840	1983 – 2012

The country has a good network of temperature stations than much of Southern Hemisphere countries (New *et al.* 2006). A station network density of between 100 and 200 stations might be required in order to define temperature variability to a reasonable degree over areas such as Australia and the United States covering areas of 7 692 024 m^2 and 9 826 675 m^2 respectively (Vose and Menne 2004). Applying this recommendation in the perspective of South Africa which is about 1 200 000 m^2 (Luüs 2005), one might argue that a total of 24 climate stations distributed across the country should be adequate in providing countrywide temperature variability over the 30-year period. Height of the stations location is of utmost importance because it is known that temperature is also influenced by elevation (Archer *et al.* 2010).

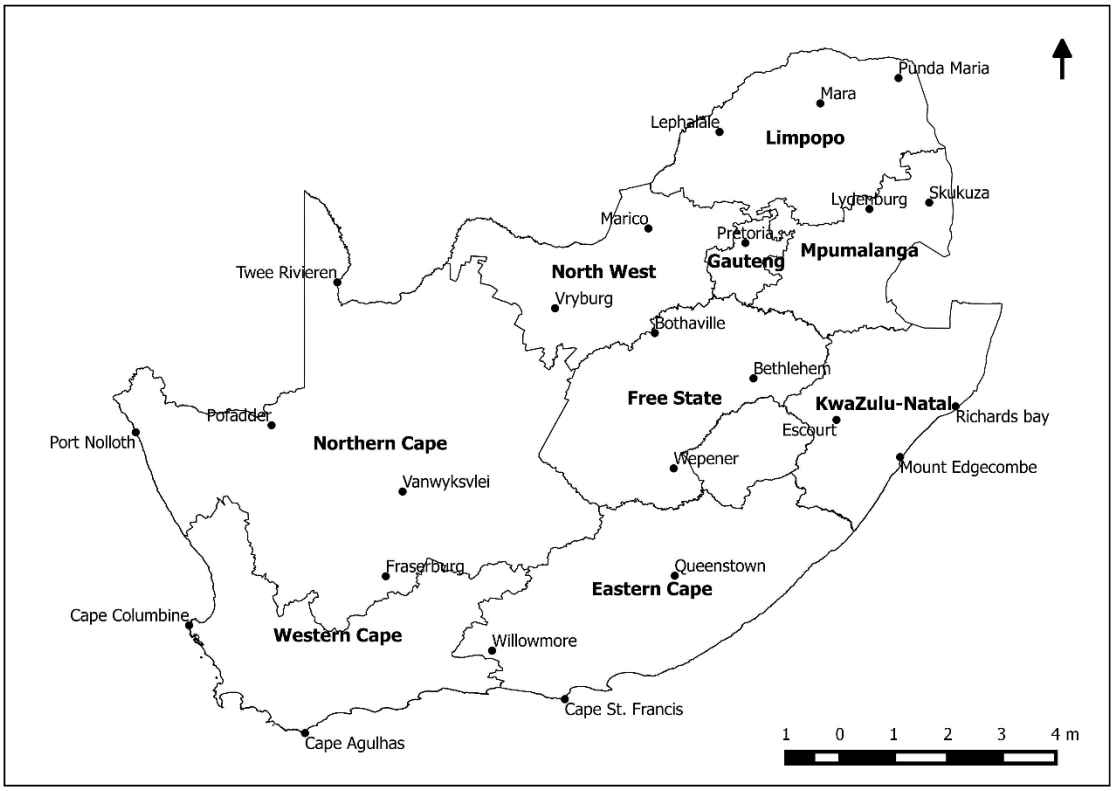

Figure 3.1: SAWS point stations with at least 95% data availability from 1983-2012.

There are several methods of filling gaps in daily data sets, and include filling gaps using regression based methods, using neighbouring stations (extrapolation approach) and can it can also be done through within one station (interpolation approach) (Allen and Gaetano 2011). Prevailing weather systems were checked during anomalously low and high T_X and $T_{N.}$ Both extrapolation and regression based methods use data from neighbouring stations, while interpolation uses days of the same station on which data is available (Tardive and Berti 2012). This work applied the interpolation method, which uses same station and uses several days before and after to reconstruct the missing data. This method was also used by Chai *et al.* (2011) in filling daily temperature gaps. Acock and Pachepsky (2000) also argued that this method tends to give better results for shorter gaps (one or few days) compared to regression based methods. It is also favourable, considering that only stations with fewer gaps were selected.

RClimDex version 1.0 software (Zhang and Yang 2004) was used to quality control the data. RClimDex is an R based statistical tool which is freely downloadable from the ETCCDMI website (http:// cccma.seos.uvic.ca/ETCCDMI/index.shtml). This software detect T_N values greater that T_X and outliers on the dataset by a standard deviation of 3.5 from the climatology of the day. This standard deviation of 3.5 has been used in the past by New *et al*. (2006). RClimDex also computes 27 core indices recommended by the World Meteorological

Organization Expert Team on Climate Change Detection and Indices (WMO ETCCDI). RClimDex version 1.0 software was also used to calculate trends of selected temperature indices (Table 3.2) relevant to this study. TN10P and TN90P represents cold and warm nights respectively, while cool and hot days are represented by TX10P and TX90P respectively.

Table 3.2: List of relevant ETCCDI indices utilized in this study

Index	Description	Units
TN10P	Annual number of days when TN < 10th percentile	days
TN90P	Annual number of days when TN > 90th percentile	days
TX10P	Annual number of days when TX < 10th percentile	days
TX90P	Annual number of days when TX > 90th percentile	days
DTR	Annual diurnal temperature range	°C

At least one station was selected in each thermal region (Figure 3.2) across South Africa. This assists in analysing heat wave characteristics of areas experiencing different temperature conditions. Kruger and Sekele (2013) performed a cluster analysis using SAWS T_X and T_N datasets to identify different thermal regions in South Africa, and Table 3.3 summarises the description of these regions which are shown in Figure 3.2.

Table 3.3: Summary of South African thermal regions

Region	Cluster	Description
coastal	Cluster A	Southern and western coastal regions which experiences Mediterranean and mild climate
	Cluster B	Eastern and southeast coastal regions experiencing temperatures greater than cluster A, and is characterized by subtropical climate
Interior	Cluster C	Northeast lowveld region experiencing high temperature all year round
	Cluster D	Subtropical western interior which is dry and characterized by high maximum temperature with an average of 30°C, and DTR is usually high
	Cluster E	Southeastern interior where temperatures are highly influenced by conditions of the Indian Ocean
	Cluster F	Northern interior which is relatively warm in austral winter than most regions in Cluster E, and usually experiences less frequent temperature extremes than cluster D

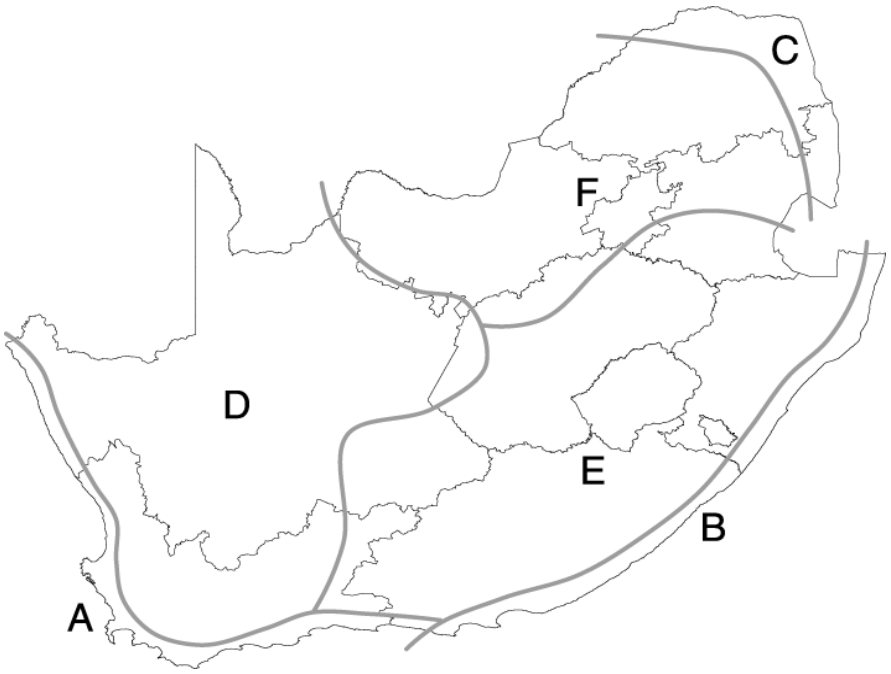

Figure 3.2: South African thermal regions from cluster analysis using annual mean T_X and T_N (Source: Kruger and Sekele 2013).

3.2.2 NCEP/NCAR Reanalysis datasets

Meteorological reanalysis datasets are obtained from a joint product between National Centers for Environmental Prediction (NCEP) which is formerly known as National Metrological Center (NMC), and National Center for Atmospheric Research (NCAR). The joint product is known as NCEP/NCAR and is an outgrowth from the Climate Data Assimilation System project (Chikoore 2005). NCEP/NCAR uses continually updating gridded datasets which represent the state of the Earth's atmosphere, incorporates observations and numerical weather prediction (NWP) models output dating back to 1948 (Kalnay *et al.* 1996).

NCEP/NCAR Reanalysis datasets that are used in this work are outgoing long-wave radiation (a), soil moisture (b), geopotential height (c), wind vector (d), relative humidity (e), and (f) omega. Kalnay *et al.* (1996) stated that these datasets are based on assimilation of surface, pibal, aircraft, ship, rawinsonde and satellite data which is quality controlled before made available online. Data from NCEP/NCAR reanalysis-2 (R-2) (Kanamitsu *et al.*, 2002) will be used. It has 17 pressure levels in the vertical ranging from 1000 to10 hPa. In this new version, known errors of NCEP- reanalysis 1 (R-1) were fixed thereby producing better reanalysis for parameters (Kanamitsu e*t al.*, 2002).

a) Outgoing long-wave radiation

Outgoing long-wave radiation (OLR) is defined as the energy which is radiating from the surface and atmosphere as infrared radiation at long wavelengths to space, and is controlled by temperature of the earth and the atmosphere above it, presence of clouds and the presence of water vapour in the atmosphere (Sapra *et al.* 2011). OLR at the top of the atmosphere (i.e. 200 hPa) is a proxy for convective precipitation. Convective clouds also block sunlight, hence cool land surface are experienced, while the complete opposite can be expected during clear skies. The National Oceanic and Atmospheric Administration (NOAA) Interpolated OLR was used. Gaps in this dataset are filled by the interpolation procedure and data is quality controlled and data that proved to be erroneous were removed.

b) Soil moisture

Soil moisture is one of the most important factors when analysing heat waves, since it is known that the interactions of soil moisture and the atmosphere play a vital role in the projected summer climates (Rowell 2005; Vidale *et al.* 2007). Persistence of the anticyclonic circulation over an area promotes subsidence and results in negative soil moisture anomalies resulting from precipitation deficits (Fischer *et al.* 2007). This study used soil moisture content in order to determine its role in the occurrence of heat waves in South Africa.

Soil moisture dataset from NCEP used in this study are estimates derived from radiation and precipitation, and characterized soil moisture climatology of the earth surface. NCEP soil moisture is expressed as a fraction. For example, 0.5 refers to 5 cm of water in a 10 cm layer of soil. The saturation value of soil moisture is 0.477 and the field capacity is 0.358 (Chikoore 2005).

c) Geopotential height

The geopotential height (values in meters) represents the height of a pressure surface in the free atmosphere. It is the gravitational potential energy per unit mass at an elevation denoted by h. Areas of low geopotential height tend to be associated with a relatively cold column of air between the surface and the middle levels, while areas of high geopotential height are associated with relatively warm columns of air. Flow at the middle levels, i.e. about 500 hPa, can often be well approximated by quasi-geostrophic theory, and thus is often assumed to be approximately parallel to the height contours (Wallace and Gutzler 1981). Geopotential height can also show pressure systems that have triggered heat wave

occurrences. NCEP/NCAR R-2 daily geopotential height has a resolution of 2.5° x 2.5° global grids. Geopotential height formula is given in equation 3.1.

$$\Phi(h) = \int_0^h g(\phi, z)dz \qquad (3.1)$$

Where, $g(\phi, z)$ is the acceleration due to gravity, ϕ is latitude, and z is the geometric elevation.

d) Wind vector

The wind vector represents the motion of the air masses over the ground and is described by both wind direction and wind speed. Wind vector also helps in illustrating the contribution of horizontal advection to the occurrence of heat wave in South Africa. There is evidence that heat waves are associated with warm air advection (e.g. Miralles *et al.* 2014). Wind vector also provides advection of air given by equation 3.8.

$$\frac{DT}{Dt} = \frac{\partial T}{\partial t} + u.\nabla T \qquad 3.8$$

Where, $\frac{DT}{Dt}$ is the total derivative, $\frac{\partial T}{\partial t}$ is the local derivative and $u.\nabla T$ is the advection term.

NCEP model assimilated wind vector was analysed at different atmospheric levels. Cloud drift satellite dataset were used in this study. This provides model derived wind directions and wind speeds in regions where data is discontinuous and sparse due to limited radiosonde observations. There is sparse radiosonde spatial coverage because it is expensive doing these observations on a daily basis. Wind vector also determines areas of wind divergence or convergence during heat waves.

e) Relative humidity

RH is defined as the quotient between vapour pressure and saturation vapour pressure (3.2) at corresponding temperature (McIntosh and Thom 1978). RH was used in this study to observe the amount of water vapour in the middle levels (at 500 hPa) of the atmosphere. It was mapped for the identified heat waves as humidity is said to affect heat retention (Cerne *et al.* 2006). NCEP RH has a daily temporal coverage at a spatial resolution of 2.5° x 2.5° backing from the first of January 1948 to present. The NCEP satellite observations are done at different atmospheric levels. Middle level (500 hPa) RH was used. RH at 500 hPa is a better predictor for the possibility of rainfall.

$$RH = e/e_s x\ 100 \qquad (3.2)$$

Where, e is vapour pressure and e_s is saturated vapour pressure.

f) Omega

g) $$\omega \equiv \frac{Dp}{Dt} \qquad (3.3)$$

Where, Dp is change in pressure and Dt is change in time.

Omega (ω) shows a vertical motion of air, positive values are showing subsidence while negative values represent uplift (Finley and Raphael 2007). Positive omega values are also associated with an increase in pressure (Finley and Raphael 2007). NCEP/NCAR reanalysis 2 data set at 500 hPa was used. This atmospheric level is selected because studies suggested that it is where a clear vertical wind direction can be depicted (e.g. Randriamahefasoa 2011). Equation 3.3 is used to calculate omega for a region. The satellite NCEP daily omega dataset also has a spatial resolution of 2.5° x 2.5°, global grids.

3.2.3 KNMI Climate Explorer

Royal Netherlands Meteorological Institute (KNMI) Climate Explorer provides access to different data portals and is known mainly for its weather forecasts and warnings, but it does a lot more in its capacity as a national data and knowledge center for weather, climate research and seismology. The KNMI Climate Explorer is a web application to analyse weather and climate data statistically. It started in late 1999 as a simple web application to analyse mainly ENSO teleconnections (Trouet and van Oldenborgh 2013). For this study, KNMI Climate Explorer was used to provide climate indices, such as Southern Oscillation Index (SOI) and Niño 3.4 SST, Standardized Precipitation Index and Normalized Difference Vegetation Index.

3.2.4 Climate indices

a) Southern Oscillation Index and Niño 3.4 SST

SOI is as the monthly, normalized mean sea level pressure (SLP) difference between Tahiti and Darwin (Figure 3.3) in the equatorial pacific (Russell *et al.* 1992). Monthly data for the SOI and Niño 3.4 SST from National Oceanic-Atmospheric Administration (NOAA) CPC were used in this study and was obtained through KNMI Climate Explorer for the study period. CPC satellite data is compiled based on current and historic oceanic conditions and atmospheric conditions above oceans. Monthly southern oscillation indices were then averaged in each year from 1982 to 2012. There are several ENSO indices; However SOI has proven to be a more useful predictor for seasonal rainfall (Nicholls and Katz 1991). El Niño-Southern Oscillation (ENSO) is a naturally occurring phenomenon that involves fluctuating ocean temperatures in the equatorial Pacific Ocean. Warm ENSO events are

referred to as El Niño events while cold ENSO events are said to be La Niña. The development and intensity of both La Niña and El Niño events are given by the SOI (equation 3.4).

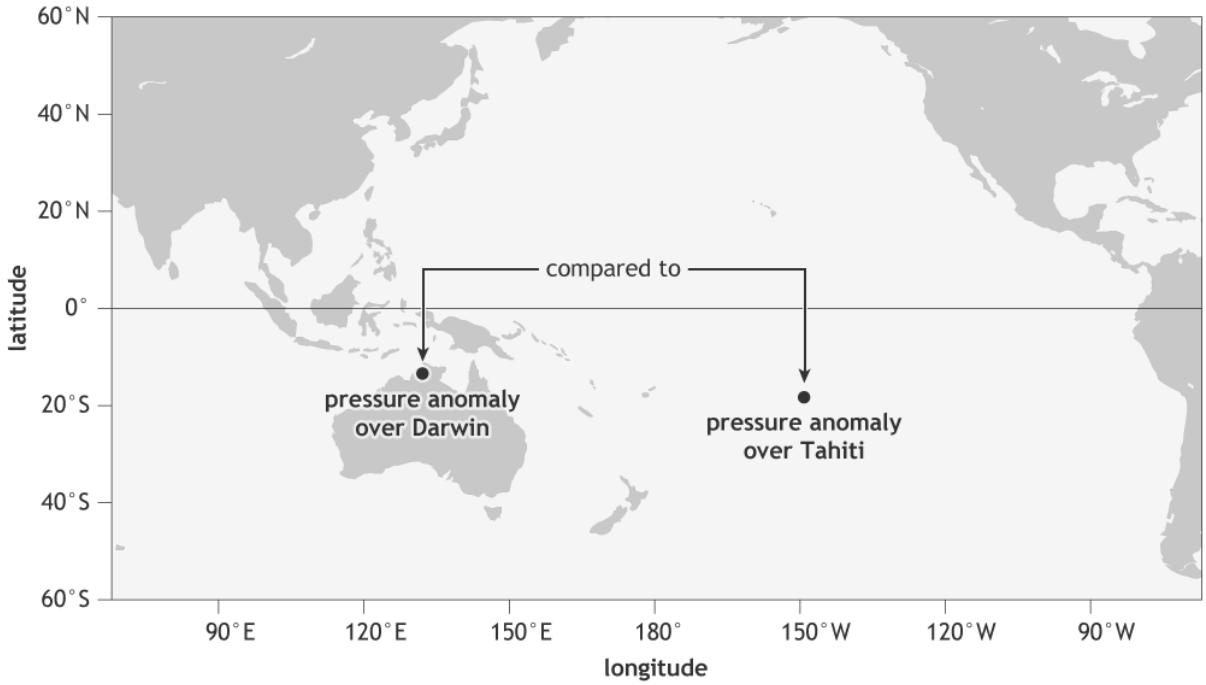

Figure 3.3: Location of the stations Tahiti and Darwin over the equatorial Pacific whose sea level pressure contribute to SOI (Source: Barnston 2015).

SOI= (Standardized Tahiti – Standardized Darwin)/ MSD (3.4)

Where,

Standardized Tahiti = (Actual Tahiti SLP - Mean Tahiti SLP) / Standard Deviation Tahiti

Standardized Darwin = (Actual Darwin SLP - Mean Tahiti SLP) / Standard Deviation Darwin

MSD = Monthly Standard Deviation = $\sqrt{}$ ($\sum$ (Standardized Tahiti - Standardized Darwin) ^{2} / N)

N = Sum of the number of months, and SLP= Sea Level Pressure

b) Standardized Precipitation Index

Standardized Precipitation Index (SPI) is the number of standard deviations that shows cumulative rainfall deviation from a climatological mean, and it was developed primarily to monitor droughts (McKee *et al*. 1993). SPI helps to determine the extent of droughts and wet periods. It can be calculated for different time scales. In this study, the SPI shows the extent of both droughts during El Niño and floods Niña events over southern Africa, and the level of both wetness and dryness (Table 3.4) over the study area. The international research

institute (IRI) map-room was used to map both droughts and floods induced by ENSO events via SPI. A description of this index is detailed by Guttman (1999).

Table 3.4: Classification for the SPI values (Source: Hayes *et al*. 1999)

SPI values	Category
2.00 and above	Extremely wet
1.50 to 1.99	Very wet
1.0 to 1.49	Moderately wet
-0.99 to 0.99	Near normal
-1.00 to -1.49	Moderately dry
-1.50 to -1.99	Very dry
-2.00 and less	Extremely dry

c) Normalized Difference Vegetation Index

Normalized Difference Vegetation Index (NDVI) was used in this work to observe vegetation distribution during heat waves. The NDVI data set was obtained from the United States Geological Survey (USGS) via KNMI Climate Explorer. This index is defined as a normalized ratio of visible regions with wavelengths between 0.58 µm to 0.68 µm and near infrared between 0.725 µm to 1.1 µm (Tucker 1979). A detailed description is given in Tucker *et al.* (1991). This index is a proxy for vegetation (Yi 2012) and also helps in identifying regions where vegetation is most impacted by heat waves. NDVI provides a degree of vegetation cover over a large region in the earth surface. Regions with no vegetation or limited vegetation are easily recognized, while dense vegetation appears very intensely in NDVI imagery. This index identify ice and water as well. Vegetation is also a proxy of spatial rainfall patterns. Previous studies illustrated that there is a joint occurrence between heat waves and droughts (e.g. Lyon 2009), but it is also known that droughts are associated with sparse vegetation cover (Karnieli 2010).

Table 3.5: NDVI typical values for several cover types (Source: Holben 1986)

Cover Type	RED	NIR	NDVI
Dense vegetation	0.1	0.5	0.7
Dry Bare soil	0.269	0.283	0.025
Clouds	0.227	0.228	0.002
Snow and Ice	0.375	0.342	-0.046
Water	0.022	0.013	-0.257

Typical examples of NDVI can be seen in Table 3.5. NDVI values show how dense the vegetation is at a given region. Bare vegetation is shown by values below 0.3 while denser vegetation is shown by values above 0.5 (Jury *et al.* 1997). Vegetation cover also indicates possible reflectance (Figure 3.4), which also contributes in warming the atmosphere. The following equation (3.5) is used when calculating NDVI.

$$\mathrm{NDVI} = \frac{\mathrm{NIR} - \mathrm{VIS}}{\mathrm{NIR} + \mathrm{VIS}} \qquad (3.5)$$

Where, NIR is near infrared and VIS is visible wavelengths or bands.

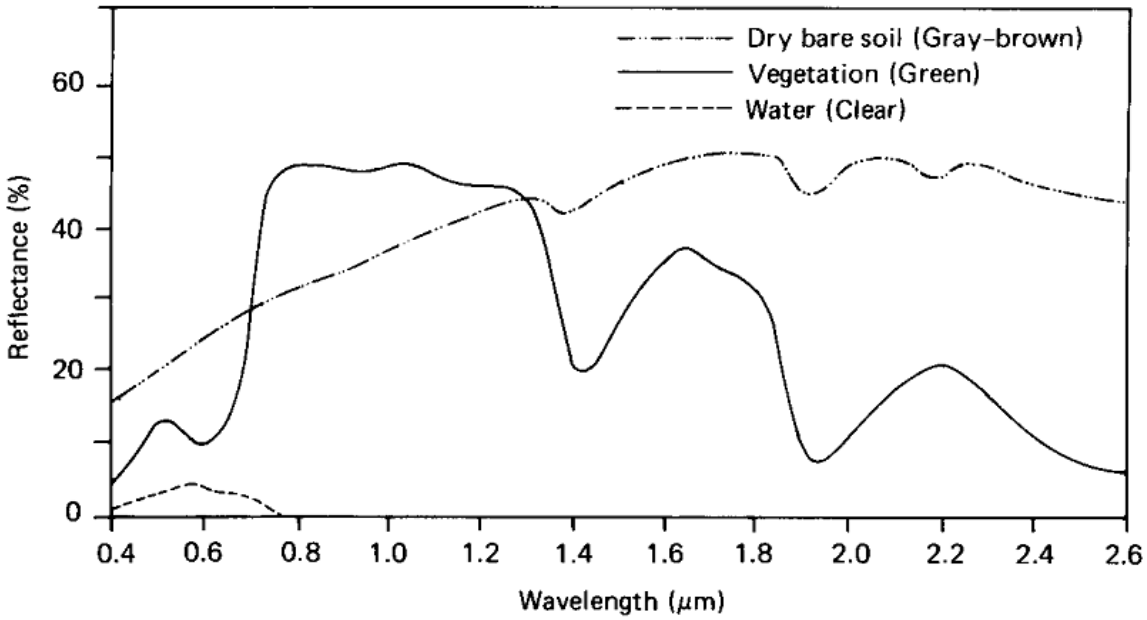

Figure 3.4: Typical reflectance curves of different land cover (Source: Lillesand and Kiefer 1994).

3.3 Methods of analysis

3.3.1 Identifying heat waves

It has been noted that there are several definitions of heat waves in different regions across the world. This work adopted the SAWS definition that a heat wave is “when for at least three days the maximum temperature of a certain region is five degrees higher than the mean maximum for the hottest month for a particular station”, which is also similar to the one used by Meehl and Tebaldi (2004). Threshold values from SAWS are shown in Figure 3.5. Fischer and Schär (2010) defined heat waves as events of at least consecutive 6 days. It is evident that different studies have used different threshold when defining a heat wave, based on factors such as weather conditions of the area of interest being considered. In this study, the 3-day duration is taken because it does not exclude possibility of detecting shorter

lasting heat waves. Heat wave is also defined in terms of the 3-day period in the American Meteorological Society (AMS).

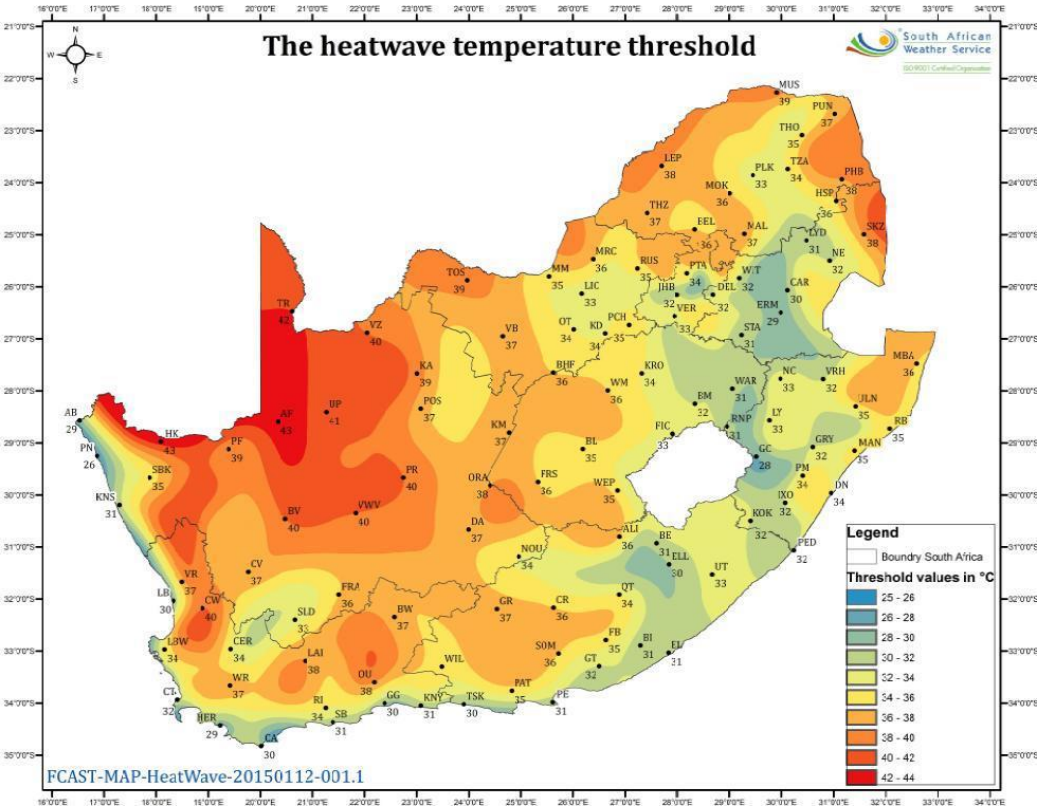

Figure 3.5: Heat wave temperature thresholds from SAWS.

Hottest month during the austral summer (October-March) was identified, and average daily T_X for that month was computed. Three consecutive days during a heat wave season, each with T_X 5°C higher than daily average T_X of the hottest month is said to be a heat wave. Heat wave season is defined as the period between the first and the last heat wave during the austral summer. This work then followed the method of Fischer *et al.* (2007) and uses two measures in determining the severity of heat waves: (a) maximum heat wave duration and (b) number of hot days.

3.3.2 Time series analysis

a) Trends analysis

Temporal patterns of South African temperatures were analysed in this study. This provides a background of areas which are hotter and cooler areas across the country. Trend analysis was applied to monthly means of T_X, T_N and DTR from 1983 to 2012. Annual T_X, T_N and DTR are also investigated in order to determine inter-annual temperature trends over the country. DTR was computed by subtracting daily average T_N from daily average T_X. Monthly

means were calculated from the daily T_X and T_N. Trend analysis was also applied when investigating changes in the number of hot and cold days per year. This study adopted forecasts terms used at SAWS (Table 3.6).

Table 3.6: Daily temperature forecast terms used at SAWS, as of 1 May 2008

Highest day temperature (Maximum)	
Extremely hot	$40°C \leq T_X$
Very hot	$36°C \leq T_X < 40°C$
Hot	$32°C \leq T_X < 36°C$
Warm	$25°C \leq T_X < 32°C$
Cool	$18°C \leq T_X < 25°C$
Cold	$10°C < T_X < 18°C$
Very cold	$T_X \leq 10°C$
Lowest day temperature (Minimum)	
Extremely cold	$T_N \leq -10°C$

Simple linear regression technique was then employed in historical temperature data to establish trends in the occurrence and duration of heat waves. This technique involves regression equation with coefficient of determination. Coefficient of determination represents the fraction of variability between two variables. In this work it was used to express variability of atmospheric temperatures with time. It explains how close the points are to the line. A decreasing trend is indicated by negative regression equation whereas an increasing trend is indicated by a positive regression equation.

For the ETCCDI temperature indices (Table 3.2), Kendall's tau based slope estimator has been used to compute the trends and statistical significance. This method was previously used in the analysis of temperature trends by New *et al*. (2006). This method was selected because it doesn't assume any distribution for the dataset or the trend linearity (Hollander and Wolfe 1973). If slope error greater than the slope estimate we can't trust slope estimate. A trend is said to be statistically significant at 95% level of confidence if p-value is less than 0.05. An example of a statistical significant trend produced using RClimDex is given in Figure 3.6.

Trend analysis was also adopted in observing historical trends of both annual heat wave frequency and average heat wave duration of heat waves over the study period (i.e. 1983-2012). Frequency and duration of heat waves during non-ENSO, warm and cold phases of ENSO seasons were studied. Table 3.7 provide ENSO seasons based on the Oceanic Niño Index (ONI) from Climate Prediction Center (CPC) National Oceanic and Atmospheric

Administration (NOAA), which is one of ENSO monitoring indices calculated by averaging SST anomalies of the east central portion of the Pacific (5°S-5°N, 120-170°W) (Jan 2015; NOAA CPC 2015). Jan (2015) further stated that warm ENSO (cool ENSO) event is said to be very strong if the SST anomaly for overlapping 3-month period is ≥ 2 (≤-2), strong if between 1.5 and 1.9 (-1.5 and -1.9), moderate if between 1 and 1.4 (-1 and -1.4) and weak if between 0.5 and 0.9 (-0.5 and -0.9). Normal conditions are observed between ONI of -0.5 and 0.5.

Table 3.7: Historical El Niño and La Niña (Source: Jan 2015)

El Niño seasons				La Niña seasons		
Weak	Moderate	Strong	Very strong	Weak	Moderate	Strong
1951-52	1963-64	1957-58	1982-83	1950-51	1955-56	1973-74
1952-53	1986-87	1965-66	1997-98	1954-55	1970-71	1975-76
1953-54	1987-88	1972-73		1964-65	1998-99	1988-89
1958-59	1991-92			1967-68	1999-00	
1968-69	2002-03			1971-72	2007-08	
1969-70	2009-10			1974-75	2010-11	
1976-77				1983-84		
1977-78				1984-85		
1979-80				1995-96		
1994-95				2000-01		
2004-05				2011-12		
2006-07						

b) Correlation analysis

Spatial correlation analysis was then used to investigate austral summer T_X and SOI from 1983 to 2012. Correlation was also done for Niño3.4 sea surface temperature and T_X. This helps to determine the influence of ENSO cycles to heat wave occurrences, since SOI is an indicator of ENSO events. The index >1 is identified as a La Niña and the index < -1 is identified as an El Niño. Non-ENSO season is when SOI is between -1 and 1. South-eastern part of southern Africa experiences dry conditions or droughts during the warm phase of ENSO which also play a role in conducive conditions for heat waves (Hunt 2007). For this

study, the correlation was done with a lag time of one month because the Pacific affects South Africa via teleconnections.

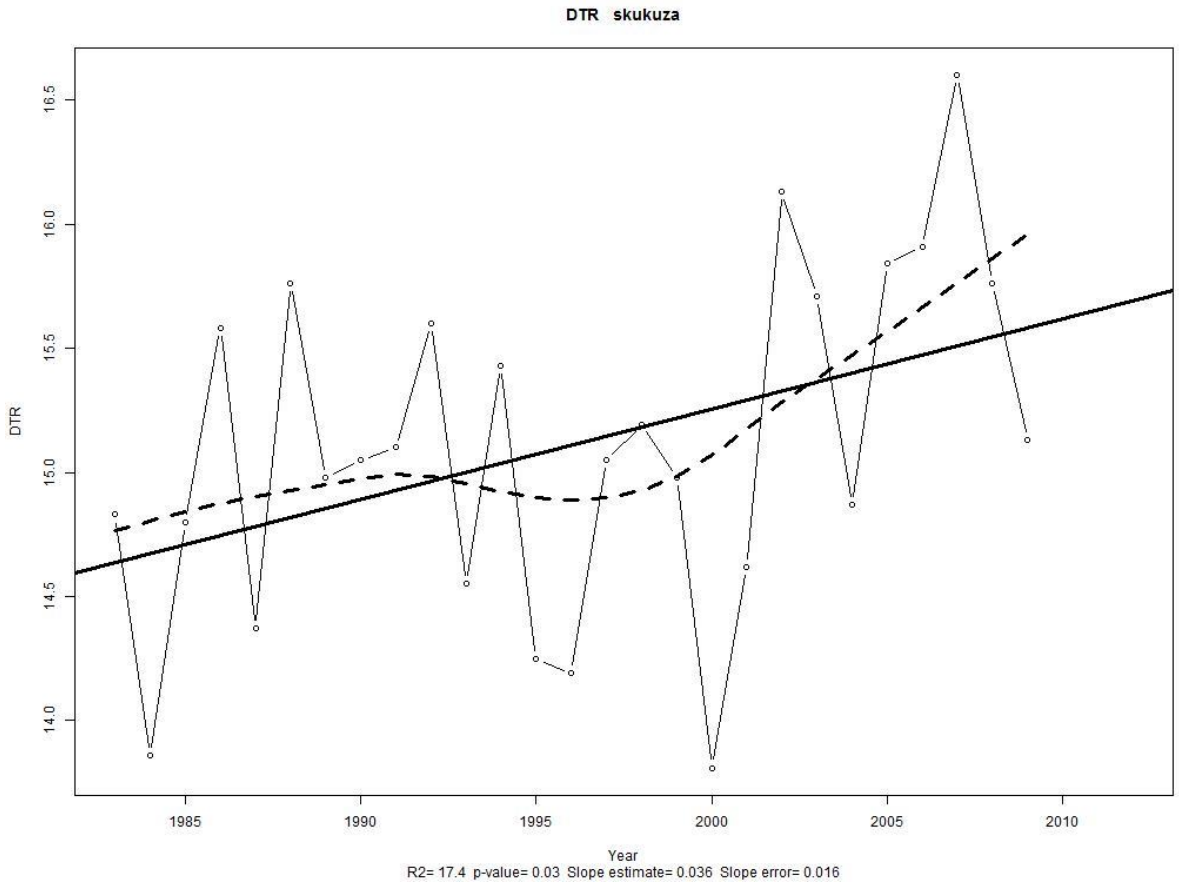

Figure 3.6: RClimDex output of trend analysis of DTR for Skukuza, for the period 1983–2012. Thin line and circles indicate time series and index values, bold line indicates linear trend and dotted line indicates decadal-scale variations based on Lowess smoother (Source: Cleveland, 1979).

3.3.3 Composite Analysis

Composite analysis is widely applied in climatological studies to detect characteristics which prove to be common (e.g. Chikoore 2005). This technique is also referred to as a superposed epoch analysis (Laken and Calagavic 2013), and is a technique which show better trends as compared to trends shown by individual cases. In this study, composite analysis was used to show characteristics of austral summer heat wave events in the interior of South Africa. It was also used to show vertical motion at the middle levels (500 hPa) over South Africa during heat wave events occurring during ENSO seasons. High pressure systems are associated with descending air, and this method investigated whether this is the case with heat waves as several studies suggest that heat wave occurrences are linked to the presence of a high pressure system.

3.3.4 Case study approach

While a composite analysis is very useful in providing a general picture about similar events, but sometimes it has a potential to group events which are diverse (Chikoore 2005), hence a case study approach then is vital. A case study approach was used in achieving an in-depth knowledge about the structure of the atmosphere during heat waves over South Africa. Case study approach is a widely used method of analysis in the field of climatology (e.g. Palecki *et al.* 2001). Longest lasting heat waves were selected in each thermal region (Figure 3.2) in order to investigate how the structure of heat wave varies across South Africa. SAWS T_X was mapped over the whole country to determine how the average T_X varies spatially during each selected heat wave period. NCEP data sets such as soil moisture, OLR, wind vector and RH were mapped during each selected heat wave. LST was also mapped during months were longest lasting heat waves occurred. Vertical motion of heat waves occurring during ENSO seasons was also investigated, and then compared to circulations and patterns of heat waves on non-ENSO seasons.

It is well documented that high atmospheric temperatures causes thermal discomfort in human beings (e.g. Yousif and Tahir 2013). Yousif and Tahir (2013) defined thermal comfort as the condition of mind that expresses satisfaction with the thermal environment and is assessed by subjective evaluation. The fact that the degree of vulnerability to heat waves differs across South Africa necessitate the need to investigate variability of thermal discomfort in different areas across the country. Studies investigated thermal discomfort using different indices in different regions across the world (e.g. Yousif and Tahir 2013).

This study used two indices to calculate thermal discomfort of different thermal regions of South Africa: (a) Thom's Discomfort Index (TDI) (Thom 1959) and (b) discomfort index from SAWS (DI). Both the index of Thom (1959) given in equation 3.6 and DI given in equation 3.7 evaluate the impact of heat stress on an individual taking into account both average RH and dry-bulb temperature (T). These indices were calculated for days when the longest heat waves occurred in each thermal region over the current climate. TDI was widely used in the past (e.g. Epstein and Moran 2006; Bartzokas *et al.* 2013; Yousif and Tahir 2013). TDI provides discomfort degree of a population at certain region (Table 3.8). T and RH during selected heat waves will be used for the calculations. SAWS indicated that there is no discomfort when DI is less than 90; DI ranging from 90 to 100 indicates it is very uncomfortable, DI of 100 to 110 indicated that it is extremely uncomfortable, while DI greater than 110 is hazardous to health. DI indicates the level of discomfort while TDI indicate the level of discomfort relating that to the population density affected. Tourism contribute to the economy of South Africa so understanding thermal discomfort levels in the country will assist tourists in deciding on a certain destination, with less or no discomfort.

Table 3.8: Thom's degree of discomfort (Source: Thom 1959)

Conditions	TDI
No discomfort	Less than 21
Under 50% of population feels discomfort	Between 21 and 24
Over 50% of population feels discomfort	Between 25 and 27
Most of population suffers discomfort	Between 28 and 29
Everyone feels stress	Between 30 and 32
State of medical emergency	Greater than 32

$$TDI = T - 0.55(1 - 0.01RH)(T - 14.5) \quad (3.6)$$

$$DI = 2T + RH(T + 24)/100 \quad (3.7)$$

3.3.5 The Grids Analysis and Display System

Using the Grids Analysis and Display System (GrADS), which is a free desktop tool on the internet that can be implemented on DOS based computers and available UNIX workstations (Doty 1995) was used to map NCEP/ NCAR R-2. NCEP/ NCAR R-2 data were displayed to analyse the synoptic circulation of heat wave events over South Africa. Wind vector data set was mapped at different atmospheric levels (i.e. 950 hPa, 500 hPa and 200 hPa) in order to understand changes of wind speed and direction with height during heat waves. This tool allows for an easy manipulation and display of earth science datasets.

Geopotential height and RH was mapped at 500 hPa which is the steering level and OLR at the upper level (200 hPa) to provide the nature of clouds formation if there are clouds during specified periods. This assists in understanding large scale circulation patterns during identified heat waves. Soil moisture was mapped days before and during the identified heat waves. NCEP/NCAR R-2 data sets were also used for this purpose. Soil moisture deficits of a particular region lead to extremely high land surface temperatures to that particular region (Fink *et al.* 2004), hence warming the atmosphere above.

GrADS was used to plot geopotential height, wind vector and anomalies of interpolated OLR, soil moisture and RH. Rather than mean composites, to show deviation from the meteorological means in order to get a better understanding of the synoptic conditions during heat waves over South Africa. NCEP/NCAR perform data assimilation using a forecast system (Kalnay *et al.* 1996), and a larger number of this data is available from Physical Sciences Division (PSD) (http://www.esrl.noaa.gov/psd/) and it is in 4-times daily format.

3.3.6 The Conformal Cubic Atmospheric Model

Current and future climate model output obtained from the Conformal Cubic Atmospheric Model (CCAM) was used in this study for present and future heat wave trends in South Africa. The periods of 2010 to 2039, 2040 to 2069, and 2070 to 2099 were considered as the future climates and the signal and effects of climate change is expected to be higher during these periods compared to the present climate were anthropogenic influences are expected to be smaller. However the threshold used for the definition of a heat wave for all the periods is derived from the present day climate. This makes it easier for characteristics of heat waves in the present and future climates to be comparable. The CCAM model provided projections of future heat wave frequency, duration and intensity.

CCAM is based on conformal cubic grids, and it is an atmospheric model which is semi Lagrangian and semi implicit and it solves hydrostatic primitive equations (Engelbrecht *et al*. 2011) and can be employed for simulations of a regional climate since it also supports a global resolution grid variable (McGregor and Dix 2008). CCAM is a global model, but it can also be employed as a Regional Climate Model (RCM) by running the model in stretched-grid variable-resolution mode (Engelbrecht *et al.* 2009). Rotstayn (1997) indicated that CCAM also include a prognostic cloud scheme, in addition to a land surface scheme suggested earlier by Kowalczyk *et al.* (1994) which include three layers of snow, soil moisture and soil temperature.

The CCAM model was developed by the Commonwealth Scientific and Industrial Research Organisation (CSIRO) in Australia (McGregor 2005; McGregor and Dix 2008), and is also being used by the Council for Scientific and Industrial Research (CSIR) in South Africa. The simulations used in this study have a grid spacing of 50 km and were made using the Representative Concentration Pathways (RCP) 4.5 and RCP 8.5, and comparison between the two were also made. Six ensemble members obtained using sea ice and sea surface temperatures from six earth system model, were used in this study (Table 3.9). RCPs were developed by the Intergovernmental Panel on Climate Change (IPCC) and a detailed description is given in studies by Potgieter (2006), Moss *et al*. (2010), Engelbrecht *et al.* (2011) and van Vuuren *et al*. (2011).

Table 3.9: List of ensemble members used in this study

Model	RCP 4.5	RCP 8.5
ACCESS	✓	✓
CCSM4	✓	✓
CNRM	✓	✓
GFDL	✓	✓
MPI	✓	✓
NorESM1M	✓	✓

In South Africa, CCAM has been used in the past to simulate future climate (e.g. Engelbrecht *et al.* 2009; Engelbrecht *et al.* 2011). Other studies used CCAM for short-range weather forecast at high resolution of about 15 km (e.g. Rautenbach *et al*. 2005; Potgieter, 2006). It was found that CCAM performs well for 24-hour forecast for a period of up to four days (Potgieter 2006). It was also found that CCAM is also good in simulations of minimum and maximum temperature, and rainfall annual cycles (Roux 2009). This work used CCAM to simulate future heat waves in South Africa.

3.4 Theoretical framework of the study

A theoretical framework of this study is offered here (Figure 3.7) based on the methods undertaken to achieve the main work of this study. Monthly and annual temperature trends are determined using trend analysis, and maximum temperature dataset was used to identify heat waves over South Africa. Using trend analysis, seasonal frequency and average duration of heat wave are studied across the country, and a case study approach is applied to understand the meteorological structure of these events. CCAM was then used to model trends of heat wave frequency and duration in the warmer future climates.

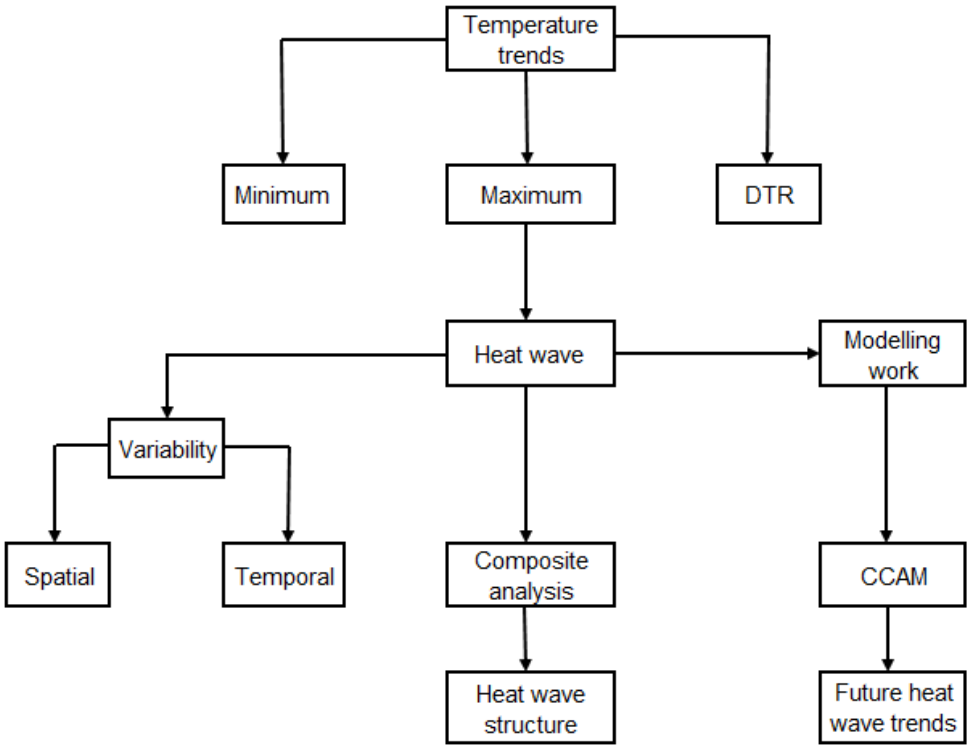

Figure 3.7: Schematic illustration of analysis involved in this study.

3.5 Summary

This chapter has described data sets and data sources used and the methods of analyses applied to achieve the objectives of this study. Maximum temperature is the major dataset used to identify heat waves in different regions across the country. Different threshold have been used because different thermal characteristics in the country. NCEP/NCAR daily composites of Geopotential height, RH, OLR, wind vector and soil moisture were mapped in order to understand the meteorological structure of heat waves. CCAM was used to model future heat wave characteristics. The chapter also provided a theoretical framework of the study.

The next chapter provide trends of DTR, minimum and maximum temperatures over different parts of South Africa. The chapter also provides heat wave occurrence spatial variability over time. Frequency, duration and averaged maximum temperature during the identified heat waves are discussed in the next chapter.

CHAPTER 4

HEAT WAVE VARIABILITY OVER SOUTH AFRICA

4.1 Introduction

A positive global general trend of temperatures is observed owing to global warming of the earth's atmosphere, with narrowing diurnal temperature range (DTR) (e.g. Makowski *et al.* 2008), but that may not necessarily be the case with regional temperature trends as microclimates vary from place to place. The atmosphere is known to be chaotic and there is observed variability in trends of anthropogenic contributions to a warming climate, such that it is crucial to analyse temperature trends over the country using recent datasets.

In this study heat waves are identified using daily maximum temperature, because changes in this dataset over time can impact the frequency and duration of heat wave occurrences. Kruger and Sekele (2013) identified thermal regions over South Africa, using the same dataset from the South African Weather Service (SAWS). South African thermal regions are experiencing different temperature characteristics in response to phenomena affecting weather and climate in the distinct regions. Weather of South Africa is influenced by both South Atlantic anticyclone and South Indian anticyclone, owing to its latitudinal location (22°-34°S and 16°-32°E). The frequency and duration of extreme temperature events may also vary as trends in the number of hot days are not the same in the country's thermal regions.

Land-atmospheric interactions have a crucial role in warming the atmosphere (Guo *et al.* 2011). Heat waves also depend on the temperature of the earth surface, so trends of land surface temperature should have a significant role in the nature of heat waves. Intense heating of a dry surface can result in negative rainfall anomalies (Fischer *et al*. 2007) and lead to occurrences of intense heat waves over a region.

The aim of this chapter is to analyse temperature trends over South Africa in the present climate, 1983 to 2012. The chapter discusses heat wave spatial variability over the country and their average duration and frequency and changes over time. Trends of temperature data from 24 selected climate stations are discussed in section 4.2; however only heat wave trends identified by 22 stations are discussed in section 4.3 as no heat waves were recorded in two stations (Cape Agulhas and Mount Edgecombe).

4.2 Temperature trends over South Africa

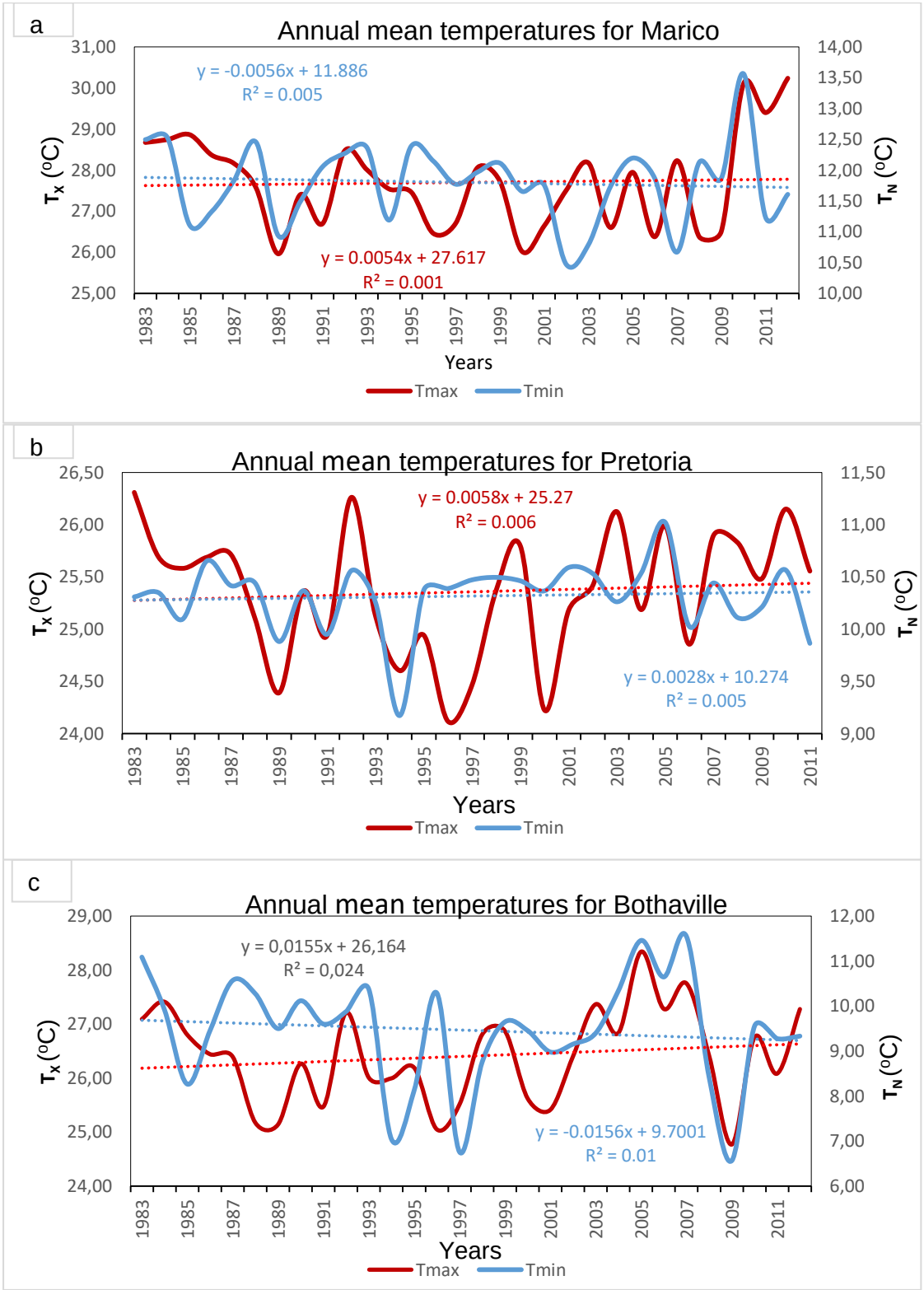

Figure 4.1: Inter-annual variability of maximum and minimum temperatures (°C) for (a) Marico, (b) Pretoria and (c) Bothaville from 1983 to 2013.

4.2.1 Annual temperature cycles

The northern interior of South Africa experiences weak positive annual maximum temperature trends in regions such as Marico, Pretoria and Bothaville (Figure 4.1). These regions also experience insignificant changes in annual minimum temperatures. While other parts of the country experience annual minimum temperature trends which are almost divided between negative and positive, much of the subtropical western interior experiences negative trends in annual minimum temperatures over the 30-year period.

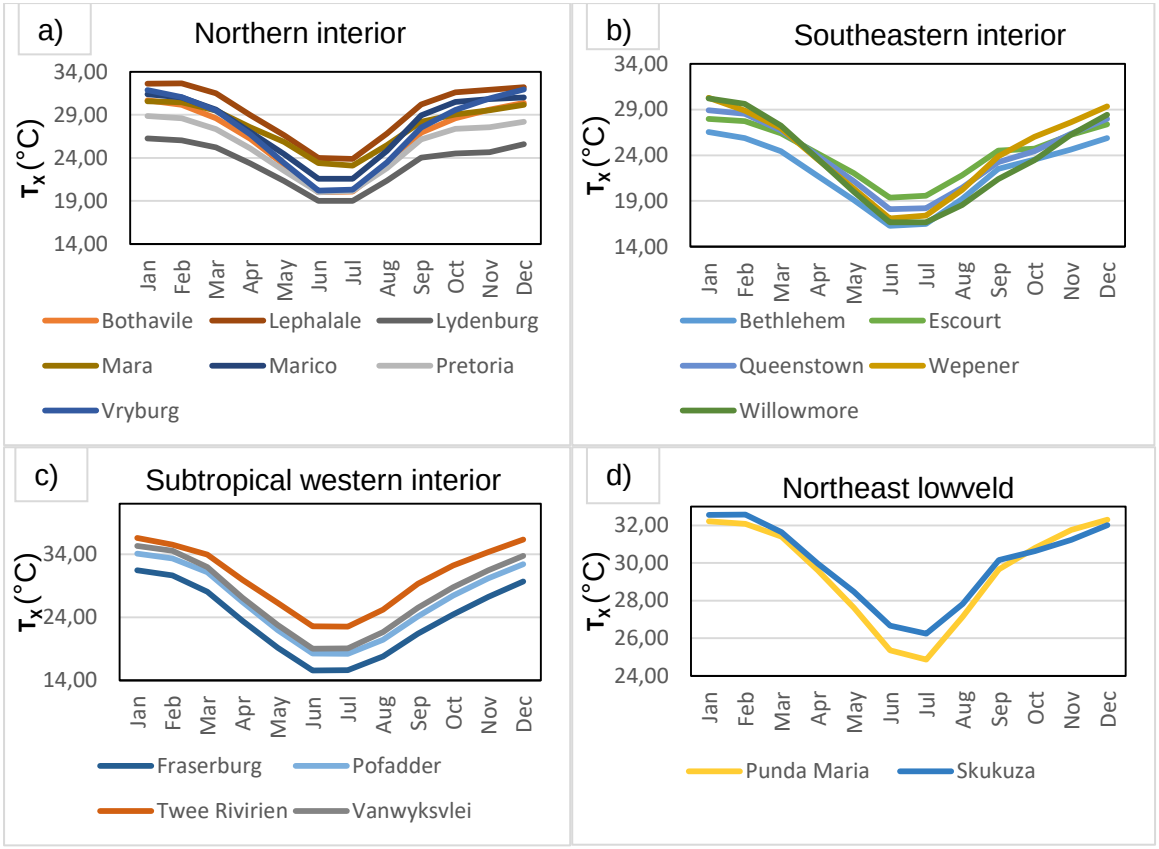

Figure 4.2: Monthly mean maximum temperatures over (a) Northern Interior (b) South-eastern interior (c) Subtropical western interior and (d) Northeast lowveld of South Africa from 1983 to 2012.

Monthly means of both maximum and minimum temperatures over much of South Africa follow a similar pattern. Higher maximum temperature values are observed during December to February (DJF), while much of the country is relatively cool during the austral winter, with lower monthly maximum temperatures observed particularly between June and July (Figure 4.2). However there are no significant monthly maximum temperature changes throughout the year over areas such as Port Nolloth in cluster A (Figure 4.3a) as a shorter range (18-20.7°C) is observed.

Monthly maximum temperature of south-west and south coastal regions are lower when compared to the entire country. Coastal areas such as Cape Columbine, Cape Agulhas and Cape St. Francis experience maximum temperatures well below <25°C throughout the year and well below 20°C (Figure 4.3a) during austral winter months (April-September). These areas usually experience cold fronts which lead to a drop in atmospheric temperature after their passage. South-east coastal region experiences warmer maximum temperatures compared to south and south-west coasts. Richards Bay is warmer than all the South African coastal regions throughout the year with lowest average temperature of 22.98°C in July. Coastal regions are experiencing moderate maximum temperatures than inland areas, as a result of the ocean cooling effect by both South Atlantic and South Indian Oceans on coastal regions

Much of cluster D experiences intense warming in DJF, with areas in the northern parts such as Twee Rivieren experiencing maximum temperature reaching 36.6°C (Figure 4.2c) in January. Cluster D is a thermal region with little to no vegetation (Figure 1.3); hence more radiation reflectance occurs and warms the atmosphere. Areas in the north-east parts of the country, such as the lowveld of the country in cluster C are the hottest regions during summer in the entire subtropical eastern part of South Africa. These region which include Punda Maria and Skukuza are also the warmest winter regions of the country with maximum temperature >25°C in June-August (JJA) (Figure 4.2d). Strong maximum temperature gradients are observed in the more elevated central interior ranging from 16-24°C in winter (June to July) and 26-33°C in summer (DJF).

Monthly maximum temperature trends over much of South Africa are consistent with monthly minimum temperature trends most cases (Figure 4.4). An exception was only observed where monthly minimum temperature decreases drastically in winter over Port Nolloth, with no significant changes in monthly maximum temperatures throughout the year. Minimum temperatures of coastal regions hardly drop below 0°C (Figure 4.3b), while inland regions experiences varying minimum temperature with only Bethlehem and Wepener well below 0°C in winter (Figure 4.4b). Bethlehem minimum temperatures range from -0.58 to -1.24°C while Wepener is the coldest with temperature ranges from -1.56 to -2.18°C between June and July. All selected climate stations recorded average monthly minimum temperature <25°C from 1982 to 2012. Richards Bay and Mount Edgecombe are the only coastal regions with DJF minimum temperature exceeding 20°C throughout the year (Figure 4.3b).

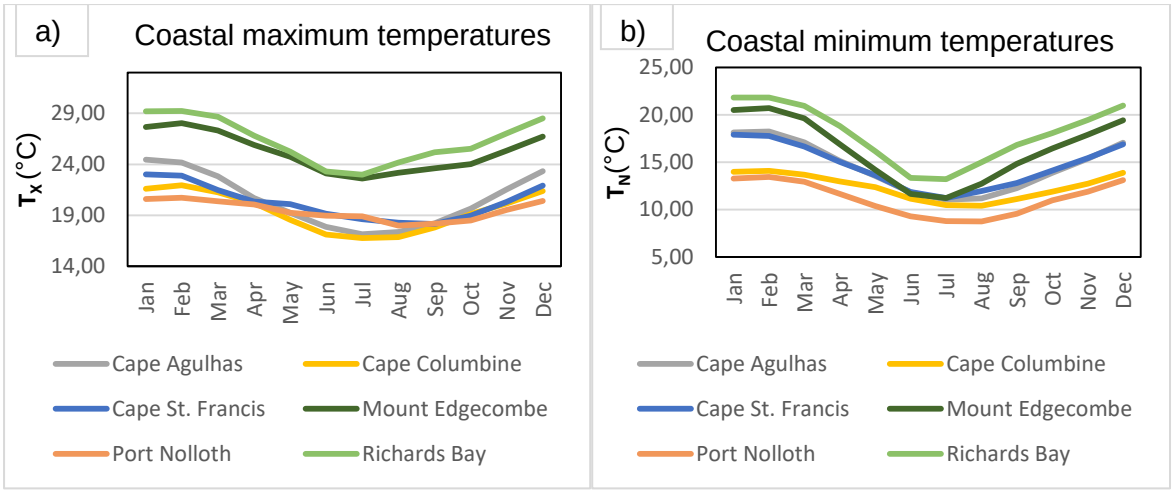

Figure 4.3: Monthly mean (a) maximum and (b) minimum coastal temperatures (°C) from 1983 to 2012.

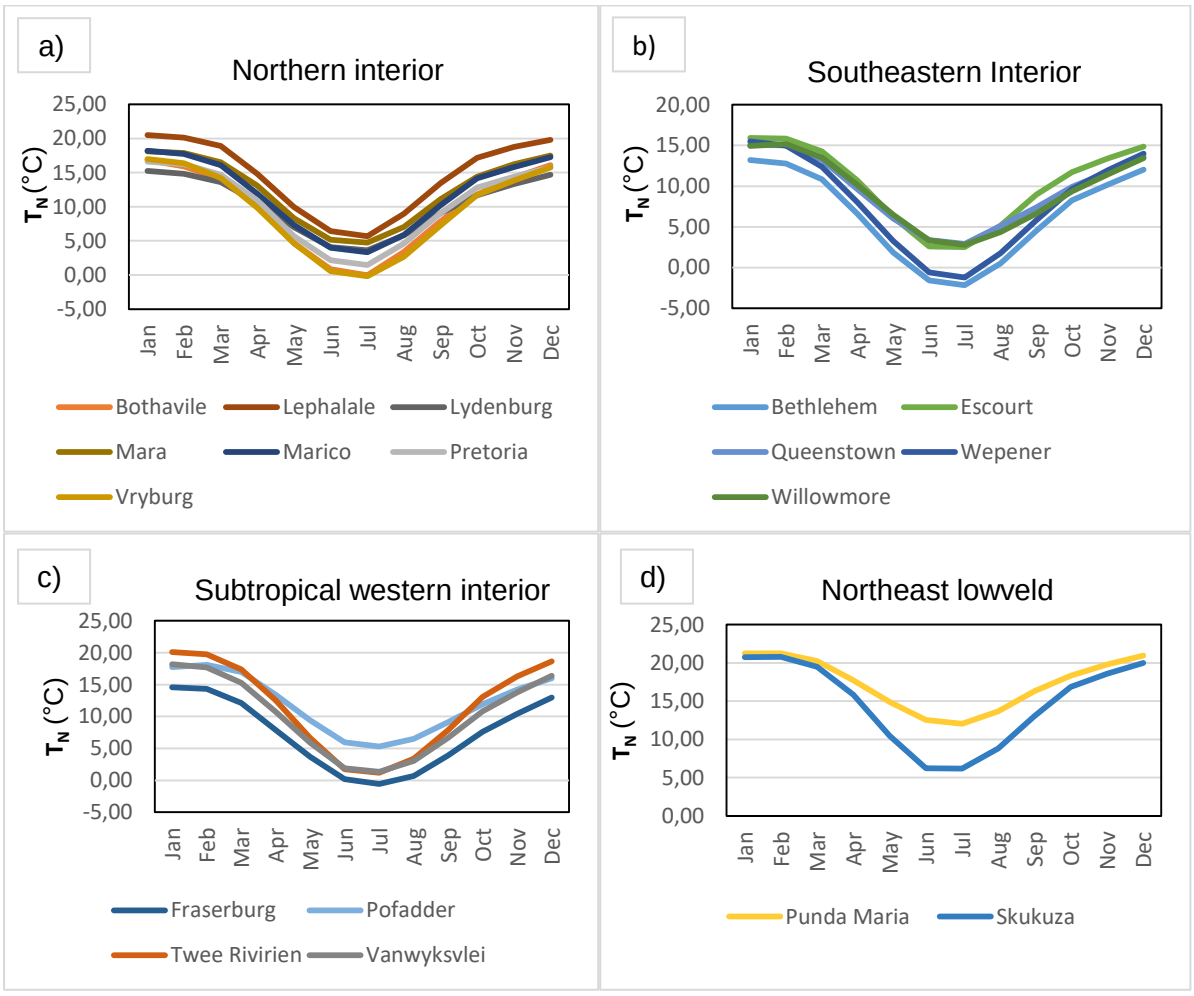

Figure 4.4: Monthly mean minimum temperatures (°C) over (a) Northern Interior (b) South-eastern interior, (c) Subtropical western interior and (d) Northeast lowveld of South Africa from 1983 to 2012.

4.2.2 Interannually variability

South Africa experienced different inter-annual temperature trends from 1983 to 2012. The country experienced increasing annual maximum and minimum temperature in other regions, while complement temperature conditions are observed in other regions (Table 4.1). Twenty-one of the 24 selected climate stations across South Africa have positive annual maximum temperature trends, while only three stations show negative annual maximum temperature trends. Cape St. Francis, Wepener and Willowmore are the stations with negative annual maximum temperature trends, and both Wepener and Willowmore are in the south-eastern interior of the country, within the same thermal region.

4.2.3 Diurnal temperature range

Mean monthly DTR is large during the austral winter in most interior parts of South Africa. An average of 17.3°C is observed from all the selected interior stations during the mid-winter (JJA) season. Eastern and southeast coastal region of the country also show the same pattern as most interior stations (Figure 4.5). While all selected stations in northeast lowveld, southern and northern interior have larger mean monthly DTR in winter which then decreases in austral summer, Pofadder in cluster D is the only station that showed the opposite pattern. Pofadder has a mean DTR of 13.1°C in JJA but 16°C during DJF. Mean monthly DTR of station in cluster A show different patterns, where DTR at Port Nolloth is larger in summer than in winter while Cape Columbine is showing the opposite. Minor mean monthly DTR differences are observed over Cape Agulhas.

Annual DTR reflect the annual trend magnitudes of both maximum and minimum temperatures during the study period. Much of the country show positive trends of annual DTR, with 13 of the 24 stations being statistically significant at the 95% level of confidence. Only 3 stations showed negative annual DTR trends (Pofadder, Pretoria and Wepener). This is because the two stations, Pofadder and Pretoria, are experiencing positive trends of both Maximum and minimum temperatures however minimum temperatures rising at a higher rate. Annual DTR is narrowing at Wepener because of the negative trend of maximum temperature but minimum temperature is experiencing a positive trend. Most of the stations with stronger significant positive trends are in the eastern half of South Africa.

Table 4.1: Annual maximum and minimum temperature trends from 1983 to 2012

Region		Positive trend		Negative trend	
		T_X	T_N	T_X	T_N
Inland	Bothaville	✓	✓		
	Bethlehem	✓	✓		
	Fraserburg	✓	✓		
	Lydenburg	✓	✓		
	Pofadder	✓	✓		
	Pretoria	✓	✓		
	Punda Maria	✓	✓		
	Escourt	✓			✓
	Lephalale	✓			✓
	Marico	✓			✓
	Mara	✓			✓
	Vryburg	✓			✓
	Willowmore	✓			✓
	Skukuza	✓			✓
	Twee Rivieren	✓			✓
	Vanwyksvlei	✓			✓
	Wepener		✓	✓	
	Queenstown			✓	✓
Coastal	Cape Agulhas	✓	✓		
	Cape Columbine	✓	✓		
	Mount Edgecombe	✓	✓		
	Port Nolloth	✓			✓
	Richards bay	✓			✓
	Cape St. Francis			✓	✓

4.3 Extreme temperature trends

4.3.1 Cold and warm nights

The selected stations across South Africa all experienced negative trends in cold nights and 21 stations are statistically significant at 95% level of confidence (Table 4.2). Stations in the central plateau, northern and eastern parts (such as Punda Maria, Mara, Lephalale, Pretoria, Lydenburg, Mount Edgecombe, Richards bay, and Queenstown) of the country show strongest negative trends in cold nights. Warm nights show opposite trends than cold nights. However, it is noticeable that the positive trends are smaller in magnitude than the

decreasing trends of cold nights. A total of 18 stations show statistically significant positive TN90P trends at the 95% level of confidence.

Table 4.2: Trend results for selected temperature indices from 1983 to 2012 (* indicates significance at the 95% level of confidence)

Station Name	TN10P (days)	TN90P (days)	TX10P (days)	TX90P (days)	DTR (°C)
Bethlehem	-0.063*	0.092*	-0.057*	0.151*	0.007
Bothaville	-0.324*	0.077	-0.034	0.275*	0.045*
Cape Agulhas	-0.199*	0.392*	-0.199*	0.392*	0.01
Cape Columbine	-0.211*	0.158*	-0.046*	0.141*	0.001
Cape St. Francis	-0.067*	0.165*	-0.184*	-0.107*	0.031*
Escourt	-0.127*	0.108*	-0.012	0.213	0.032*
Fraserburg	-0.06	0.19*	-0.04	0.244	0.003
Lephalale	-0.354	0.453*	-0.155	0.834*	0.052*
Lydenburg	-0.163*	0.052	-0.092*	0.336*	0.014
Mara	-0.322*	0.027*	-0.042	0.356*	0.038*
Marico	-0.186*	0.113	0.148*	0.027	0.006
Mount Edgecombe	-0.326*	0.206*	-0.019	0.176*	0.008
Pofadder	-0.063	0.151*	-0.012	0.186	-0.006
Port Nolloth	-0.116*	0.018*	-0.063*	0.218*	0.035*
Pretoria	-0.314*	0.049	-0.023	0.028	-0.005
Punda Maria	-0.438*	0.116*	-0.038*	0.137*	0.034*
Queenstown	-0.329*	0.208*	-0.174*	0.051	0.001
Richards bay	-0.339*	0.283*	-0.143*	0.515*	0.069*
Skukuza	-0.283*	0.109	-0.114*	0.2	0.036*
Twee Rivieren	-0.262*	0.065*	-0.122*	0.832*	0.111*
Vanwyksvlei	-0.118*	0.062	-0.076*	0.091	0.018*
Vryburg	-0.298*	0.123*	0.057*	0.166*	0.039*
Wepener	-0.035*	0.173*	-0.18	0.1*	-0.037*
Willowmore	-0.117*	0.305*	-0.165*	0.183*	0.024*

4.3.2 Cool and hot days

Table 4.2 also indicate trends of cool (TX10P) and hot days (TX90P). TX10P indices are negative in 23 of the 24 stations, indicating a general decreasing trend in cool days across South Africa. Vryburg in cluster F is the only selected station showing a positive trend. A total of 15 of the 24 stations were significantly negative with strongest negative trends in south and south-east coastal regions. Hot days show increasing trends from 1983 to 2012, with an exception of Cape St. Francis in the eastern coast of cluster B. A total of 16 TX90P

are statistically significant at the 95% level of confidence with central and northern regions of the country showing strongest trends.

4.4 Heat wave variability

4.4.1 Spatial and temporal variability

South Africa experiences a considerable spatial variability of heat wave occurrences over time (Figure 4.6). The country experienced higher heat wave frequency in the more equator ward regions, with Punda Maria (22.68°S, 31.02°E) recording 45 heat waves from 1983 to 2012. The north-east regions experience more heat wave occurrences in the subtropical eastern parts of South Africa, and these low-lying regions are warm throughout the year.

Most regions experience heat waves during the austral summer, particularly in DJF (Figure 4.7), with the exception of subtropical western to south-west coastal regions experiencing heat waves mainly between May and August (Figure 4.8-4.9). Northern parts of South Africa also experienced over 12 heat waves between September and November (SON) during the study period (Figure 4.10). The western coastal regions of South Africa experiences most heat waves in winter when subtropical anticyclones are more equator-ward and when a continental high becomes more established. Port Nolloth experienced most (71) heat wave occurrences (Figure 4.11) between 1983 and 2012, 66 of which occurred between April and September.

The average heat wave frequency per season varies across South Africa during the present day climate (Table 4.3). Port Nolloth experiences a high average heat wave frequency per season than all the stations, followed by Punda Maria. However, on average there is no season where the country cannot experience heat wave occurrences. There is no uniform recurrence pattern of heat wave occurrences. Some seasons have high heat wave frequency, while no heat waves are observed during other seasons. More than one heat wave can be observed in a season.

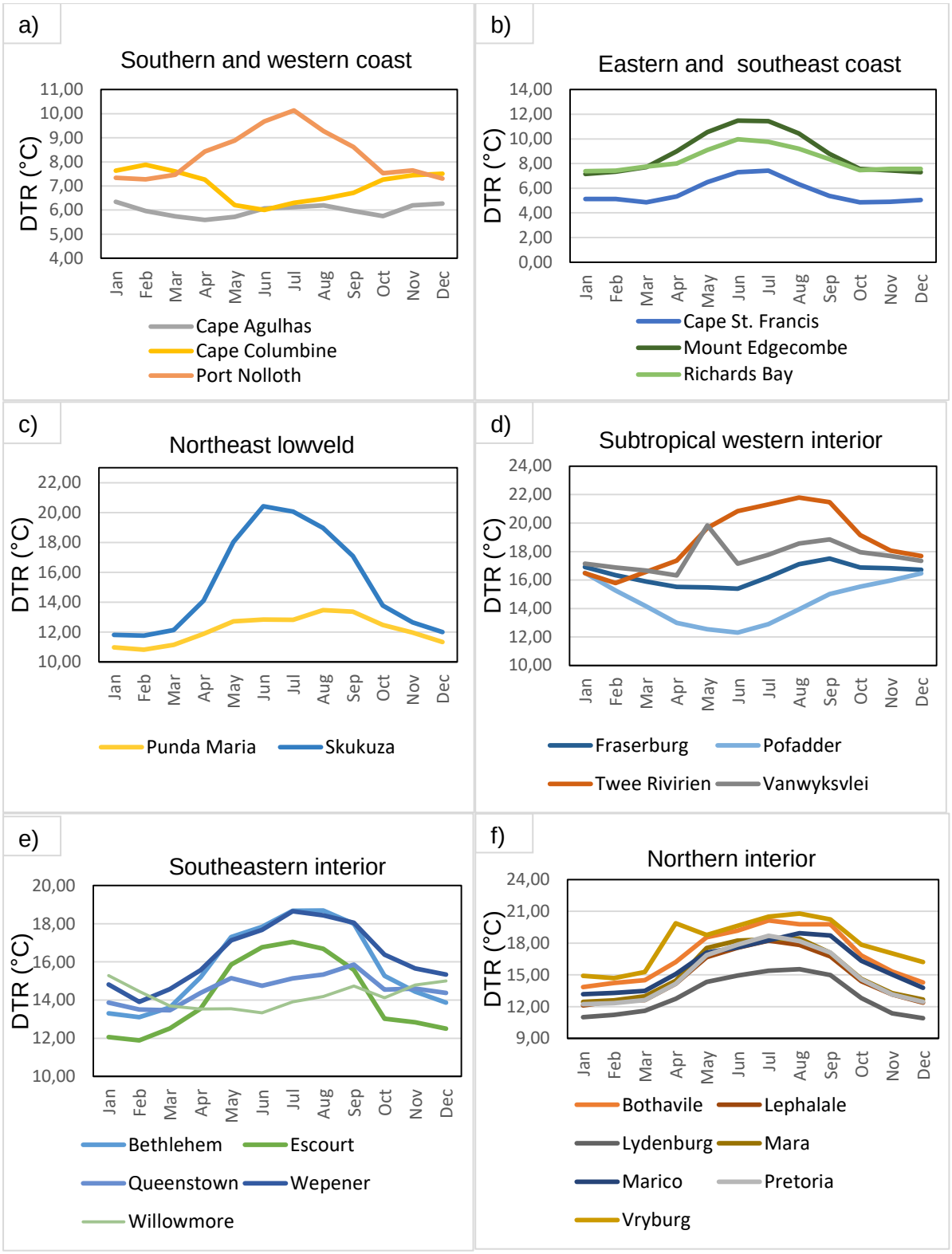

Figure 4.5: Monthly mean DTR (°C) over (a) Southern and western coast, (b) Eastern and southeast, (c) Northeast lowveld, (d) Subtropical western interior and (e) south-eastern interior and (f) Northern interior of South Africa from 1983 to 2012.

Table 4.3: Hottest month per station and its average maximum and minimum temperatures, and average number of heat waves per season.

Station Name	Hottest month	Average T_X (°C)	Average T_N (°C)	Average number of heat waves per season
Bethlehem	January	26.53	13.12	0.3
Bothaville	January	30.67	16.82	0.9
Cape Agulhas	January	24.46	18.22	0.0
Cape Columbine	February	21.96	14.08	0.5
Cape St. Francis	January	23.00	17.88	0.2
Escourt	January	27.96	15.90	0.6
Fraserburg	January	31.47	14.56	0.2
Lephalale	February	32.65	20.13	0.9
Lydenburg	January	26.25	15.24	0.1
Mara	January	30.58	18.13	1.1
Marico	January	31.37	18.21	1.2
Mount Edgecombe	February	28.05	20.70	0.0
Pofadder	January	34.08	17.71	0.2
Port Nolloth	February	20.71	13.44	2.4
Pretoria	February	28.84	16.60	0.2
Punda Maria	December	32.30	20.96	1.6
Queenstown	January	28.91	15.05	0.8
Richards bay	February	29.23	21.81	0.2
Skukuza	February	32.57	20.80	0.7
Twee Rivieren	January	36.58	20.10	0.4
Vanwyksvlei	January	35.32	18.18	0.2
Vryburg	December	31.94	15.75	0.7
Wepener	January	30.28	15.48	0.2
Willowmore	January	30.22	14.94	0.8

Cape Agulhas and Mount Edgecombe were the only stations where no heat wave was recorded during the study period. Both regions are located in the coasts and weather and climate of these regions is highly influenced by adjacent oceans. Atmospheric temperatures of these regions hardly experienced hot weather conditions for prolonged periods as the adjacent oceans act as cooling factor. Monthly mean minimum temperatures of both Cape Agulhas and Mount Edgecombe are >10°C (Figure 4.3b) during their coldest months (June-July).

4.4.2 Heat wave duration

Section 4.4 has shown that heat waves that occurred in South Africa between 1983 and 2012 may last from three days up to a record of 11 days as recorded by Marico during the strong El Niño season of 1982/1983. Average heat wave duration during the study period

also vary in different regions across the country (Figure 4.12). Heat waves in most of the northeast lowveld (cluster C), high lying interior and equator-ward regions (northern parts of Cluster D, and cluster E and F) of the country experience an average duration greater than 4.5 days during the study period. Most stations in these regions are characterized by high maximum temperatures (>32°C) during the austral summer. Wepener in cluster E recorded the highest average heat wave duration of 6 days.

Subtropical eastern parts, eastern and southeast coastal regions experience an average duration between 3 and 4.3 days, with the Mediterranean climate region of South Africa experiencing the lowest average duration of that region. Cape Agulhas in cluster A and Mount Edgecombe in cluster B did not record heat wave events between 1983 and 2012; hence the average heat wave duration in these regions is below the minimum duration (3 days) of a heat wave event.

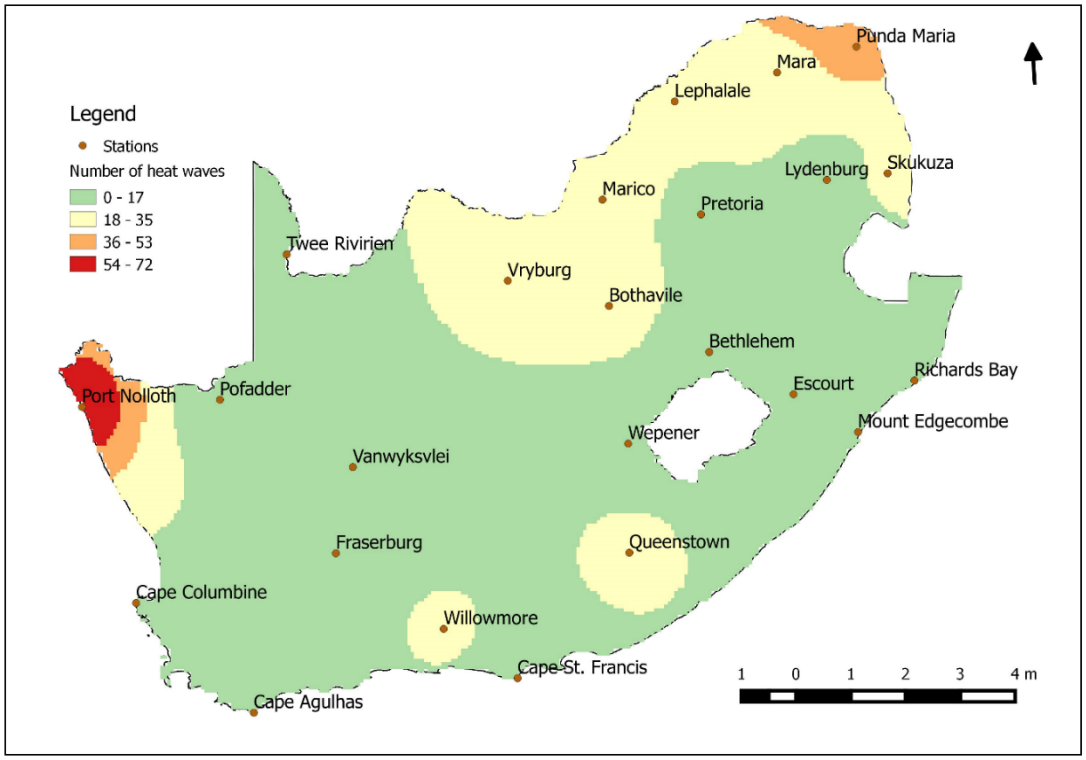

Figure 4.6: Annual spatial variability of heat waves (shaded) over South Africa from 1983 to 2012.

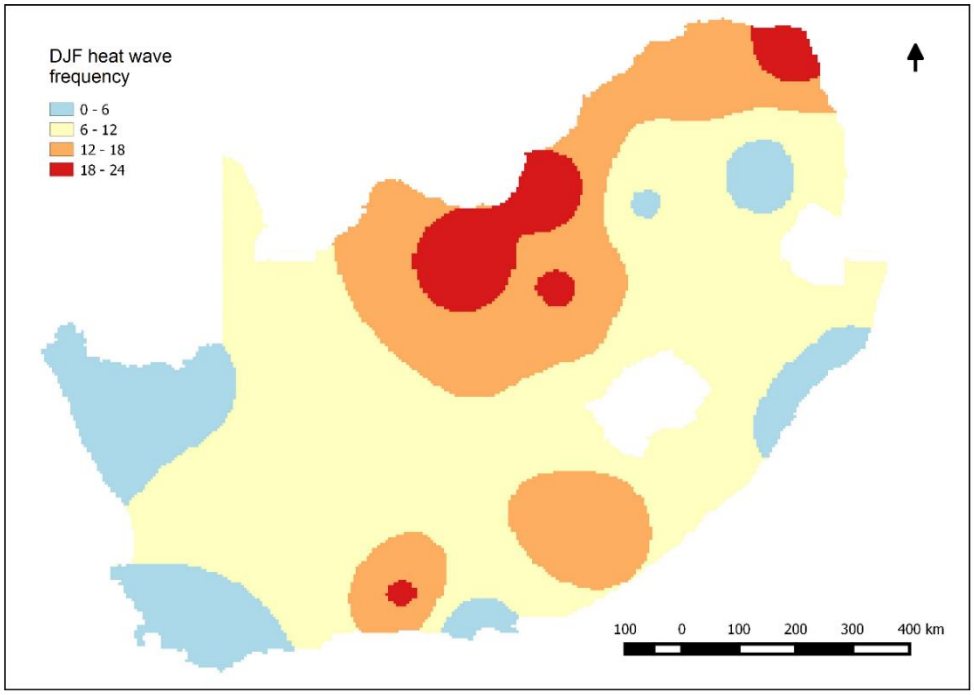

Figure 4.7: DJF heat wave frequency (shaded) over South Africa from 1983 to 2012.

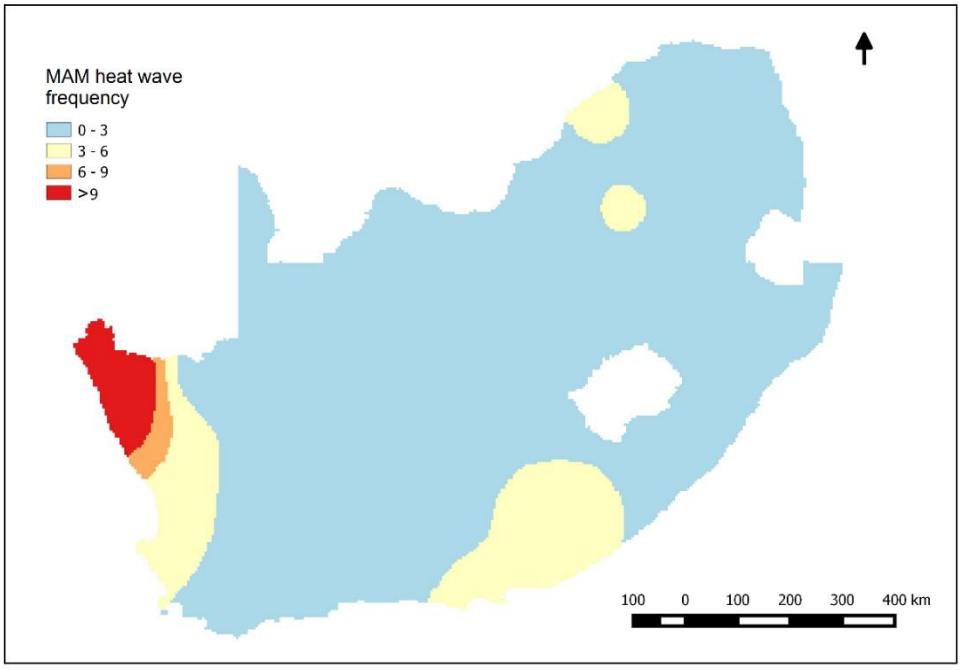

Figure 4.8: MAM heat wave frequency (shaded) over South Africa from 1983 to 2012.

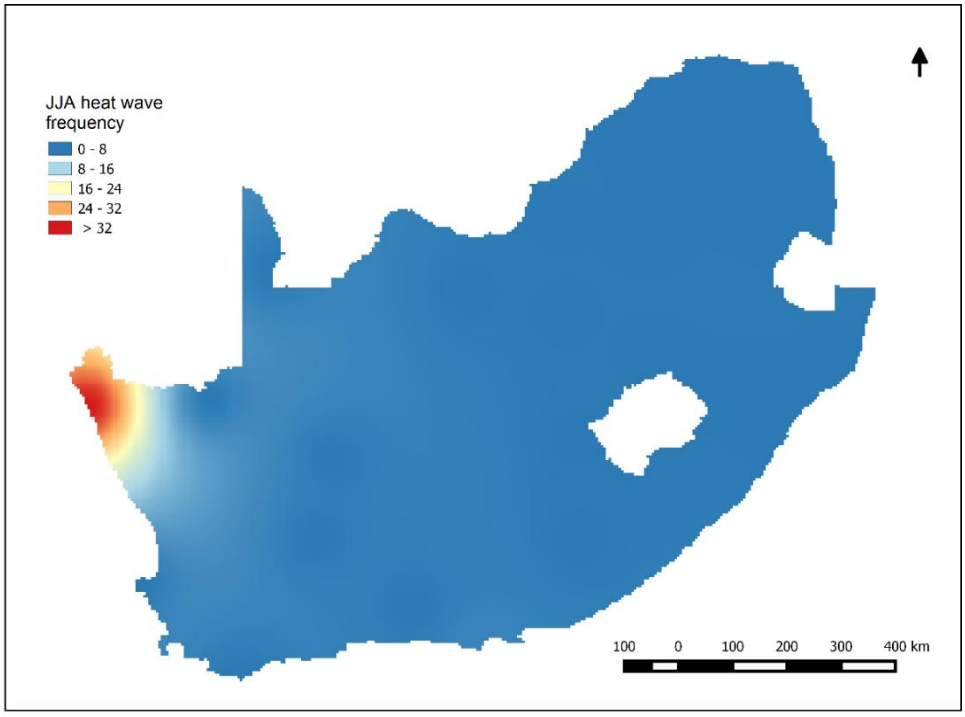

Figure 4.9: JJA heat wave frequency (shaded) over South Africa from 1983 to 2012.

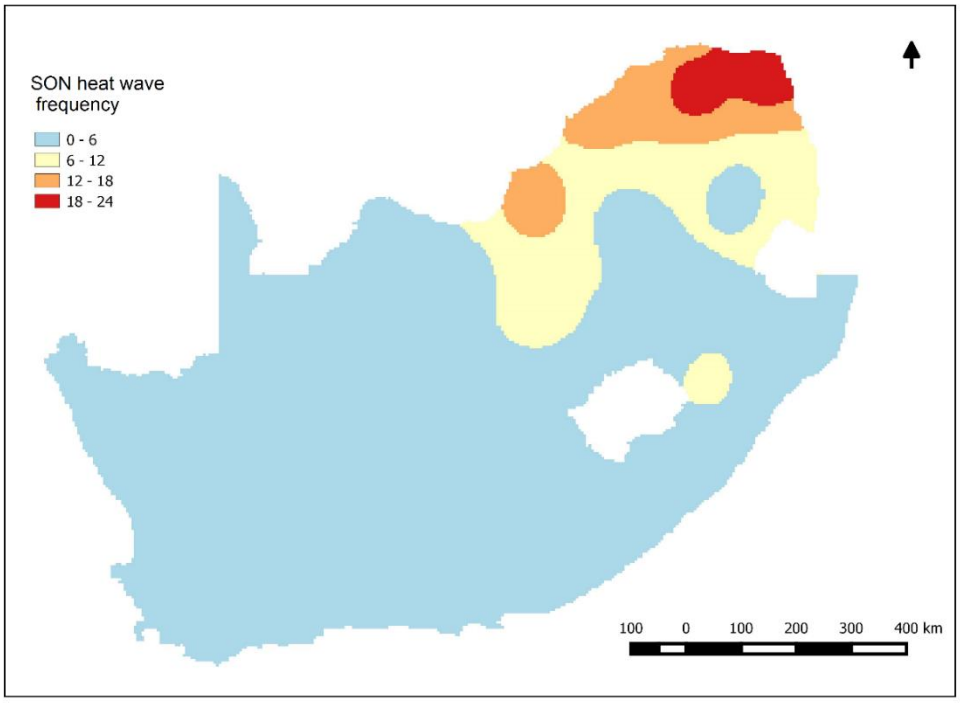

Figure 4.10: SON heat wave frequency (shaded) over South Africa from 1983 to 2012.

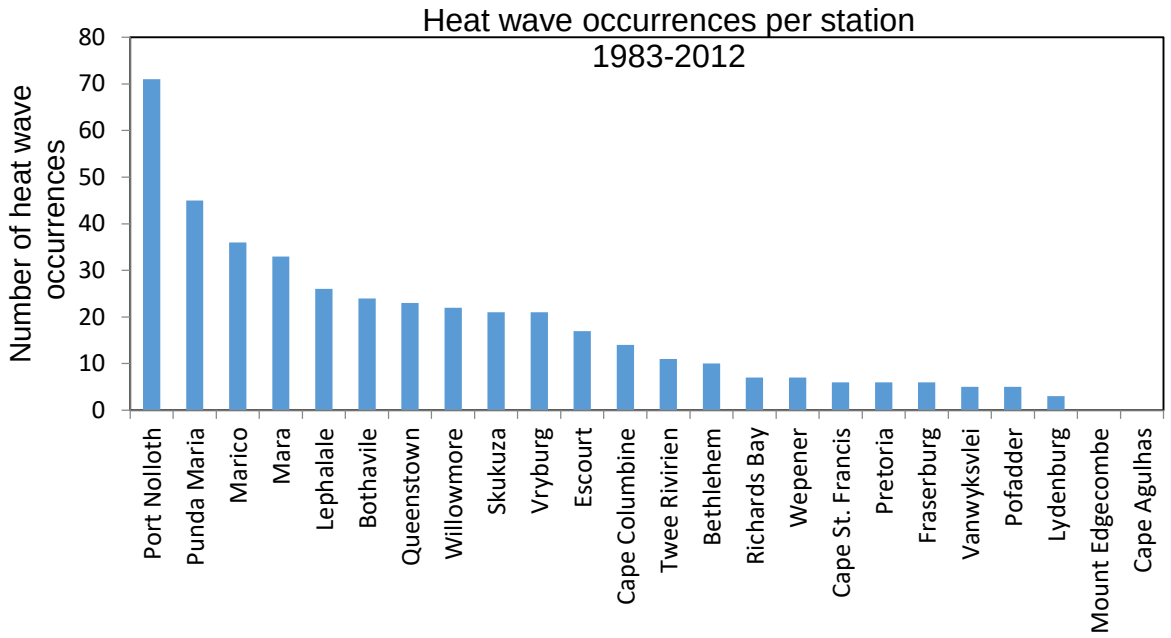

Figure 4.11: Number of heat wave occurrences from each selected climate station over South Africa from 1983 to 2012.

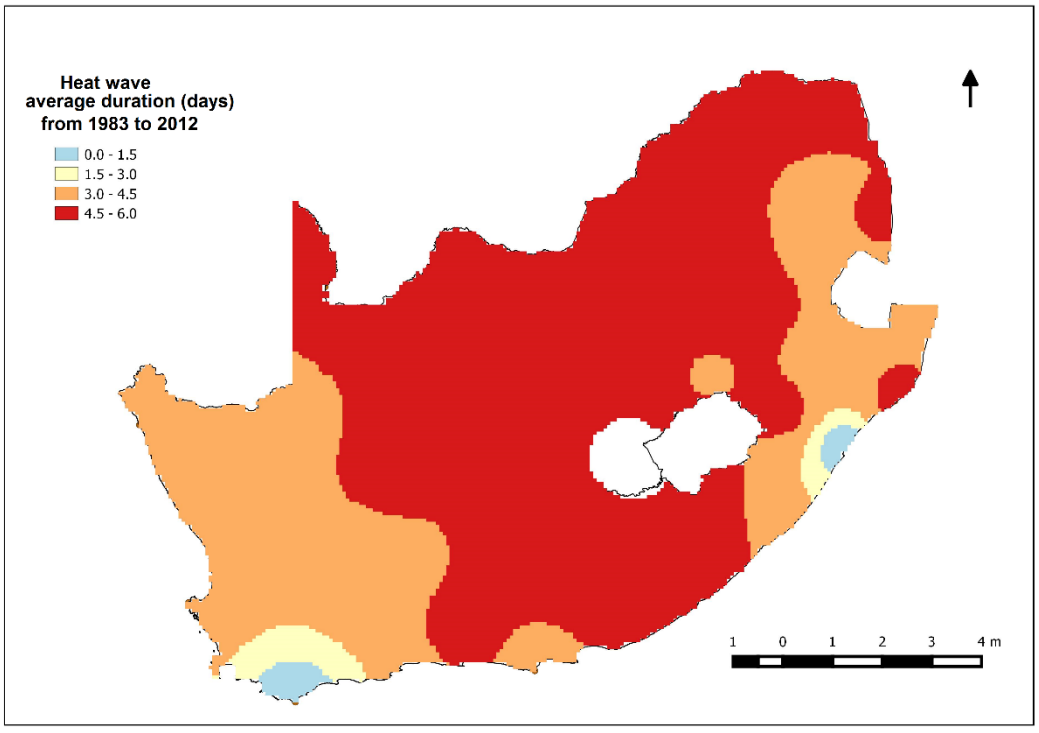

Figure 4.12: Interpolated heat wave average duration over South Africa from 1983 to 2012. Duration less 3 days should be ignored (an artefact from interpolation process).

4.5 Heat waves and ENSO

Temperature over South Africa is also influenced by El Niño-Southern Oscillation (ENSO) events. The cluster C region is affected the most by the El Niño. This region experiences high maximum temperatures during warm ENSO events, as shown by a negative October to March correlation between maximum temperature and SOI (Figure 4.13). Except for the north-east lowveld, there is a fairly weak maximum temperature and Southern Oscillation Index (SOI) correlation in much of the country during the austral summer. Niño 3.4 sea surface temperature (SST) correlation with maximum temperature shows a strong positive correlative over cluster C and fairly weak correlation in other parts of the country (Figure 4.14.

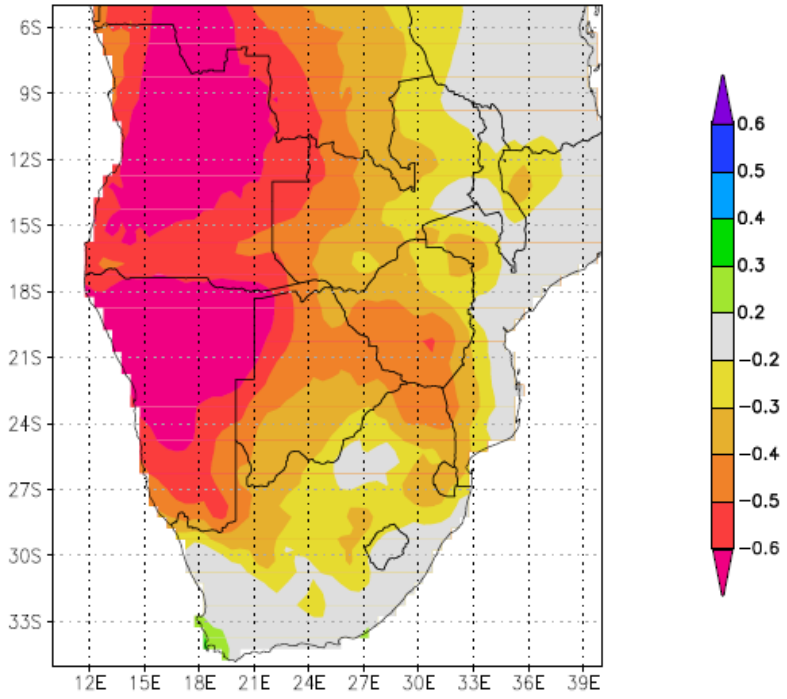

Figure 4.13: Austral summer correlation of Southern Oscillation Index and maximum temperature from 1983-2012, p<10%.

The 1991/1992 summer season recorded most heat waves over much of the country in the study period. Stations in the northern parts of South Africa such as Punda Maria and Mara recorded their longer lasting heat waves during this moderate El Niño season (Table 3.6). Most of South Africa's longest lasting heat waves per station (Table 4.4) are observed during the negative phase of SOI. The longest lasting heat waves in Marico (11 days) and Escourt (5 days) both occurred during the one strongest El Niño seasons (1982/1983) of the study period. While other heat waves were observed during weak and moderate El Niño events, stations in the northern interior of the country such as Pretoria and Lydenburg experienced their longest lasting heat waves during the 2011/2012 weak La Niña season.

Table 4.4: Longest lasting heat waves per station (* indicate stations that recoreded the longest lasting heat waves per thermal region).

Thermal region (Cluster)	Cluster stations	Longest lasting heat wave				
		Date from (dd/mm/yy)	Date to (dd/mm/yy)	Number of days	Average T_X (°C)	Average T_N (°C)
A	Cape Agulhas	–	–	–	–	–
	Cape Columbine	15/1/2000	19/1/2000	5	31.1	15.9
	Port Nolloth*	4/6/2000	9/6/2000	6	32.2	15.6
B	Cape St. Francis	15/5/1991	19/5/1991	5	31.7	15.4
	Richards bay*	6/2/2010	12/2/2010	7	35.8	23.9
	Mount Edgecombe	–	–	–	–	–
C	Skukuza	18/10/2010	25/10/2010	8	42	27.1
	Punda Maria*	23/2/1992	2/3/1992	9	40.2	25.5
D	Fraserburg	3/1/1993	7/1/1993	5	38.5	19.8
	Pofadder	3/1/1993	7/1/1993	5	41.4	24.3
	Twee Rivieren*	4/1/2012	11/1/2012	8	42.3	21.3
	Vanwyksvlei	6/2/1998	10/2/1998	5	42.1	22.2
E	Bethlehem	17/12/1994	22/12/1994	6	32.4	12.9
	Willowmore	21/1/2007	27/1/2007	7	36.4	18.8
	Queenstown*	3/2/1992	12/2/1992	10	36.2	17.8
	Wepener	28/1/1987	4/2/1987	8	36	18.8
	Escourt	27/9/1983	1/10/1983	5	35.1	12.7
F	Bothaville	30/11/2009	6/12/2009	7	38.2	17.6
	Lydenburg	23/10/2011	25/10/2011	3	32.9	15.0
	Mara	30/11/1992	6/12/1992	7	36.8	17.0
	Marico*	17/2/1983	27/2/1983	11	37.8	18.5
	Pretoria	9/11/2011	13/11/2011	5	34.5	15.7
	Vryburg	8/12/1997	16/12/1997	9	38.1	18.7
	Lephalale	30/1/2003	8/2/2003	10	39.5	24.3

Northern parts of South Africa are experiencing most heat waves in one season. Lephalale experienced most heat wave occurrences, up to 8 during the 2002/2003 moderate El Niño season with an average duration of 4.6 days were observed. Punda Maria experienced second most number of heat waves (6) during the weak El Niño of 2006/2007 with an average duration of 3.3 days. While heat waves usually jointly occur with droughts, heat wave events are more localized but droughts tends to be widespread, such was observed

during ENSO induced dryness of 1982/1983, 1991/1992, 2002/2003 and 2006/2007 seasons (Figure 4.15).

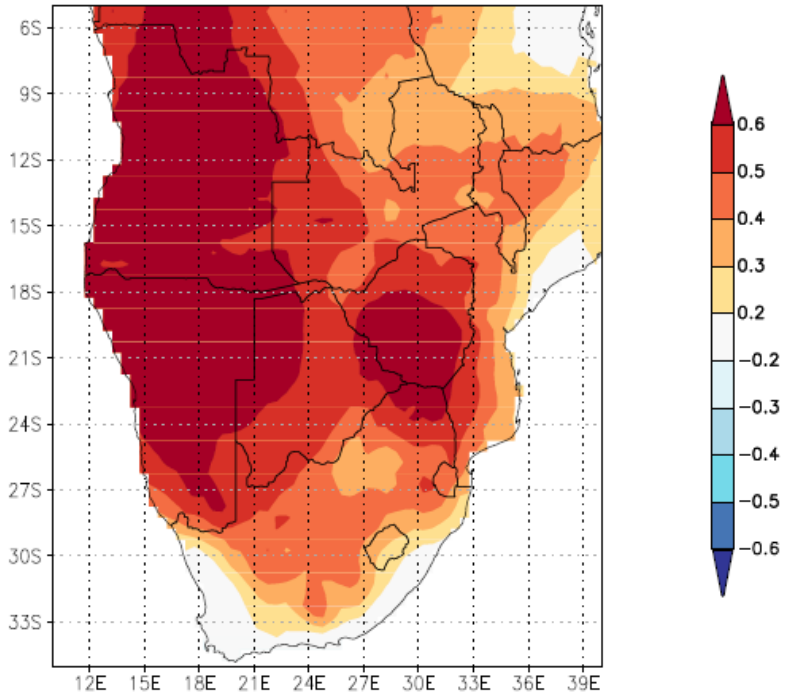

Figure 4.14: Austral summer correlation of Niño 3.4 sea surface temperature and maximum temperature from 1983-2012, p<10%.

Least number of heat waves in South Africa is usually observed during non-ENSO and cool ENSO seasons. Punda Maria recorded only 2 heat waves, one 4-day (7-10 October 1988) lasting heat wave and the other lasting for 3 days (23-25 December 1988) during the 1988/1989 strong La Niña season. The 1993/1994 and 2005/2006 non-ENSO seasons also experienced 2 heat waves respectively in regions such as Punda Maria and Port Nolloth. The only season where one heat wave occurred in a season was during the 1996/1997 non-ENSO over Richards, Lephalale and Port Nolloth. Another heat wave that occurred during a non-ENSO season of 1992/1993 was widespread over Northern Cape and was the longest lasting heat wave at Pofadder and Fraserburg.

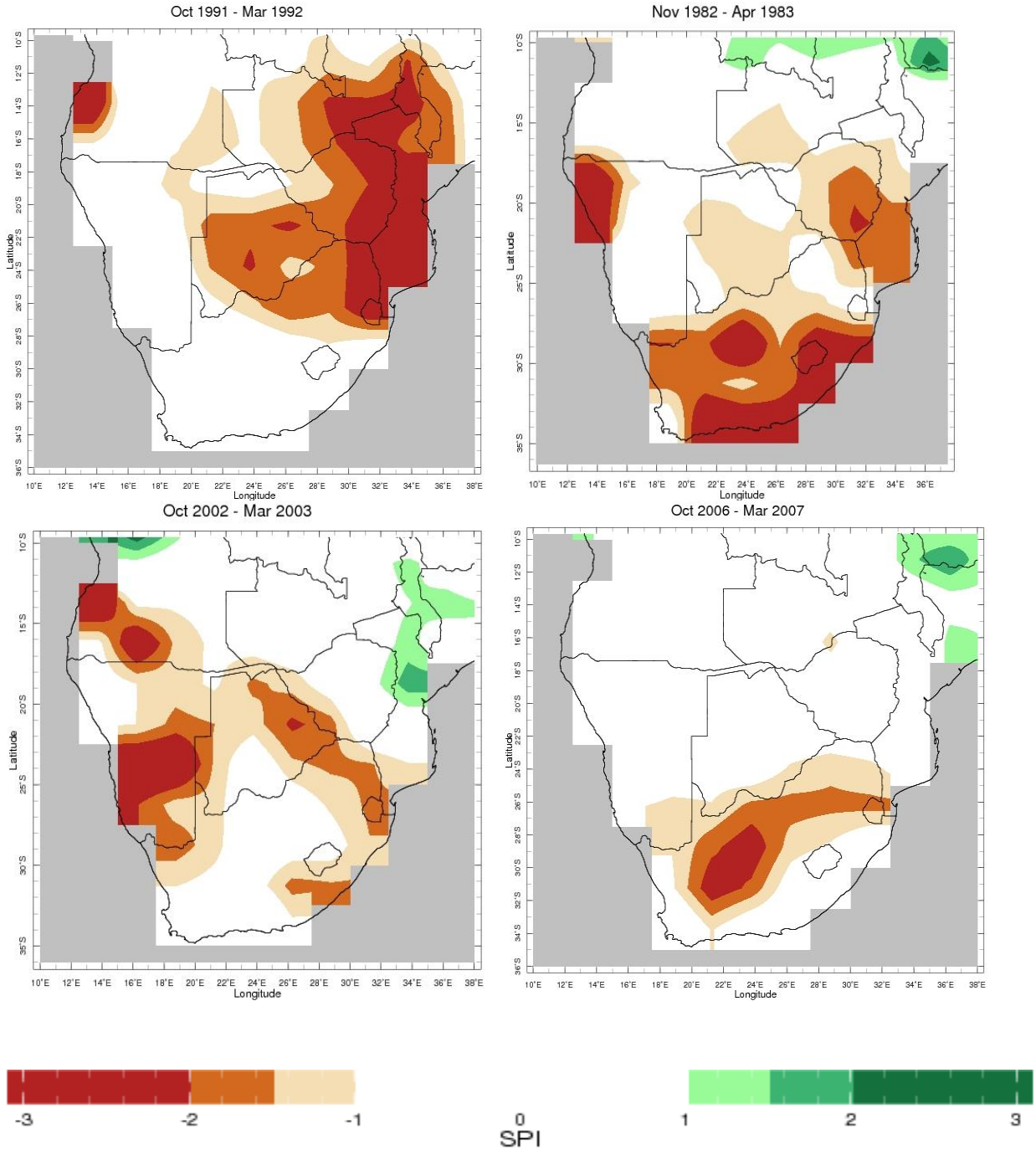

Figure 4.15: Standardized Precipitation Index of positive phase of ENSO seasons (1991/1992, 1982/1983, 2002/2003).

4.6 Summary

Recent temperature trends over South Africa have been investigated. Monthly maximum and minimum temperatures follow the same pattern in most station, however the temperature trends differs spatially. It was observed that there are no major seasonal temperature changes over coastal regions, while inland areas are hotter in summer but relatively cool or cold in winter, particularly in the plateau. Both annual maximum and minimum temperature in most regions indicate that the country is becoming warmer over time. The north-east lowveld

is the inland region which is warmer throughout the year, while Richards is the coastal region which is the warmest all year-round.

Out of the 24 selected stations, 21 shows a general increasing trends of both maximum and minimum temperatures, while only 3 stations in the central interior not depicting significant changes during the study period. The country is also characterized by changes in daily extreme temperatures. Cold night and cool days over South Africa between 1983 and 2012 have general negative trends while warm and hot days experience the opposite trends. It is believed that the daily extreme temperatures play a certain role in the trends of heat weave frequency. All selected stations indicate that DJF is the hottest period across the entire country, and it is also the period where most heat waves were observed. Larger differences between maximum and minimum temperatures are observed in winter in where heat wave occurrences are less frequent in most parts of the country. From the analysis, the following has been noted about heat waves characteristics over South Africa:

a) Heat waves are unusual events in the present climate (1983-2012) over much of South Africa, with 20 of the selected 24 stations experiencing less than one heat wave per season. Only Mara, Marico, Punda Maria (All three in the eastern half of the country) and Port Nolloth in the subtropical western coast experienced more than one heat wave per season.
b) Most parts of South Africa experience heat waves in austral summer, with an exception of the subtropical western coast. Regions such as Port Nolloth along the western coast experiences most of its heat wave events in winter.
c) Heat wave frequency is relatively higher in inland regions than in coastal regions. Coastal regions such as Cape Agulhas and Mount Edgecombe did not record a heat wave during the 30-year study period.
d) Eastern Half of South Africa experiences more heat waves than the western half in austral summer.
e) DTR is usually stronger in winter when heat waves are less frequent in most parts of the country
f) Heat wave occurrences are affected by ENSO events, with the northern and north-east parts of the country being most influenced. High frequency and longer duration heat waves is observed during El Niño seasons.
g) While heat waves and ENSO induced droughts usually co-occur, heat waves are more localized while droughts are more widespread.
h) Heat waves can last up to 11 days over inland regions, while a maximum duration of 7 days in coastal regions was recorded at Richards Bay from 6-12 February 2010.

i) Heat waves last longer in the central interior and north-west lowveld with a seasonal average duration ranging from 4.5 to 6 days.

The next chapter provides atmospheric conditions which are conducive for heat wave occurrence over South Africa. It also discusses circulation patterns associated with heat waves in different parts of the country.

CHAPTER 5

METEOROLOGICAL STRUCTURE OF HEAT WAVES OVER SOUTH AFRICA

5.1 Introduction

The nature and trends of extreme weather events are likely to change due to anthropogenic contributions to climate change (Meehl *et al*. 2000). Global increase of mean temperature increases the probability of extreme warm days (Mahlman 1997; Griffiths 2005). The precedent chapter provided temperature trends and heat wave spatio-temporal variability over South Africa and also indicated changes in the heat wave frequency in response to El Niño-Southern Oscillation (ENSO) cycles. This chapter seeks to understand how mean temperature trends links to the trends of heat wave frequency and duration in different parts of the country.

Geopotential height at 500 hPa is used to determine pressure systems associated with heat wave occurrences as they are extensively been linked to persistent anticyclonic circulations (e.g. Palutikof *et al.* 1996; Palecki *et al*. 2001; Galarnean *et al*. 2012). Coastal low pressure systems are associated with hot and dry conditions (Ramuligho 2012), and may also provide conducive conditions for heat waves. The identified events are divided into warm ENSO, cool ENSO and non-ENSO seasons. Mapped relative humidity (RH), outgoing longwave radiation (OLR), soil moisture and wind vector anomalies during the identified heat waves are discussed in the subsequent sections. Longest lasting heat wave per thermal region were selected as different case studies.

The aim of this chapter is to identify systems that trigger conducive conditions for heat wave occurrences and details the meteorological structure and circulation patterns of the identified longest lasting heat waves over each thermal region of South Africa. Heat waves have negative impacts on livelihoods but have not received rigorous attention in the whole southern Africa. South Africa has good temperature station network (MacKellar *et al*. 2014) that can assist in determining how heat waves vary spatially.

5.2 Heat waves over the interior

Heat wave occurrences are dominant in austral summer in most parts of South Africa, particularly between December and February where most climate stations record their hottest maximum temperatures. Composite analyses of circulation patterns during DJF heat waves in South Africa from 1983 to 2012 were performed to provide a general structure of

heat waves during this season over the interior of South Africa. The composite analysis also indicate that the surface is usually drier during heat waves (Figure 5.4).

Heat wave occurrences are mainly due to a persistent presence of a middle level (500 hPa) high pressure system indicated by geopotential height which dwells and stagnates over the interior (Figure 5.1a) of South Africa for few days up to weeks. The high-pressure system results in subsidence of air which warms as it sinks towards the surface. The high also induces anticyclonic circulations in the middle levels which weakens with decreasing height (Figure 5.2b) as a result of friction. DJF heat waves in the interior are also associated dry conditions and less cloud cover indicated by positive 200 hPa outgoing longwave radiation (OLR) anomalies over the eastern half of the country (Figure 5.3). The eastern half experiences negative relative humidity (RH) anomalies.

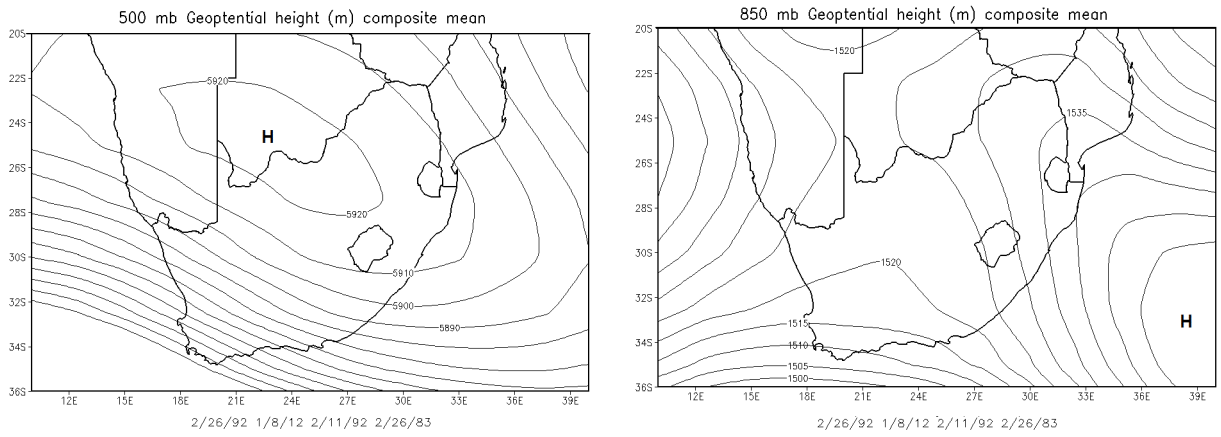

a) b)

Figure 5.1: Composite of geopotential height (m) at a) 500 hPa and b) 850 hPa during longest lasting DJF heat waves per thermal region in the interior of South Africa from 1983 to 2012.

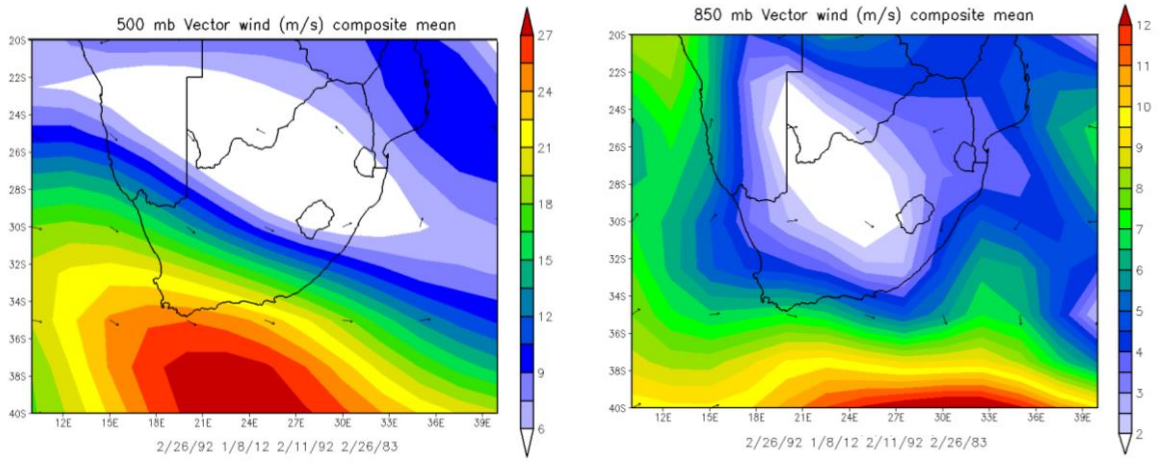

a) b)

Figure 5.2: Composite of wind vector (m/s) at a) 500 hPa and b) 850 hPa during longest lasting DJF heat waves per thermal region in the interior of South Africa from 1983 to 2012.

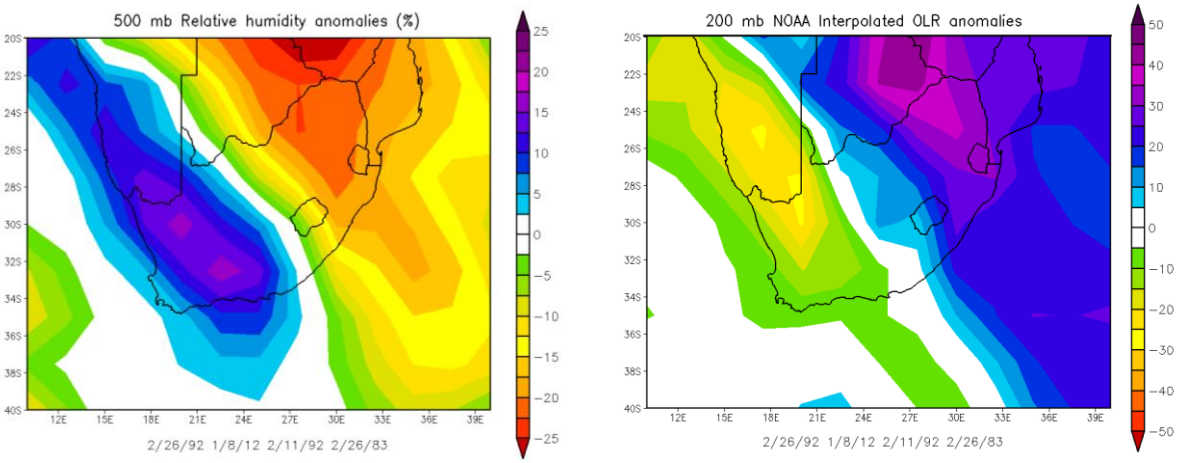

a) b)

Figure 5.3: Composite of RH anomaly (%) at a) 500 hPa and b) OLR anomaly (W/m^2) at 200 hPa during longest lasting DJF heat waves per thermal region in the interior of South Africa from 1983 to 2012.

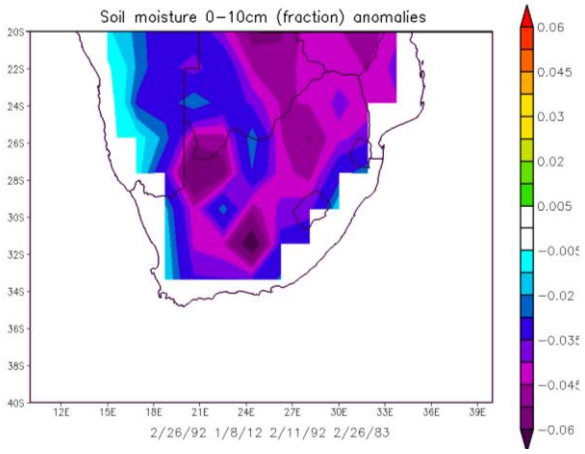

Figure 5.4: Composite of soil moisture anomaly during longest lasting DJF heat waves per thermal region in the interior of South Africa from 1983 to 2012.

5.3 Heat wave composites per thermal region (Clusters)

5.3.1 Cluster A

Case 1: 4-9 June 2000

South Africa is known to be hotter during the austral summer where warm extreme weather events are expected. Other parts such as the western subtropical coastal region also experience hot weather and heat waves during the austral winter. Port Nolloth recorded the longest lasting winter heat wave over the western subtropical coastal region which lasted from 4 to 9 June, 2000. There was a significant average daily maximum temperature gradient over the country (Figure 5.5) during this period.

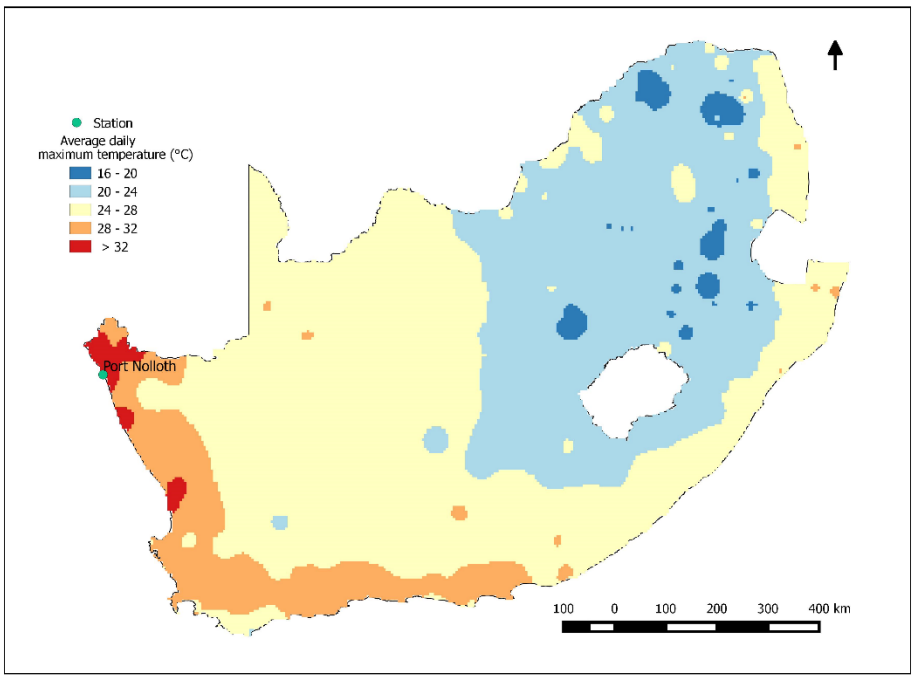

Figure 5.5: Average daily maximum temperature (°C) over South Africa between 4 June 2000 and 9 June 2000. The labelled region experienced a heat wave.

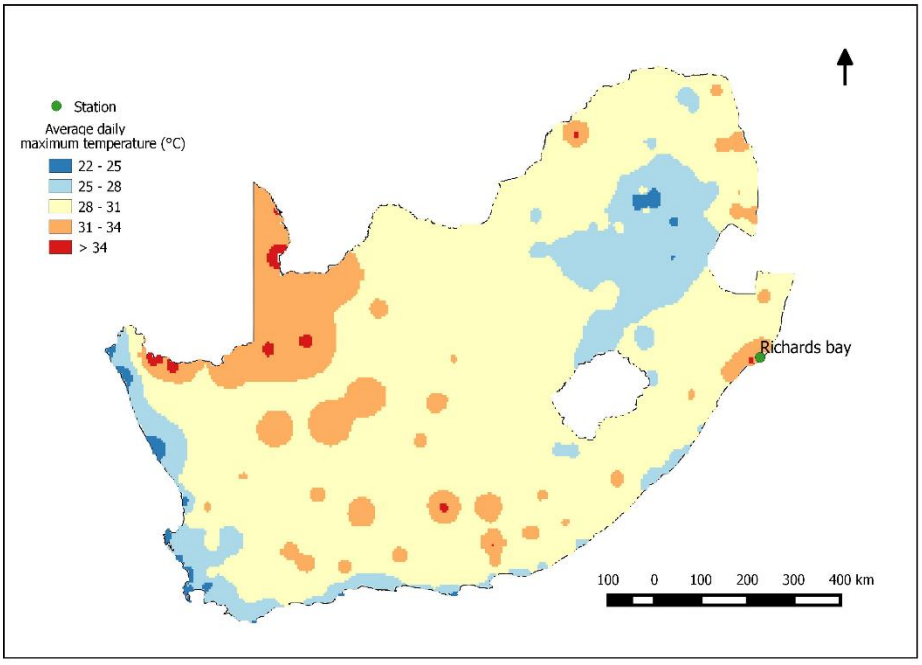

Figure 5.6: Average daily maximum temperature (°C) over South Africa between 6 February 2010 and 12 February 2010. The labelled region experienced a heat wave.

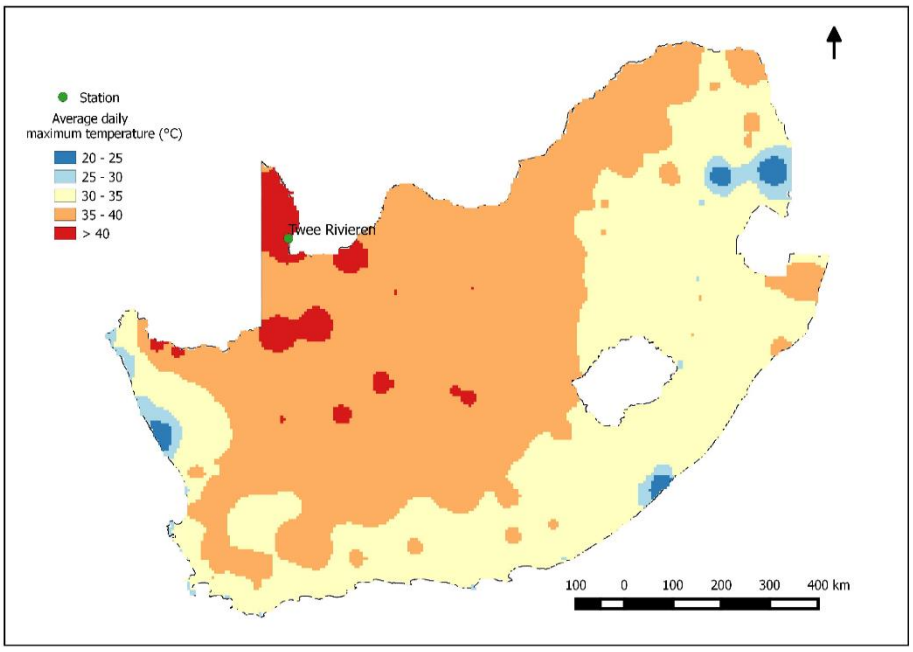

Figure 5.7: Average daily maximum temperature (°C) over South Africa between 4 January 2012 and 11 January 2012. The labelled region experienced a heat wave.

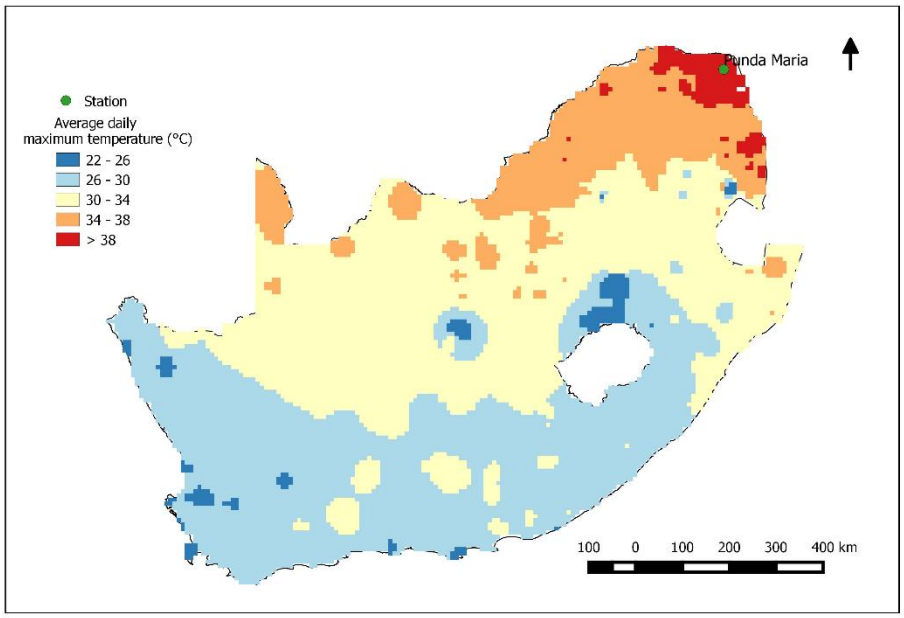

Figure 5.8: Average daily maximum temperature (°C) over South Africa between 23 February 1992 and 2 March 1992. The labelled region experienced a heat wave.

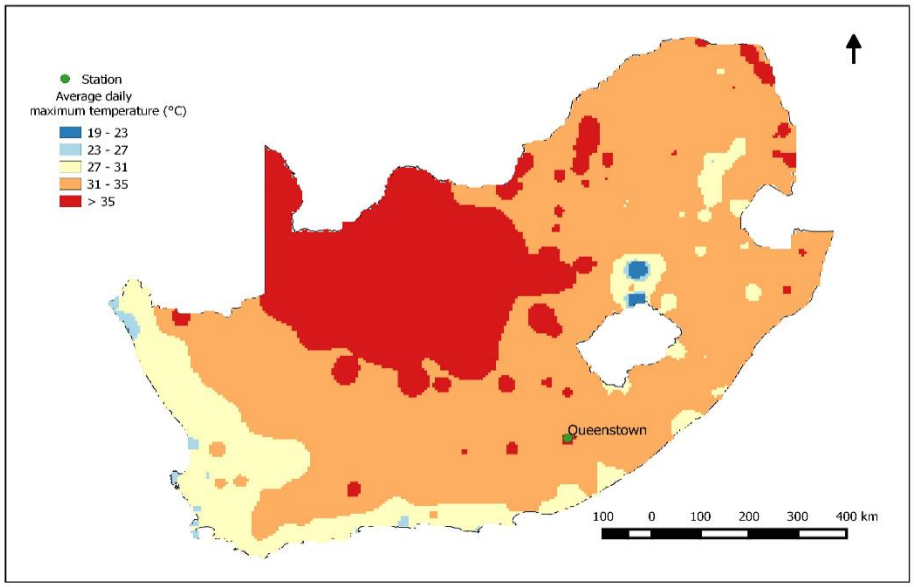

Figure 5.9: Average daily maximum temperature (°C) over South Africa between 3 February 1992 and 12 February 1992. The labelled region experienced a heat wave.

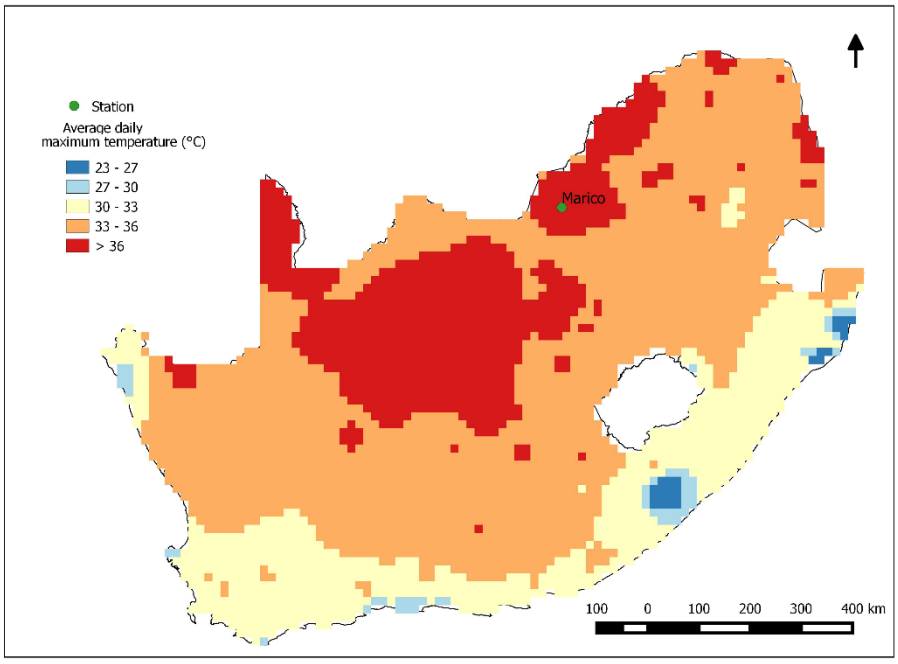

Figure 5.10: Average daily maximum temperature(°C) over South Africa between 17 February 1983 and 27 February 1983. The labelled region experienced a heat wave

Average daily maximum temperatures greater than 28°C were observed over the southern and western coastal regions and the high temperature over these regions were associated with a middle level high pressure system (Figure 5.11) which induced subsidence. The subtropical western interior also experienced warmer conditions (24-28°C) relative to the

eastern elevated regions where average daily maximum temperature was ≤24°C. The inland region in the eastern half of South Africa which experienced warmer temperature during this period was the north-east lowveld, and it is the warmest region over the eastern part of the country in winter.

a) b)

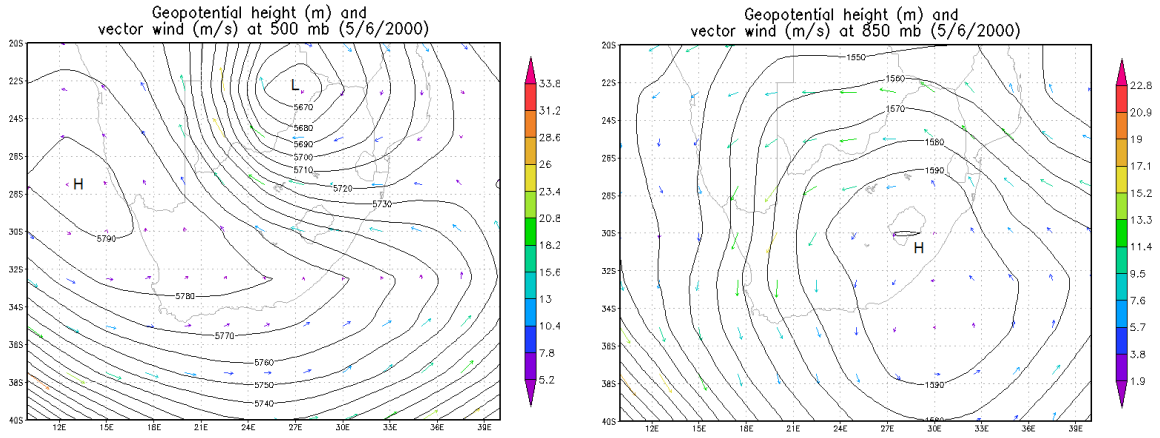

Figure 5.11: Geopotential height (m) and vector winds (m/s) at 500 hPa (a) and at 850 hPa (b) over South Africa during the 6-day lasting heat wave (4 June 2000 to 9 June 2000) over Port Nolloth. Colour bar indicates wind strength in m/s.

a) b)

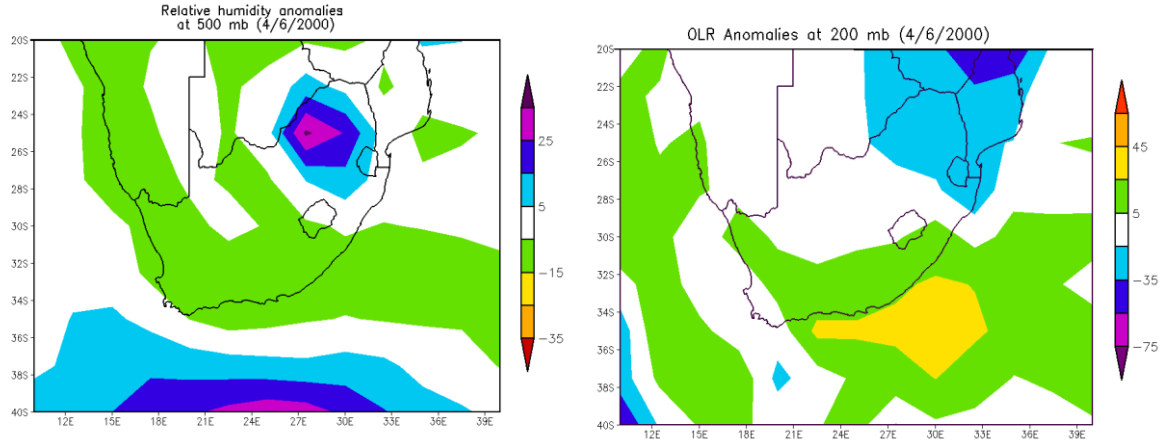

Figure 5.12: Anomalies of RH (%) at 500 hPa (a) and OLR (W/m^2) at 200 hPa (b) during the 6-day lasting heat wave in Port Nolloth from 4 June 2000 to 9 June 2000 over South Africa.

Northern parts of South Africa in areas of cluster F experienced cool conditions and an a middle level low pressure system between 4 and 9 June 2000 (Figure 5.11) which was associated with positive 500 hPa RH anomalies (Figure 5.8). During that period, a middle

level high pressure system over the subtropical west coastal region of the country was observed and associated with anticyclonic circulations and the heat wave occurrence over Port Nolloth. RH anomalies were negative over Port Nolloth during this heat wave.

The presence of the persistent middle level (500 hPa) anticyclonic circulation over much of cluster D stagnated and dwelled for the entire duration of the heat wave. There was also subsidence at the center of the 500 hPa high pressure system and 850 hPa offshore winds (Figure 5.11) over the subtropical western coast that induced berg winds and led to hot weather for extended periods over the region. Winds at 500 hPa over the region were weak hence the heat was not distributed and resulted in the 6-day lasting heat wave over Port Nolloth with average daily maximum temperature of 32.2°C.

During this period a strongly positive upper levels (200 hPa) OLR anomalies were recorded over the southern coast of South Africa and around Port Nolloth (Figure 5.12), while negative OLR anomalies were observed over the eastern parts of the country. This indicates that the subtropical western regions experienced sunny conditions, while east and northern parts of South Africa experienced cloudy conditions. OLR anomalies were decreasing from north to west of the country proving to be consistent with 500 hPa Geopotential height.

5.3.2 Cluster B

Case 2: 6-12February 2010

Temperatures were warm to hot during the heat wave at Richards Bay that lasted for 7 days (6–12 February 2010) with a daily average maximum temperature of 35.8°C (Figure 5.6). However, much of the interior of South Africa was relatively cool during this period with average maximum temperatures ranging from 28 - 31°C. An anticyclonic circulation was observed in the middle levels (500hPa) centered over the east coast of South Africa.

Most heat waves in South Africa are associated with dry conditions; however that is not always the case with heat waves over cluster B. During the 7-day lasting heat wave over Richards Bay that started from 6-12 February 2010, moist, sunny and hot conditions were experienced (Figure 5.14). This is because the anticyclonic circulations at 850 and 500 hPa (Figure 5.13) during the duration of this heat wave transported warm moist air above the Indian Ocean towards the south-east coastal region of the country. Positive 500 hPa RH anomalies at the middle levels were observed during this period over the south-east coast extending to the interior and subtropical western parts of the country. However, the northern part was relatively drier during this period.

a) b)

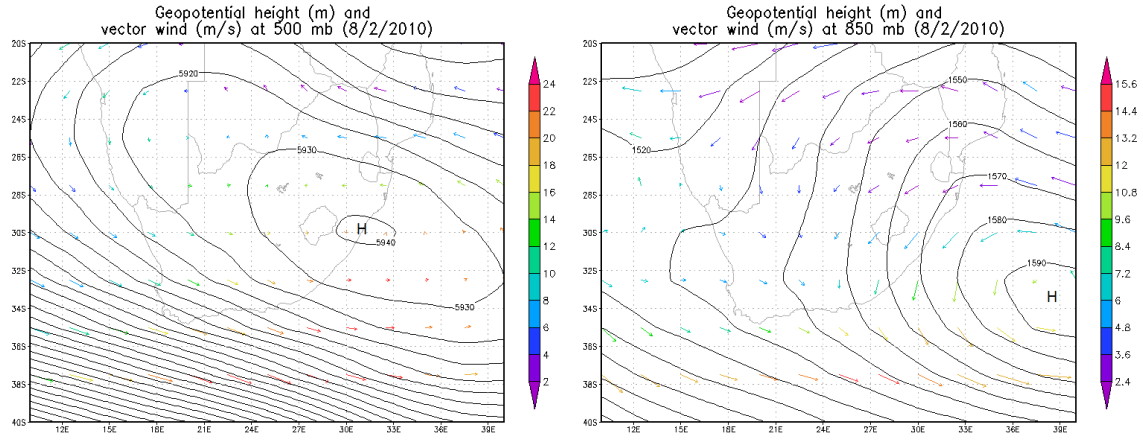

Figure 5.13: Geopotential height (m) and vector winds (m/s) at 500 hPa (a) and at 850 hPa (b) over South Africa during the 7-day lasting heat wave (6 February 2010 to 12 February 2010) over Richards Bay. Colour bar indicates wind strength in m/s.

b) b)

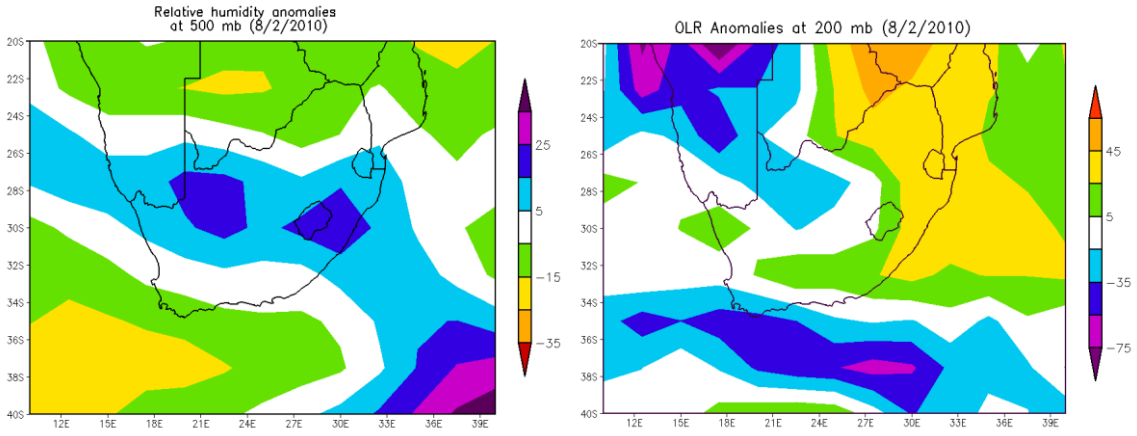

Figure 5.14: Anomalies of RH (%) at 500 hPa (a) and OLR (W/m^2) at 200 hPa (b) over South Africa during the 7-day lasting heat wave in Richards Bay from 4 June 2000 to 9 June 2000.

The entire south-east coastal area to the eastern interior of the country experienced positive OLR anomalies at 200 hPa between 6 and 12 February 2010. This suggests that sunny conditions were experienced during this period over the eastern part of South Africa when the longest lasting heat wave over cluster B was recorded at Richards Bay. The 200 hPa OLR anomalies were strongly positive on the 8th of February, 2010. The east-west decrease of OLR at 200 hPa indicates it was cloudy over the western parts of the country during this period.

5.3.3 Cluster C

Case 3: 23 February-2 March 1992

a) b)

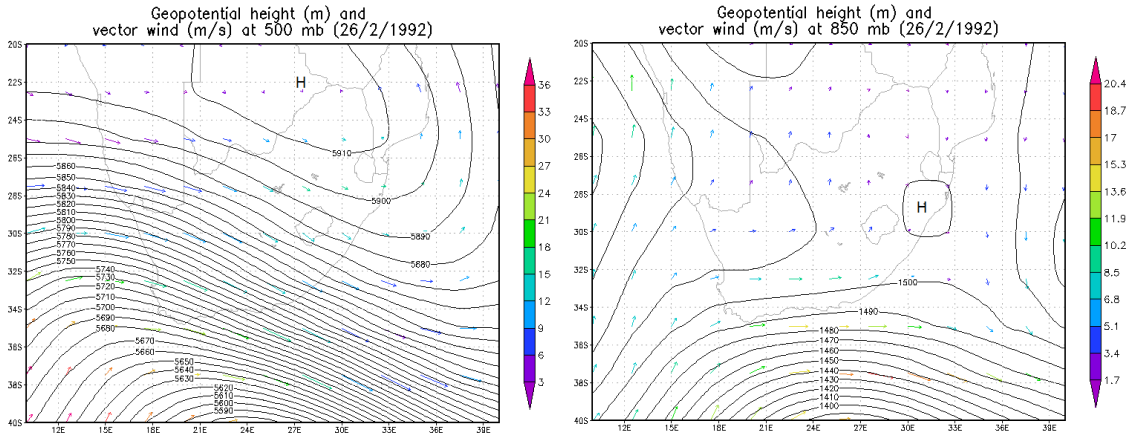

Figure 5.15: Geopotential height (m) and vector winds (m/s) at 500 hPa (a) and at 850 hPa (b) over South Africa during the 9-day lasting heat wave (23 February 1992 to 2 March 1992) over Punda Maria. Colour bar indicates wind strength in m/s.

a) b)

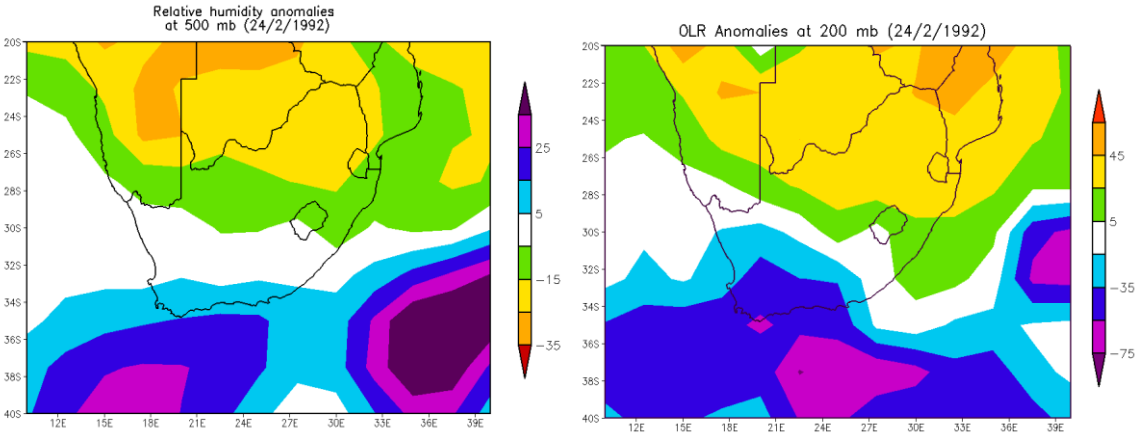

Figure 5.16: Anomalies of 500 hPa RH (%) (a) and 200 hPa OLR anomalies (W/m^2) over South Africa during 9-day lasting heat wave in Punda Maria from 23 February 1993 to 2 March 1992.

The northeast lowveld thermal region experiences high temperature all year (Figure 4.1) and has the third most lasting heat wave over the 30-year period (Table 4.2). The longest lasting heat wave over this thermal region was recorded by Punda Maria (Figure 5.3) occurred in February during the austral summer season of 1991/1992 and lasted for 9 days (23rd of February to the 2nd of March). A continental high pressure system was retreating more south-ward during this period (Figure 5.15), associated with subsidence and triggered the occurrence of the heat wave over Punda Maria, Limpopo. Continental warm and dry winds near the surface were southward towards the Limpopo province and led to extremely high atmospheric temperatures for 9 consecutive days over the region with an average of 40.2°C and 25.5°C maximum and minimum temperature respectively.

Negative RH anomaly between -20% and -15% were observed over the northeast lowveld of the country (Figure 5.16a) but increasing as you move pole-ward with the southern coasts experiencing RH which is above normal conditions.

5.3.4 Cluster D

Case 4: 4-11 January 2012

a) b)

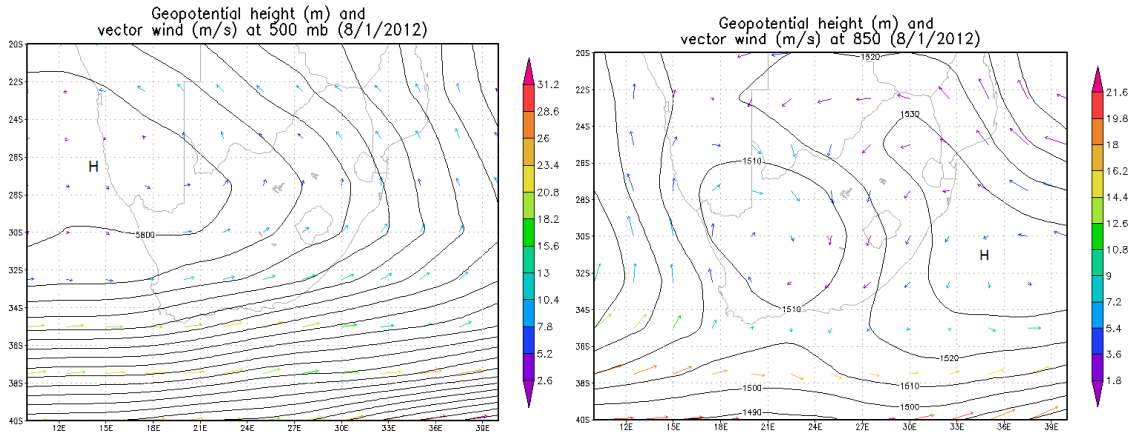

Figure 5.17: Geopotential height (m) and vector winds (m/s) at 500 hPa (a) and at 850 hPa (b) over South Africa during the 8-day lasting heat wave (4 January 2012 to 11 January 2012) over Twee Rivieren. Colour bar indicates wind strength in m/s.

a) b)

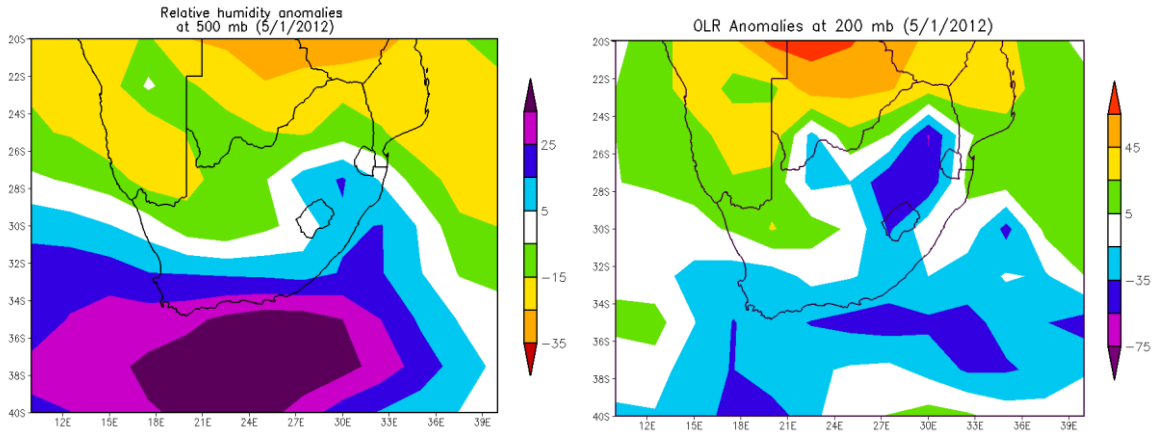

Figure 5.18: Anomalies of RH (%) at 500 hPa (a) and 200 hPa OLR anomalies (W/m^2) (b) over South Africa during the 8-day lasting heat wave in Twee Rivieren from 4 January 2012 to 11 January 2012.

Longest lasting heat wave in cluster D was recorded by Twee Rivieren (Figure 5.8) during the weal La Niña season of 2011/12. This heat wave lasted for 8 days (4-12 January, 2012) with a daily average maximum temperature of 42.3°C. The entire thermal region experienced hot conditions during this period with daily average maximum temperature between 35 and 40°C.

The heat wave was also triggered by the subsidence of air at the center a high-pressure system (Figure 5.17a) at 500 hPa passing over Twee Rivieren moving eastern. This event was associated with middle level anticyclonic circulation (Figure 5.17a) with the high pressure system near the surface further east (Figure 5.17b). Vector winds at 850 hPa are also from the Namib Desert which is hotter and drier. Strong negative 500 RH anomalies (Figure 5.18a) were observed over the equator-ward regions of Northern Cape where the heat waves occurred, indicating dry conditions. Upper level (200 hPa) OLR anomalies were well above normal (Figure 5.18b) during the period of the Twee Rivieren longest lasting heat wave, hence sunny conditions were experienced over the region.

5.3.5 Cluster E

Case 5: 3-12 February 1992

All inland thermal regions recorded fairly high maximum temperatures between the 3rd to the 12th of February 1992, with northern parts of Free State and Northern Cape where the heat wave occurred recording an average maximum temperature above 35°C (Figure 5.9). Average maximum temperatures over Cluster A were cool to warmer during this period.

However it was Queenstown that recorded the longest lasting heat wave in cluster E with an average maximum temperature of 36.2 during this period.

Anticyclonic circulations in the middle levels (Figure 5.19a) were also associated with this heat wave for the entire duration, however weakening in the last day of the heat wave. Both the observed high pressure system and positive 200 hPa OLR anomalies (Figure 5.20b) over Queenstown during this period indicate clear and sunny conditions, which might have contributed in increasing atmospheric temperatures of the region. Figure 5.20a shows negative 500 hPa RH anomalies over the eastern part of South Africa during the duration of the heat wave, hence indicating dry atmospheric conditions.

a) b)

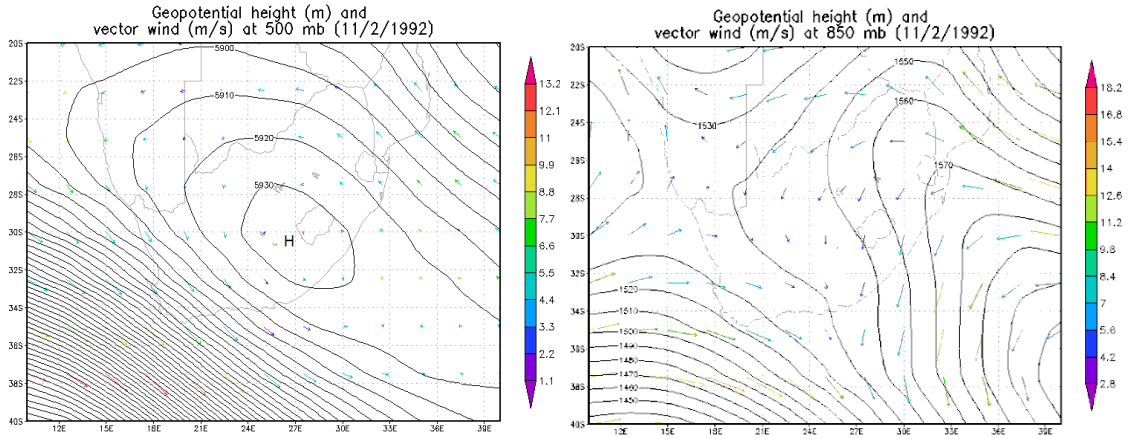

Figure 5.19: Geopotential height (m) and vector winds (m/s) at 500 hPa (a) and at 850 hPa (b) over South Africa during the 11-day lasting heat wave (3 February 1992 to 12 February 1992) over Queenstown. Colour bar indicates wind strength in m/s.

a) b)

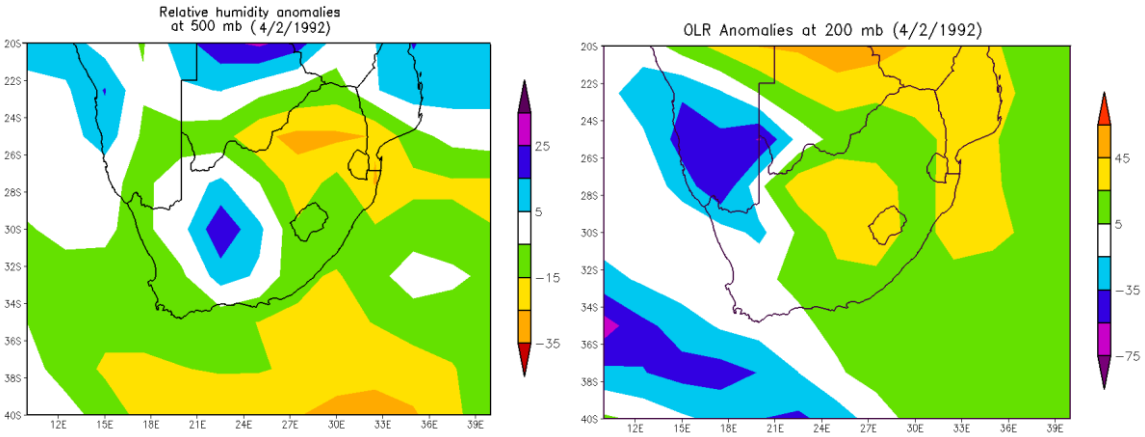

Figure 5.20: Anomalies of 500 hPa RH (%) (a) and OLR anomalies (W/m^2)at 200 (b) over South Africa during the 10-day lasting heat wave in Queenstown from 3 February 1992 to 12 February 1992.

5.3.6 Cluster F

Case 6: 17-27 February 1983

Much of the country experienced warmer to very hot average daily maximum temperatures between 17 and 27 February 1983, ranging from 23°C to over 36°C (Figure 5.10). This period recorded the longest lived heat wave over South Africa from 1983 to 2012 over Marico lasting for 11 days. Average daily maximum temperature over South Africa during the longest lasting heat wave in cluster F was the highest (> 36°C) in the elevated interior and the north-west lowveld of the country, specifically an average of 37.8°C was recorded at Marico over the 11-day period. A decrease of maximum temperature during this event was observed pole-ward and lowest average daily maximum temperatures were recorded in coastal regions.

a) b)

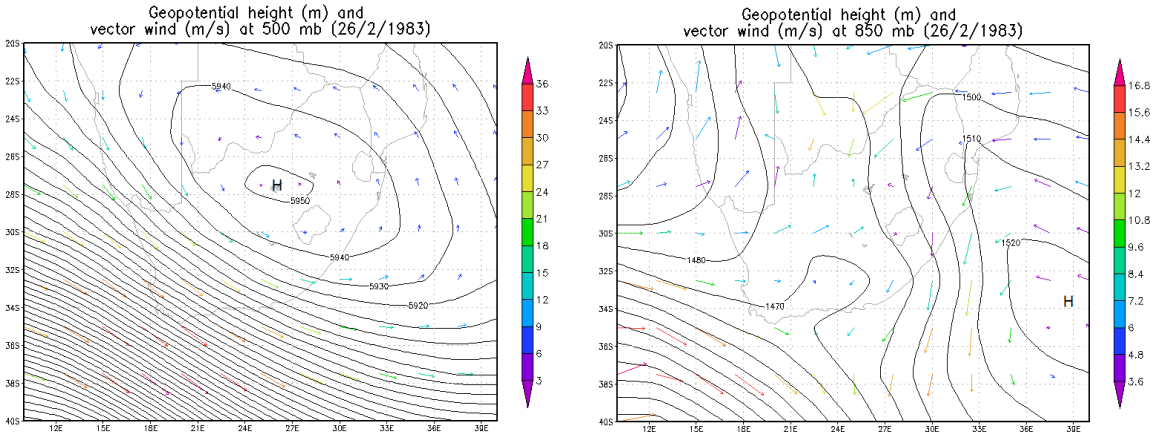

Figure 5.21: Geopotential height (m) and vector winds (m/s) at 500 hPa (a) and at 850 hPa (b) over South Africa during the 11-day lasting heat wave (17 February 1983 to 27 February 1983) over Marico. Colour bar indicates wind strength in m/s.

a) b)

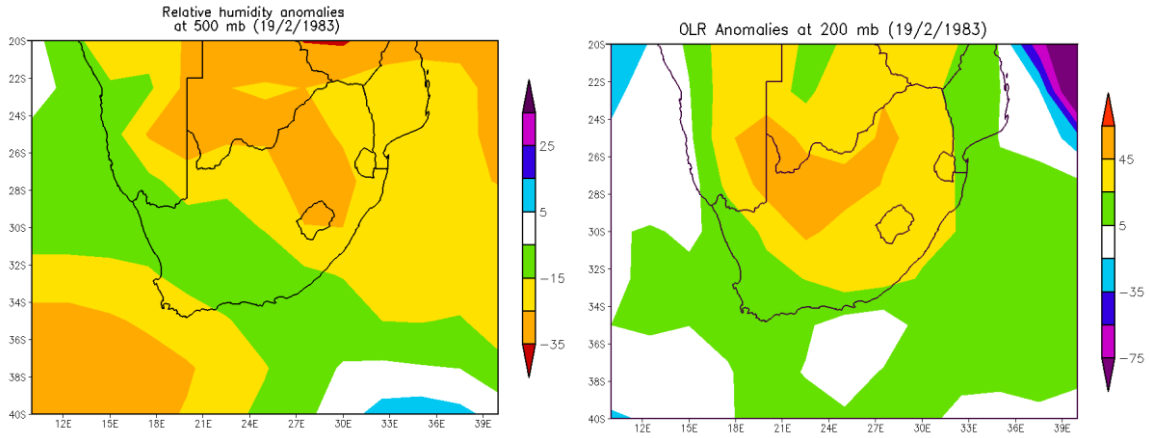

Figure 5.22: Anomalies of RH (%) at 500 hPa (a) and OLR anomalies (W/m^2) at 200 hPa (b) over South Africa during a heat wave in Marico from 17 February 1983 to 27 February 1983.

Strongly positive OLR anomalies were observed over the whole of South Africa, but decreases pole-ward (Figure 5.22b) and proved to be consistent with the mean daily maximum temperature between 17 and 27 February, 1983 over the country. The entire country was dry during this period, with the plateau experiencing strong negative RH anomalies. A persistent high pressure system was observed during February over the plateau of South Africa which coincided with the strongest El Niño season of 1982/1983.

Anticyclonic circulations at 500 hPa (Figure 5.21a) over the northern interior of South Africa and continental winds at 850 hPa towards the northern Interior of the country were observed during this heat wave. As a result, it can be concluded that the high temperatures over Marico, a station that recorded this heat wave, was caused by both the subsiding air from the continental high pressure system and warm air advection from land areas of the tropics.

All the longest lasting heat waves (Cluster A-F) are associated with anticyclonic circulations at 500 hPa. However, it weakens with decreasing height because of friction which may result from infrastructures and mountains. Subsidence at the center of high pressure systems during these systems and horizontal warm air advection contribute in increasing temperatures during heat waves. While heat waves in much of the country are associated with dry conditions, the south-east to eastern coastal regions experience warm and moist conditions during heat waves. When a certain region experiences a heat wave, other regions may experience cooler conditions as it was the case in Port Nolloth during the austral winter of the 1999/2000 season a middle level low pressure system was observed over the northern part of the country associated with cool conditions.

Negative soil moisture anomalies are observed in much of South Africa during the longest lasting heat waves per thermal region (Figure 5.23). The soil moisture deficits are clearly visible over inland clusters (C-F). The NCEP/NCAR model is unable to record land variables along coastal regions (A-B).

5.4 Vertical motion over South Africa during heat waves in ENSO seasons

It has been discussed in the previous chapter (section 4.3.1) that heat wave occurrences over South Africa are also observed during both El Niño and La Niña seasons. However, the severity differs as the most severe heat waves last for longer periods with high average maximum temperatures and occur during El Niño seasons. The longest lasting heat waves per thermal region were equally divided in the positive and negative phases of ENSO. However, it has to be noted that there was no heat wave observed in moderate and strong La Niña seasons but only during weak La Niña. Cluster A, D and F experienced their longest lasting heat waves during weak La Niña seasons while cluster B, C and E experienced their longest lasting heat waves during moderate to strong El Niño seasons. The country usually experiences different weather conditions during El Niño and La Niña seasons, however that is not the case with vertical motion during heat waves.

Composite analysis for heat wave days occurring during El Niño and those during La Niña both indicate that the interior of South Africa experiences subsidence, uplift is observed over the north-east lowveld of the country (Figure 5.24-5.25). The subsidence is more concentrated in the southern interior of South Africa during heat waves in La Niña seasons (Figure 5.24), while subsidence tends to be concentrated over the northern interior of the country during heat waves occurring during El Niño seasons (Figure 5.25).

The large scale subsidence over the interior contributed in the atmospheric warming as subsiding air warms adiabatically. This subsidence is linked to the persistent high pressure systems during heat waves, which also bring dry and clear weather conditions as rainfall is unlikely to occur at the center of a high pressure system. It must be noted that time scales of heat waves and ENSO are not the same as heat waves only make up few days of ENSO periods, however heat waves are more frequent during warm ENSO seasons.

5.5 Thermal discomfort

Regions of South Africa experiences different thermal discomforts during heat waves. Both TDI and DI indicated that Port Nolloth did not experience thermal discomfort during heat waves over 30-year period, with indices of 20 and 70 respectively (Table 5.1). Eastern parts of the country such as the eastern lowveld, east and south-east coastal regions experience high uncomfortable conditions with DI of 92 and over 50% of the population in these regions

feels the discomfort. This is because the regions also experience significant high RH during the warm to hot atmospheric conditions. However, while South Africa experienced very uncomfortable conditions in other regions during heat waves that occurred between 1983 and 2012, the country did not experience discomforts that require medical emergency.

Table 5.1: Thermal discomfort indices during the longest lasting heat waves in each cluster region

Cluster regions	Station	T (°C)	RH (%)	TDI	DI
A	Port Nolloth	21.8	57.3	20	70
B	Richards Bay	28.2	68.5	26	92
C	Punda Maria	34.1	41.7	28	92
D	Twee Rivieren	32.6	18.1	24	75
E	Queenstown	24.7	67.9	23	82
F	Marico	25.8	40.0	22	72

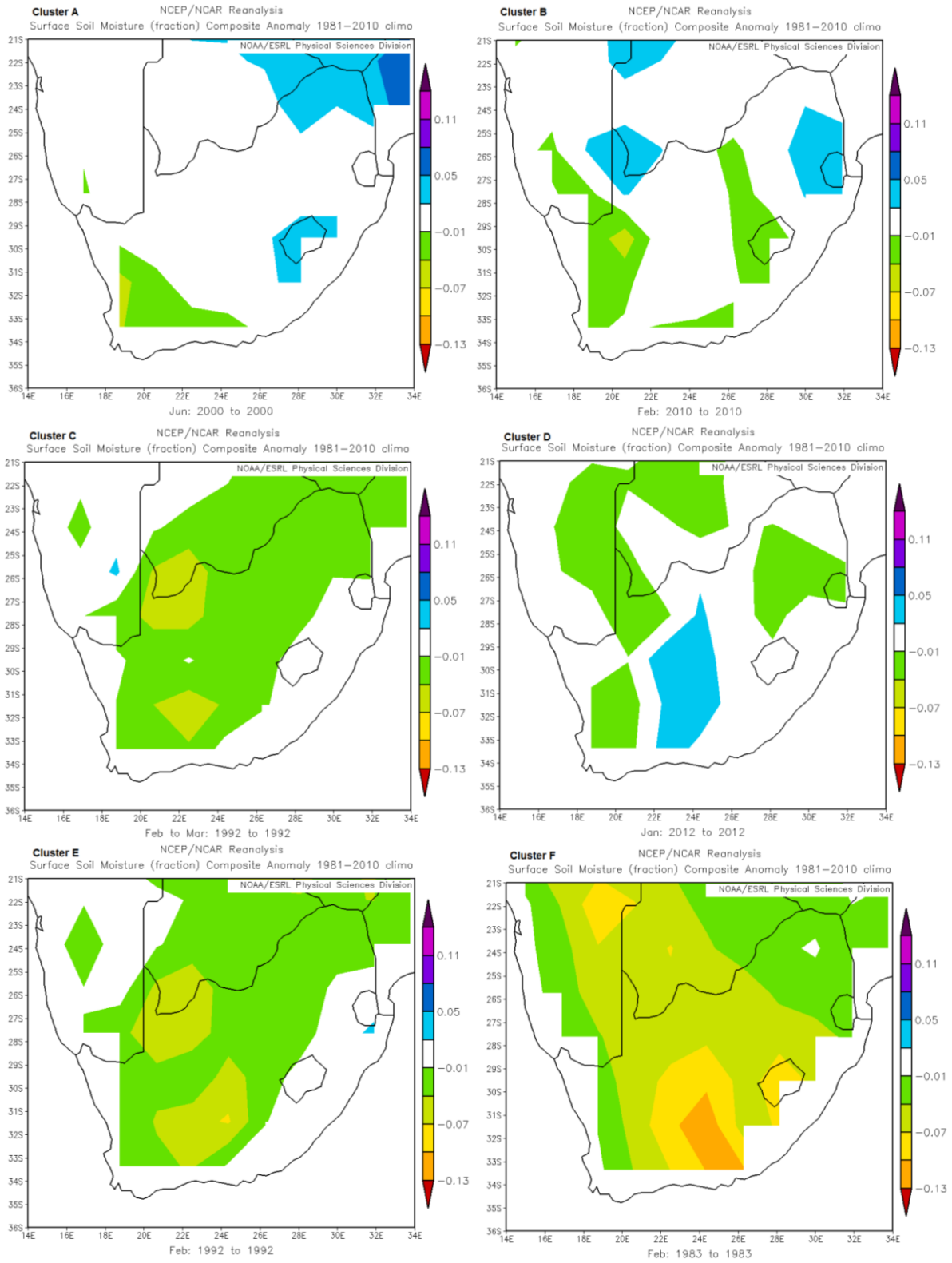

Figure 5.23: Monthly soil moisture anomalies (mm/month) over South Africa during the longest lasting heat waves per thermal regions (A – F).

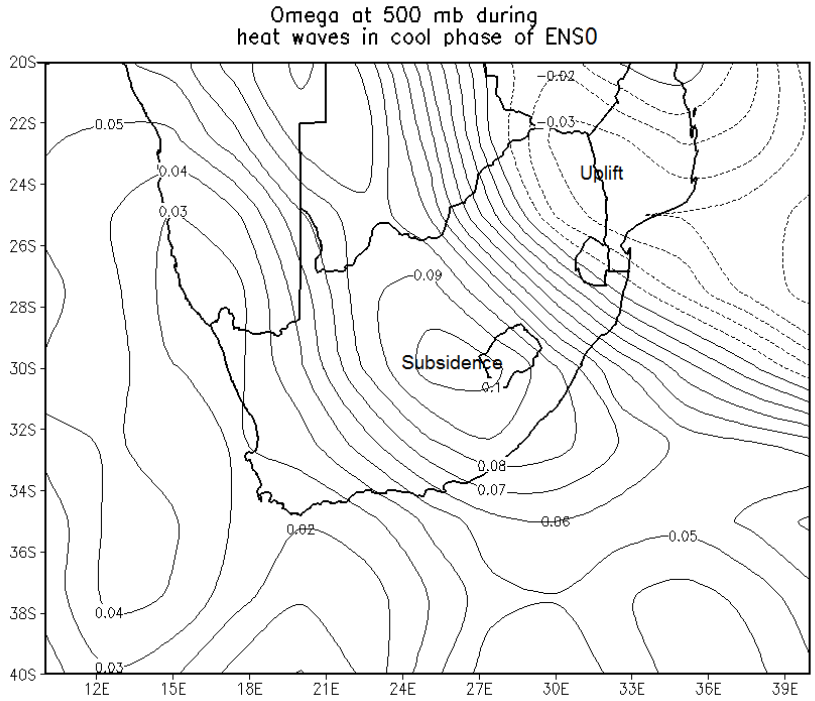

Figure 5.24: 500 hPa omega during heat waves in La Niña seasons from 1983 to 2012.

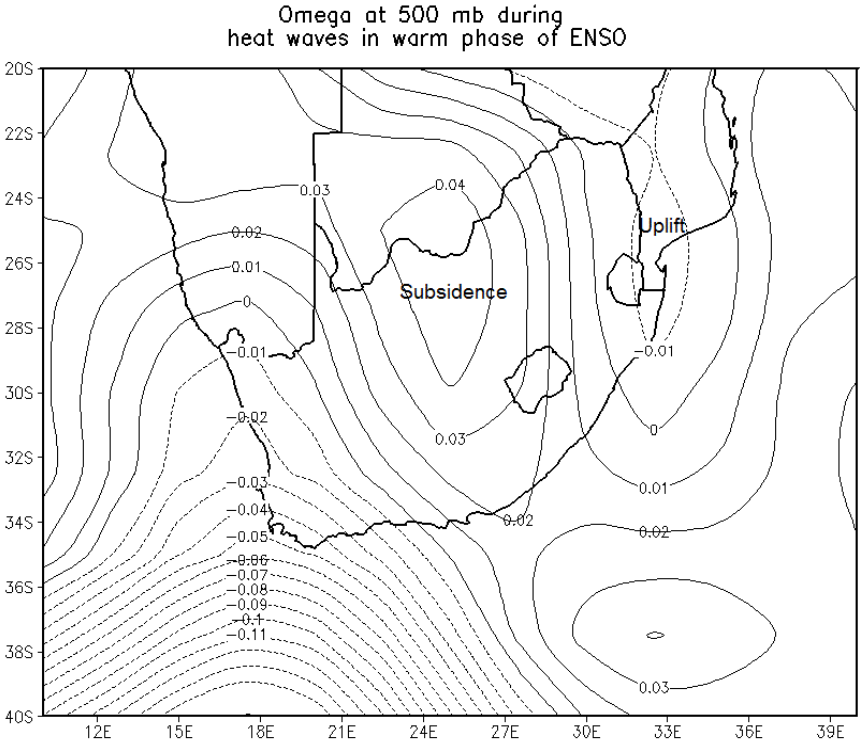

Figure 5.25: 500 hPa omega during heat waves in El Niño seasons from 1983 to 2012.

5.6 Summary

This chapter has provided the structure of heat waves in each thermal region of South Africa. Geopotential height at the middle levels was mapped to observe pressure systems associated with these events. Heat wave occurrences are associated with persistent high pressure systems which usually induce anticyclonic circulations and dry conditions over South Africa. However, that is not always the case as a 6-day lasting heat wave in Richards bay was associated with a high pressure system which lead to onshore warm and dry wind from the Indian Ocean. The following was observed about the structure of heat waves in the perspective of South Africa:-

a) The plateau and north-east lowveld of South Africa are warm (>28°C) during the identified longest heat waves in most thermal regions, with an exception of the longest lasting heat wave that occurred in winter at cluster A over Port Nolloth. Most part of the central interior was cool during the longest lasting heat wave in Port Nolloth, however the north-east lowveld was warmer.
b) Heat waves are associated with a high pressure system in the middle levels which weakens and placed south-east with decreasing height.
c) The high pressure systems induce anticyclonic circulations in the middle level and near the surface; however the anticyclonic circulation weakens near land surface areas.
d) Subsidence at the center of the 500 hPa high pressure systems and warm and dry continental winds are the main drivers that trigger heat wave occurrences.
e) Both 850 hPa and 500 hPa wind vectors transport warm and dry inland winds from countries such as Namibia and Botswana towards interior regions of South Africa during heat waves over the interior of the country.
f) During heat waves, pattern of OLR anomalies are usually consistent with average daily maximum temperature distribution during the heat wave period.
g) Composite analysis of 500 hPa omega indicates subsidence over the interior of South Africa, while the north-east lowveld experience uplift.
h) Heat waves over South Africa are also associated with dry atmospheric conditions over inland regions of the country where RH anomalies are usually negative throughout the duration of these events.
i) In cluster B, the anticyclonic circulation transport warm and moist air from the south-west Indian Ocean towards south-east coastal regions during heat waves increasing RH, hence increasing thermal discomfort over those regions.

j) Much of South Africa experiences negative soil moisture anomalies during months with longest lasting heat waves per thermal regions, particularly in the area of a certain thermal region that recorded the heat wave.
k) Subsidence over the interior of the country is observed during heat waves in both phases of ENSO.

Coastal low pressure systems are usually conducive for berg-winds over the coasts in winter and also lead to high maximum temperatures, however cannot trigger heat wave occurrences because they last few hours or less than the minimum heat wave duration and the also the cold fronts which usually follow coastal low pressure systems lower atmospheric temperatures after their passage over a particular area.

The next chapter provide characteristics of future heat waves over South Africa. Frequency, duration and intensity of heat waves in the future warming climate from CCAM outputs are detailed in the next chapter.

CHAPTER 6

FUTURE HEAT WAVES IN SOUTH AFRICA

6.1 Introduction

Heat waves are one of the most important climate-related risks in the world. Owing to climate change, characteristics of these events are also expected to change (Zacharias *et al*. 2015). Less emphasis has been put in the projection of heat waves in South Africa, Australia being a region where most heat waves studies are based in the southern hemisphere (e.g. Perkins *et al*. 2013; Nairn and Fawcett 2013; Boschat *et al*. 2014; Zacharias *et al*. 2014; Zacharias *et al*. 2015). It is expected that a global average of heat wave frequency, duration and intensity will increase owing to the increasing global mean temperatures (Min *et al*. 2011; Coumou and Rahmstorf, 2012). However, that may not necessary be the case on regional scale as temperatures vary from place to place depending on the prevailing weather features.

The aim of this chapter is to provide characteristics of heat waves over South Africa in the warmer future climate under the Representative Concentration Pathway (RCP) 4.5 and 8.5 emission scenarios. RCP 4.5 represents a future with high mitigation while RCP 8.5 represents a future with low mitigation. The simulated frequency, duration and intensity of future heat waves over South Africa as projected by the Conformal Cubic Atmospheric Model (CCAM) are discussed in this chapter. There is a strong variation of near-surface temperatures over the African continent. It has been established in this study that the southern tip of the African continent experiences most warming during the recent century (Figure 1.1), which may enhance the likelihood of hot temperature extremes over the region.

Simulations were made for the period 1971 to 2099, and the analyses is split into 30 year averages. 1983-2012 is considered as a present-day climate, three future climate periods defined as 2010-2039, 2040-2069 and 2070-2099 are also analysed. The 30-year period, 2070-2099, just before the 22nd century is considered the period where the climate change signal will be strongest. To make comparisons easier, threshold used to identify heatwaves in all four periods are those identified using present day simulations. The 10th, 50th and 90th percentiles of six ensemble members are presented separately for RCP4.5 and RCP8.5.

6.2 Simulated average T_X and heat wave threshold

Simulated 30-year average maximum temperatures during the present day climate are consistent with observed maximum temperatures throughout the year. The simulations indicate that South Africa experiences highest maximum temperatures during DJF,

particularly in the northern parts of the country. Highest values are more evident in the dry regions of the Northern Cape with averages of over 36°C (Figure 6.1). Just like with the observations, lowest average maximum temperatures are simulated to be experienced during JJA, with values averaging to less than 22°C in much of the interior and coastal regions during the 1983-2012 period (Figure 6.2). There is little variability amongst the different ensemble members for both RCP8.5 and RCP4.5. The RCP8.5 and 4.5 are similar until the year 2000, and then start to divert, however the differences until 2012 between the two scenarios are small.

Maximum temperatures are projected to increase by up to 2°C during the period 2010 to 2039 as compared to the reference period of 1983 to 2012 during summer (Figure 6.3). The increase along coastal regions is less than 1°C, with the central part of the subcontinuent expected to experience increases of over 1°C. The over 1°C change extends into Botswana and Namibia for all RCP 8.6 percentiles, while only the 90th percentile of RCP4.5 extends way into Namibia and Botswana. The winter temperatures are also projected to increase, with higher values in the RCP8.5 scenario (Figure 6.4). The RCP4.5 scenario projects increases of less than 1°C over larger part so the central interior. The coastal areas are still projected to have a lower increase as compared to inland.

The projected temperatures increases in the medium term period of 2040-2069 are larger than those projected for the present day/near term future period of 2010 to 2039 (Figure 6.5). The RCP8.5 projections are showing increases of over 3°C, while those of RCP4.5 are projected to be slightly lower. This result further confirms that the increases that are projected are due to increases in the concentration of anthropogenic greenhouse gases, which are larger for RCP8.5. The 1 to 2°C changes projected for the near future period, extend to the coastal regions, while the increases over land have become even larger. This result suggests that changes over the coastal regions are slower because of the modulating effects of the nearby water, because water has a larger heat capacity.

The climate change signal is expected to be largest in the period 2070 to 2099, because it is the furthest and the anthropogenic greenhouse gas concentrations will be largest especially in the low mitigation scenario (Figure 6.6 and Figure 6.7). The summer temperatures are projected to increase further, with increases going in excess of 7°C in the RCP8.5 scenario. The projected increase over the coastal regions is smaller further indicating the modulating effect of the oceans. All the ensemble members, both in the RCP4.5 and RCP8.5 are predicted an increase in temperature which shows that there is a high certainty in the temperature projections. The increase in the mean temperatures are expected to have an effect on the characteristic of heatwaves in the future climate.

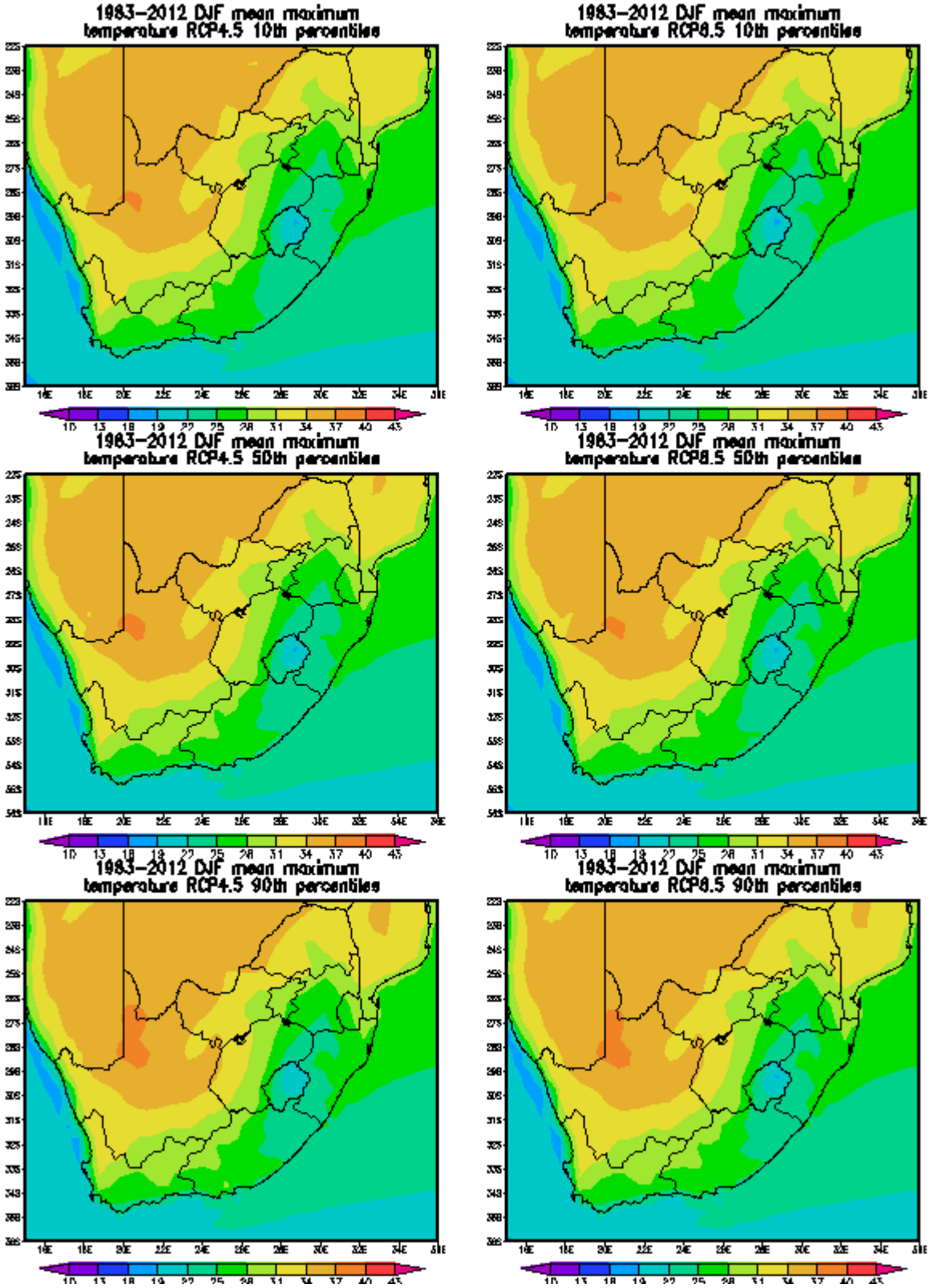

Figure 6.1: Comparisons between simulated RCP4.5 and RCP 8.5 10th, 50th and 90th percentiles of DJF average maximum temperature (°C) during 1983-2012.

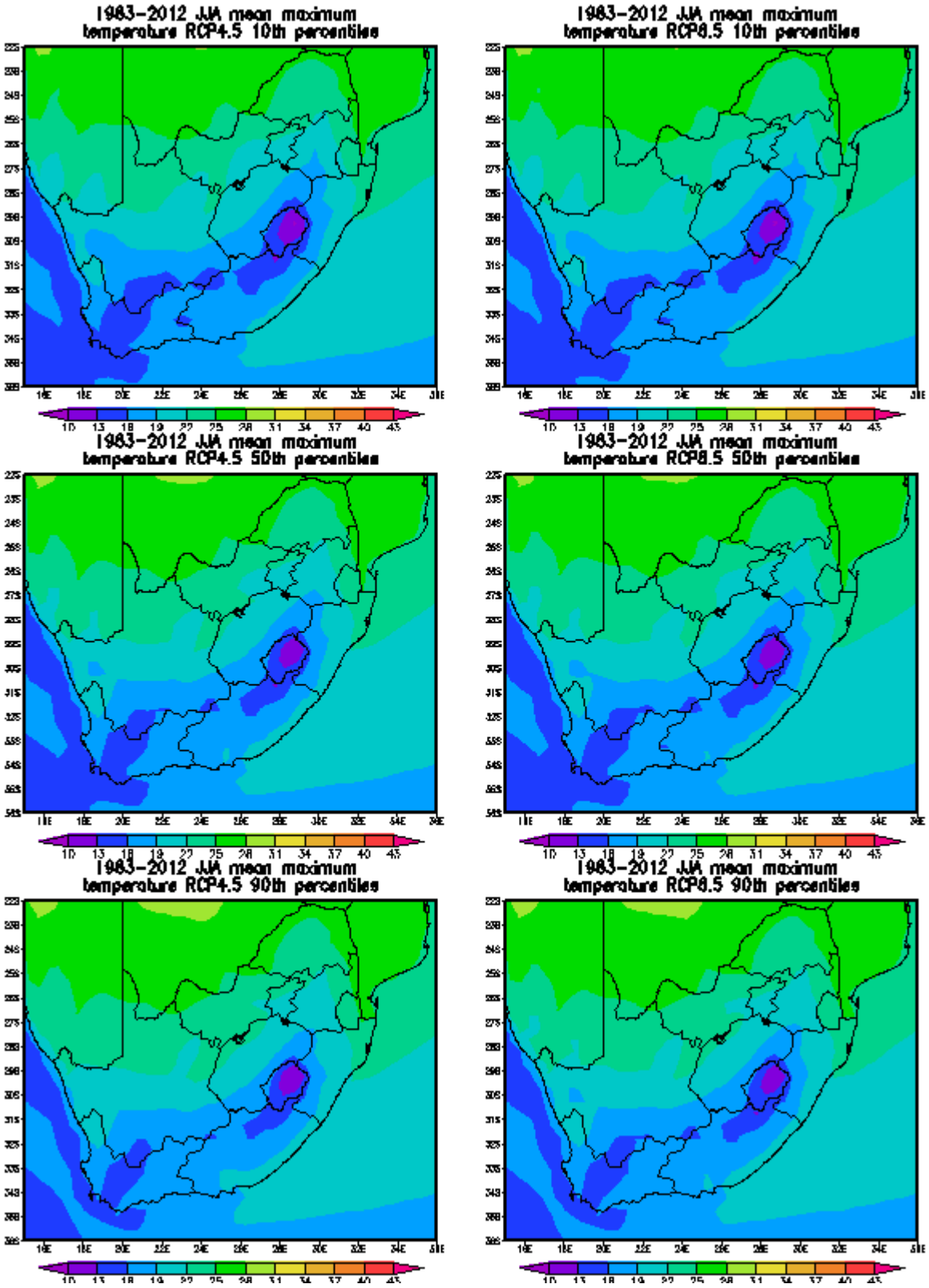

Figure 6.2: Comparisons between simulated RCP4.5 and RCP 8.5 10th, 50th and 90th percentiles of JJA average maximum temperature (°C) during 1983-2012.

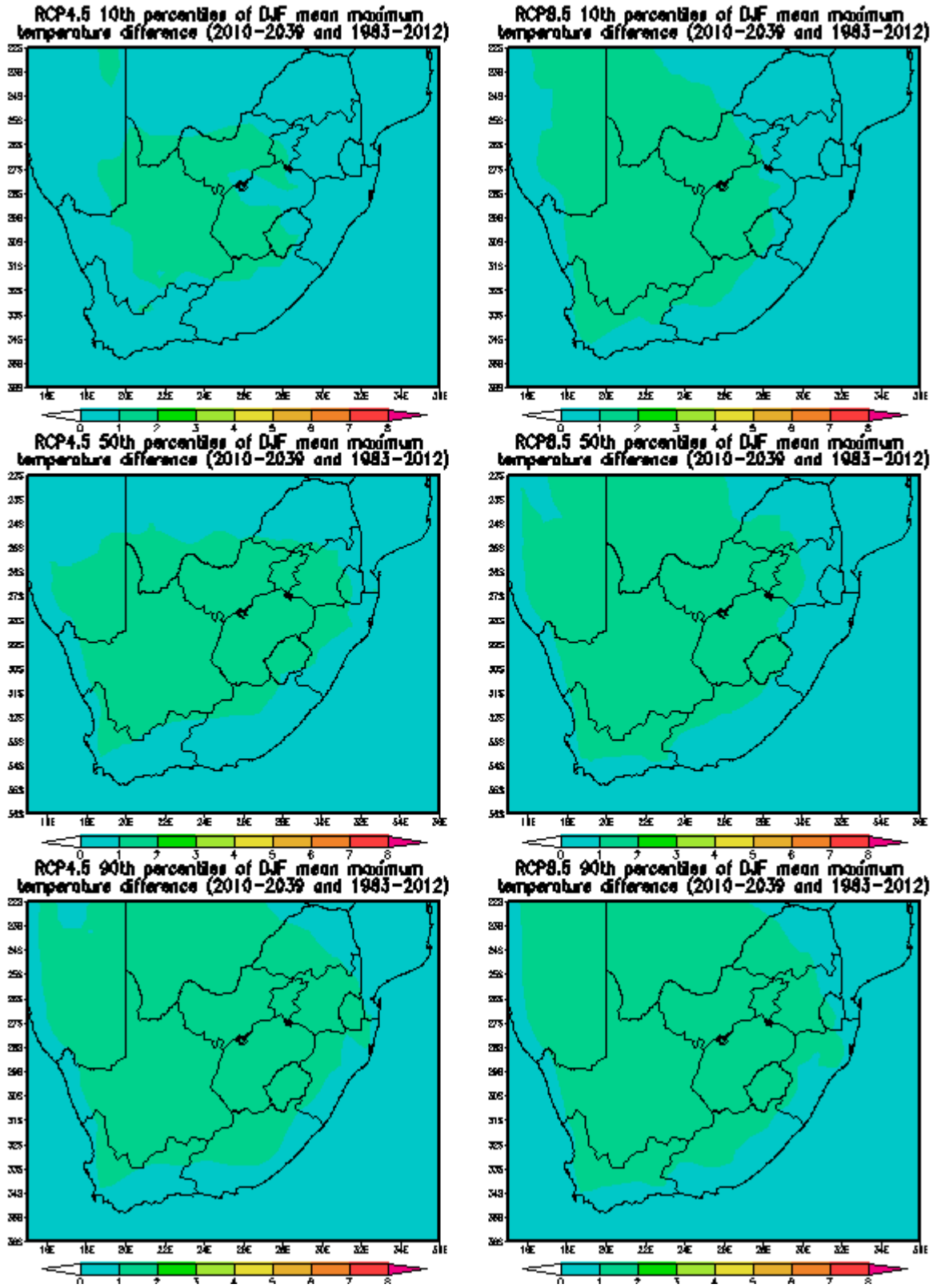

Figure 6.3: Comparisons between simulated RCP4.5 and RCP 8.5 10th, 50th and 90th percentiles of DJF average maximum temperature (°C) difference between 2010-2039 and 1983-2012.

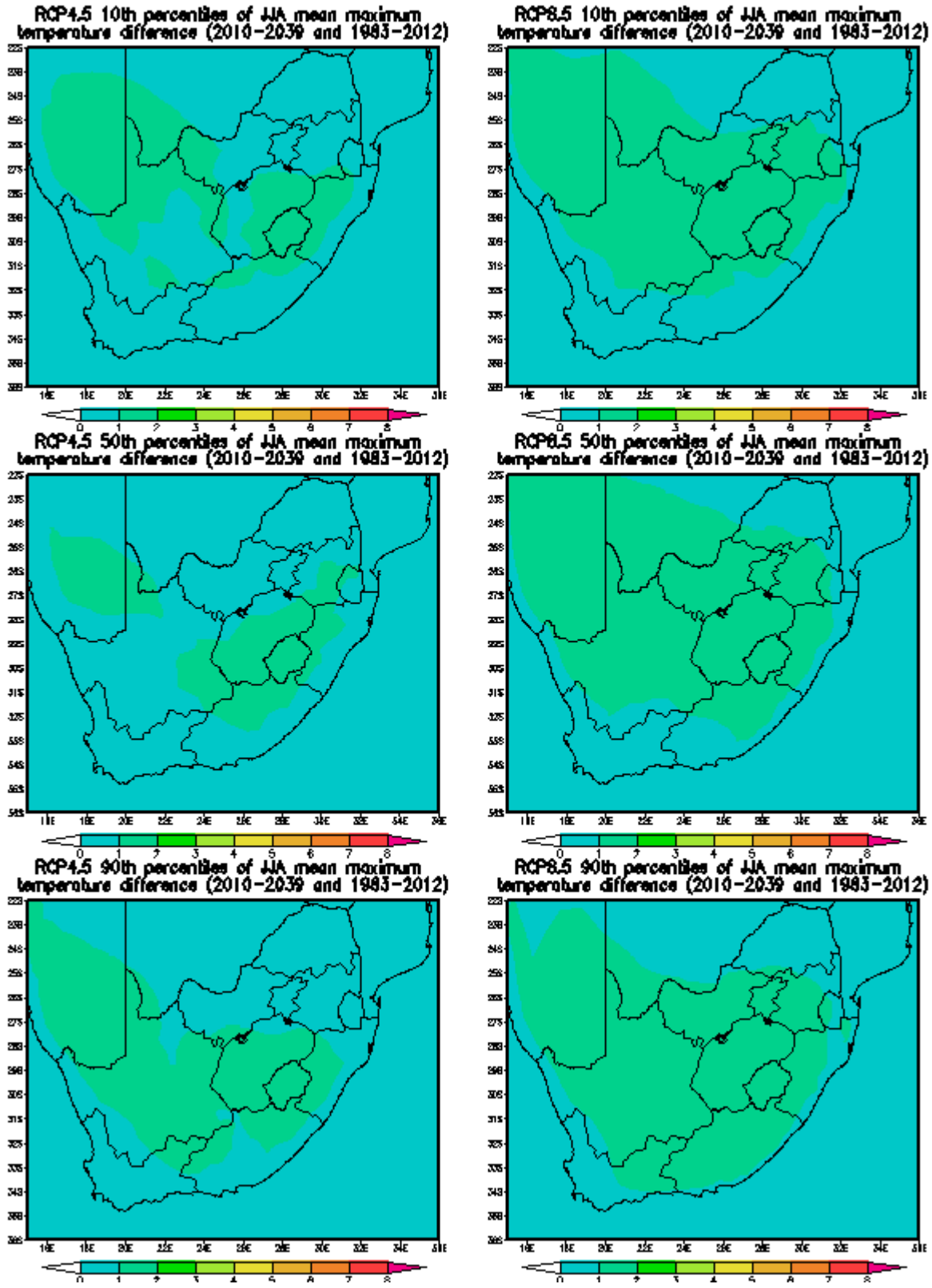

Figure 6.4: Comparisons between simulated RCP4.5 and RCP 8.5 10th, 50th and 90th percentiles of JJA average maximum temperature (°C) difference between 2010-2039 and 1983-2012.

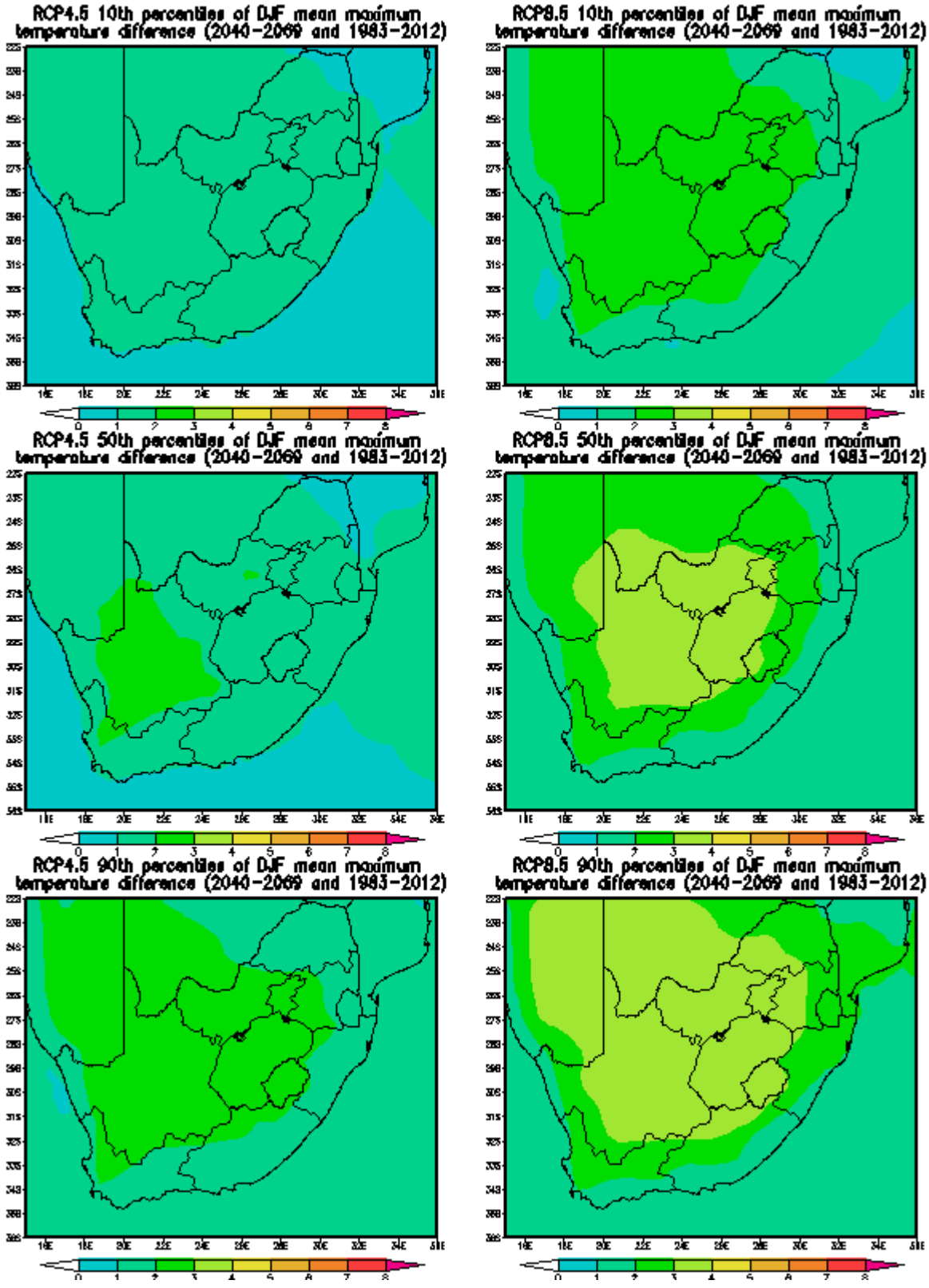

Figure 6.5: Comparisons between simulated RCP4.5 and RCP 8.5 10th, 50th and 90th percentiles of DJF average maximum temperature (°C) difference between 2040-2069 and 1983-2012.

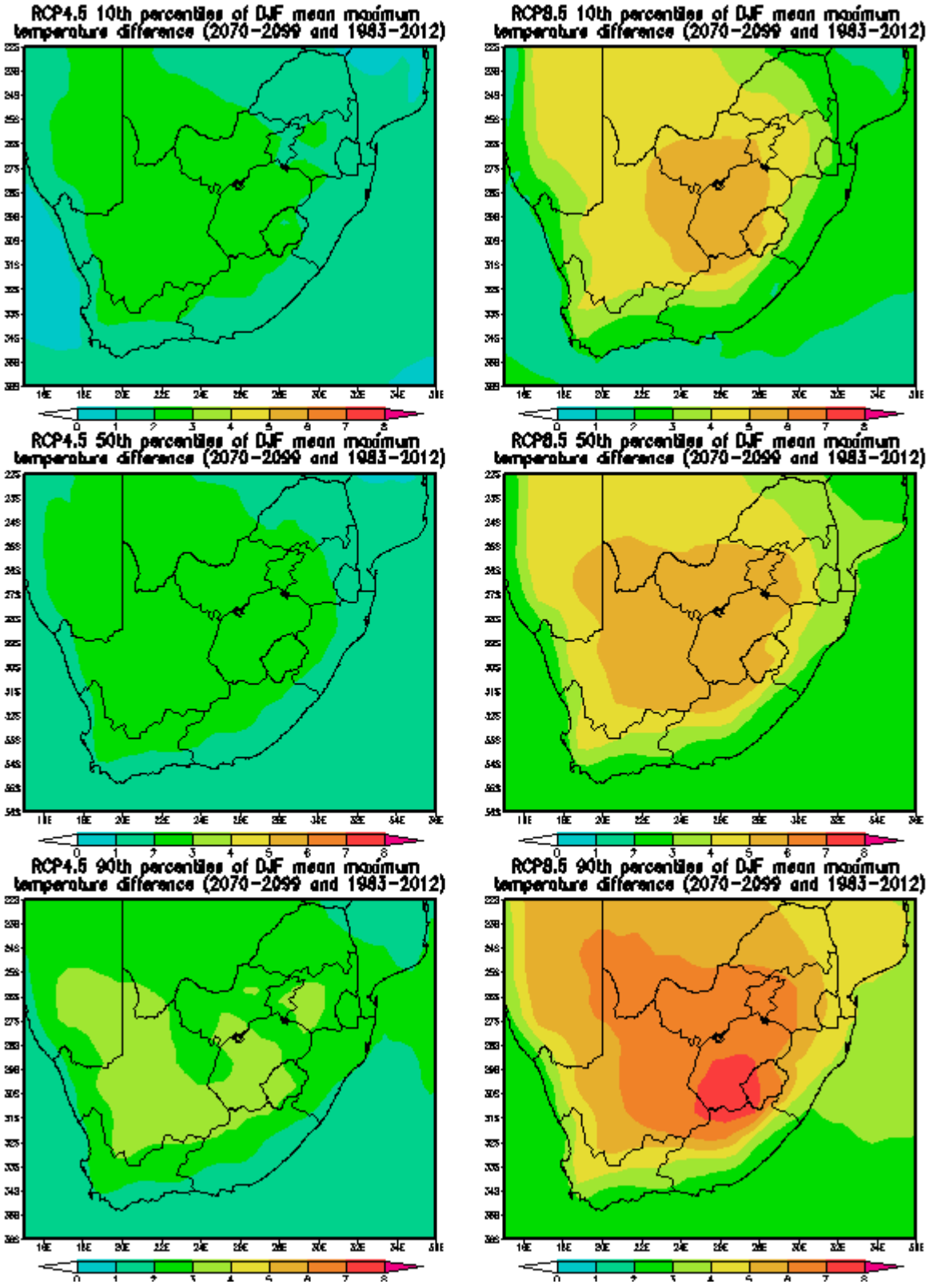

Figure 6.6: Comparisons between simulated RCP4.5 and RCP 8.5 10th, 50th and 90th percentiles of DJF average maximum temperature (°C) difference between 2070-2099 and 1983-2012.

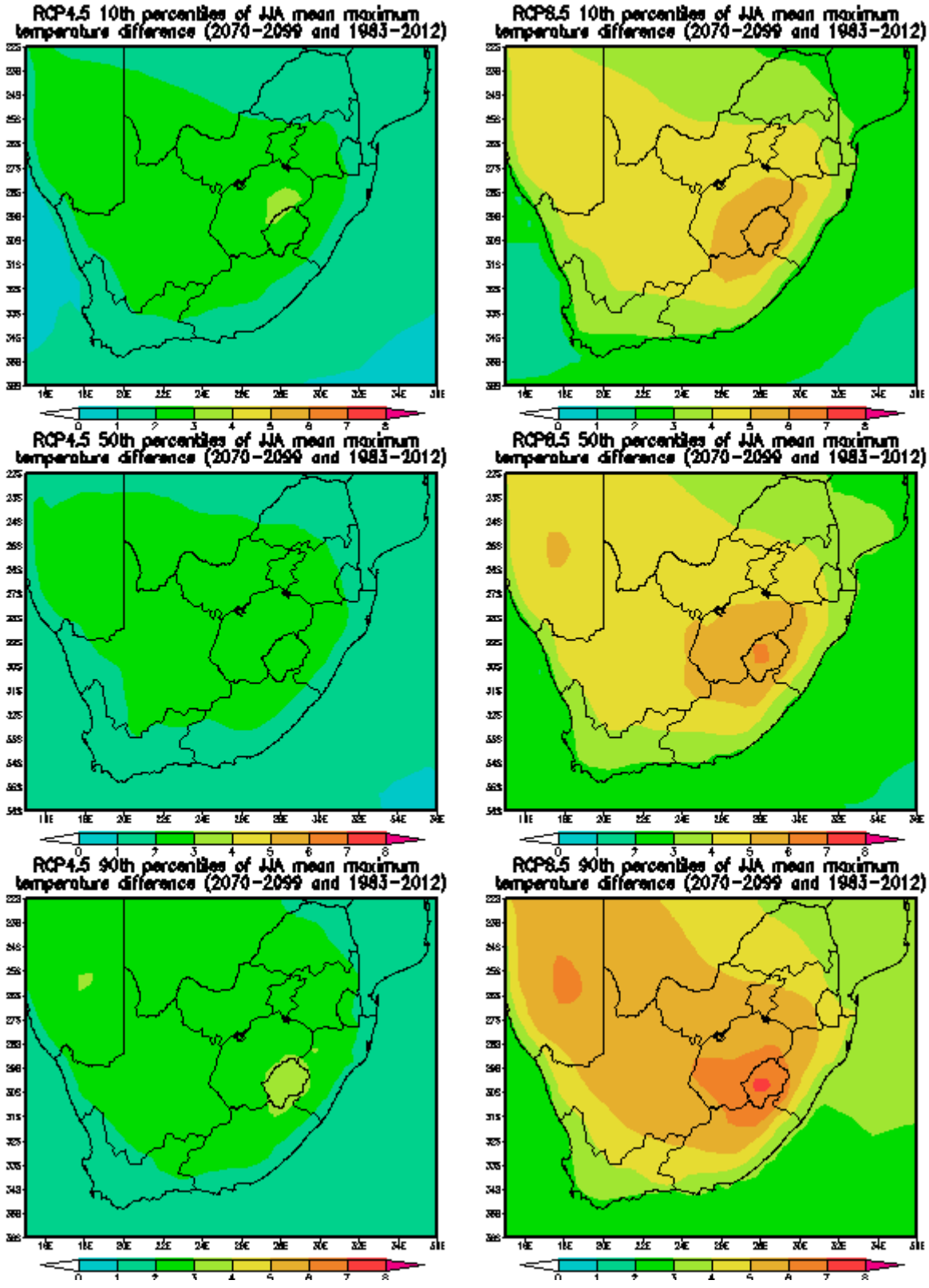

Figure 6.7: Comparisons between simulated RCP4.5 and RCP 8.5 10th, 50th and 90th percentiles of JJA average maximum temperature (°C) difference between 2070-2099 and 1983-2012.

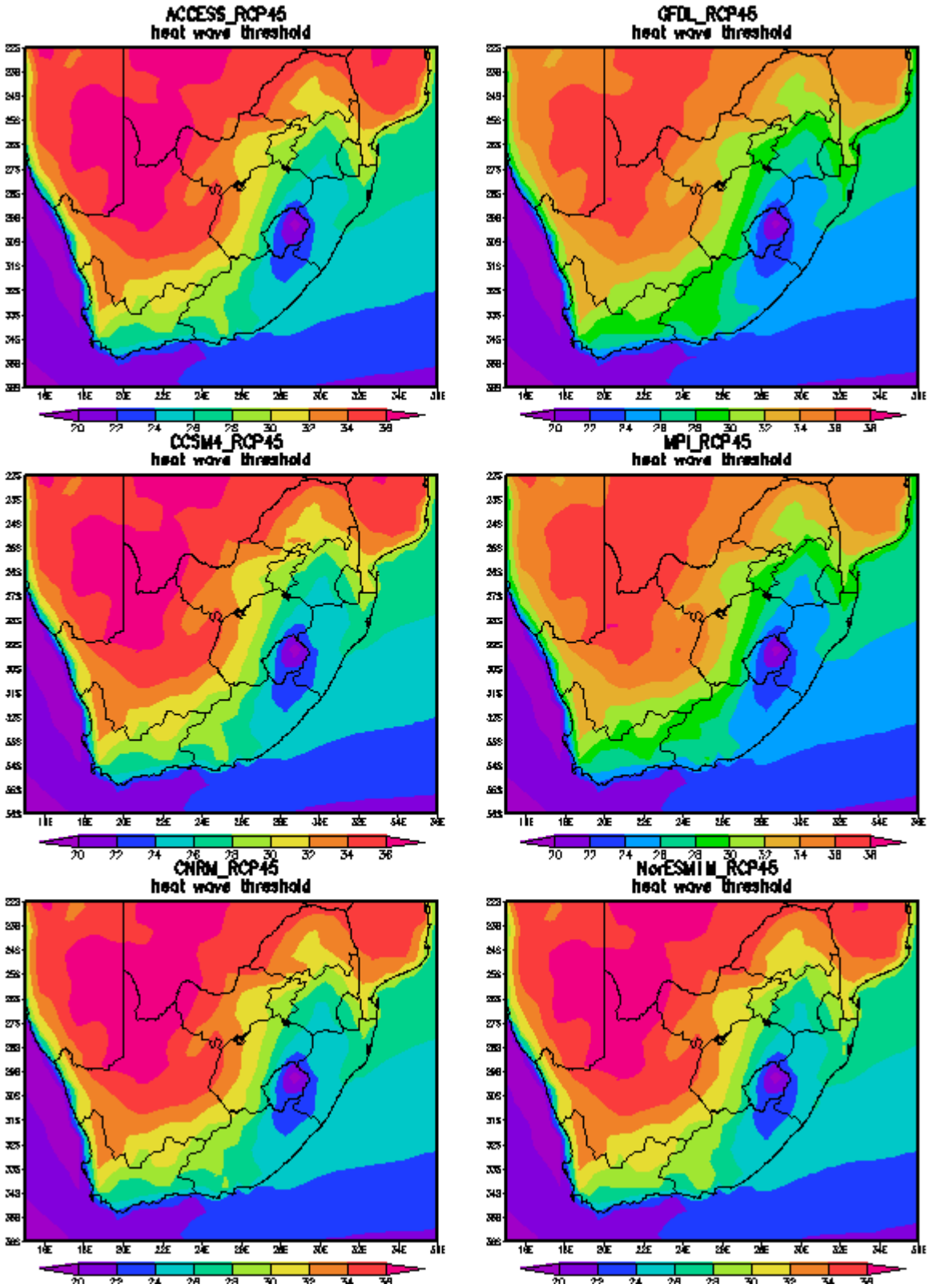

Figure 6.8: Simulated RCP4.5 heat wave thresholds (°C) of the 6 ensemble members.

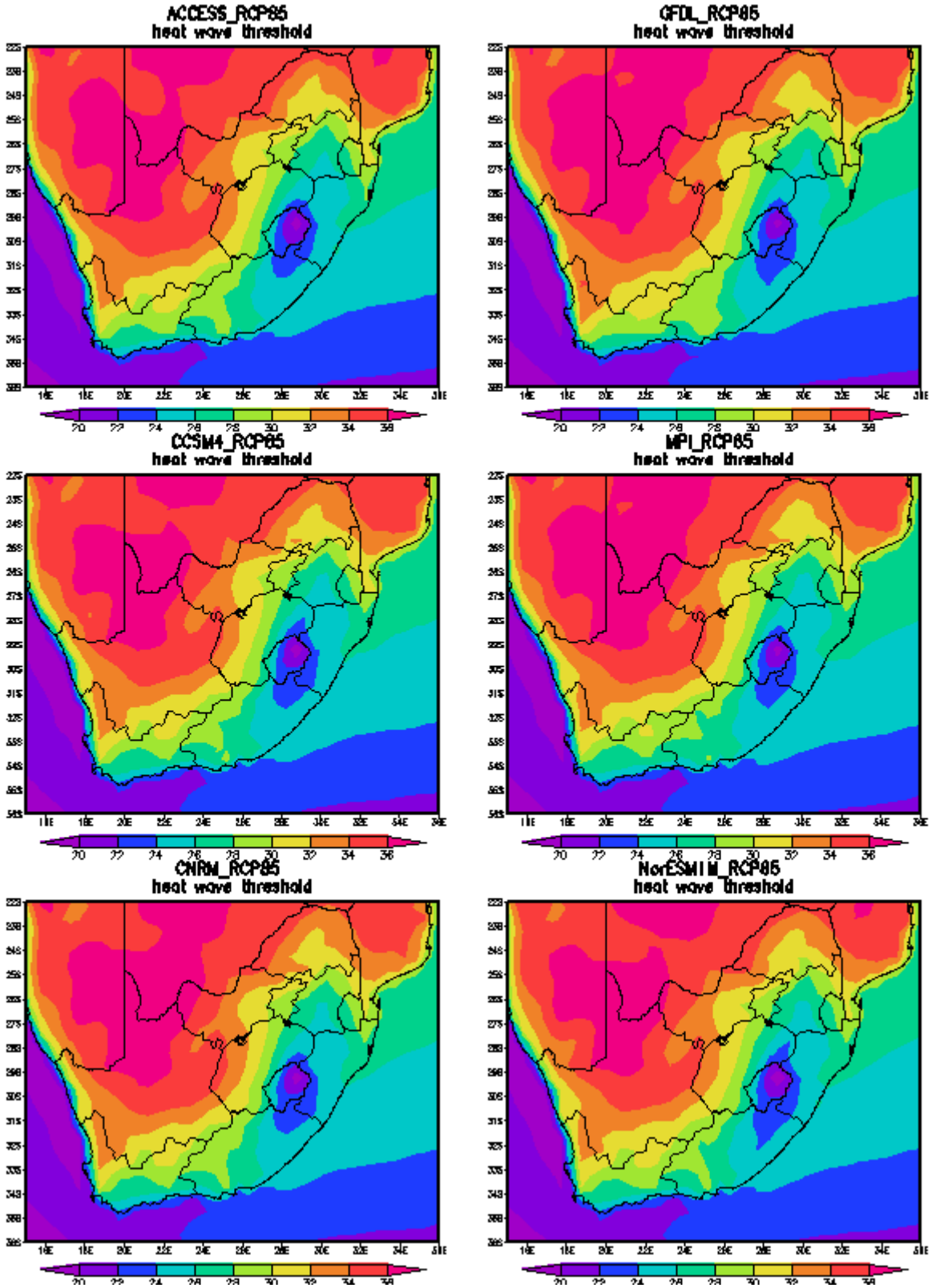

Figure 6.9: Simulated RCP8.5 heat wave thresholds (°C) of the 6 ensemble members.

The heatwaves are identified using a minimum of the days that the simulated temperature is 5°C greater than the average maximum temperature of the hottest month. This definition is used for the present day period, and threshold as determined in present day climate is also applied to future projections. Figure 6.8 and 6.9 show the values of the maximum temperature during the hottest month determined separately for each grid points, for all six ensemble members, for RCP4.5 and 8.5, respectively. The thresholds are higher in the north-east lowveld and western parts of South Africa, ranging from 32-38°C. It has been indicated in Chapter 4 that these are the regions that experience high maximum and minimum temperatures in austral summer. Simulated heat wave thresholds are well below 32°C in much of the eastern parts and coastal regions of the country. The simulated heat wave thresholds are also spatially consistent with the observed thresholds indicated in Chapter 3 (Figure 3.6). Sections 6.3-6.4 below discuss heat waves in future climates identified using the simulated thresholds.

6.3 Simulated heat waves vs. observations

The simulated heatwave frequency in present day climate looks almost similar for the different ensemble members, with the Northwest, Gauteng and Free State provinces simulated to experience the least number of heatwaves (Figure 6.10). The differences between RCP4.5 and RCP8.5 are not significant. The number of heatwaves simulated over Limpopo is high, as well as over the adjacent interior of the south and east coasts. The Northern and Western Cape provinces are also simulated to experience a large number of heatwaves. The observed structure discussed in Chapter 4 looks different from the simulations, with parts of the Western Cape and Northern Cape observed to experience the least number of heatwaves. It should however be noted that the number of grid points in the simulations is much more than the stations used for observations.

The CCAM is able to capture the seasonal differences in the number of heatwaves well (Figure6.10 – Figure 6.13). The least amount of heatwaves is simulated to occur in winter, while the highest number is simulated for summer. The number of heatwaves simulated in spring is higher than those simulated for autumn, however, both autumn and spring heatwaves are fewer than those that occur in summer, and more than those that occur in winter. The spring simulations are in agreement with observations in that they show the highest number of heatwaves over the eastern parts of the country. The observations discussed in Chapter 4 showed a similar seasonal cycle, and hence we can say the CCAM simulates present day climate perfectly, and its future projections can be considered with some confidence.

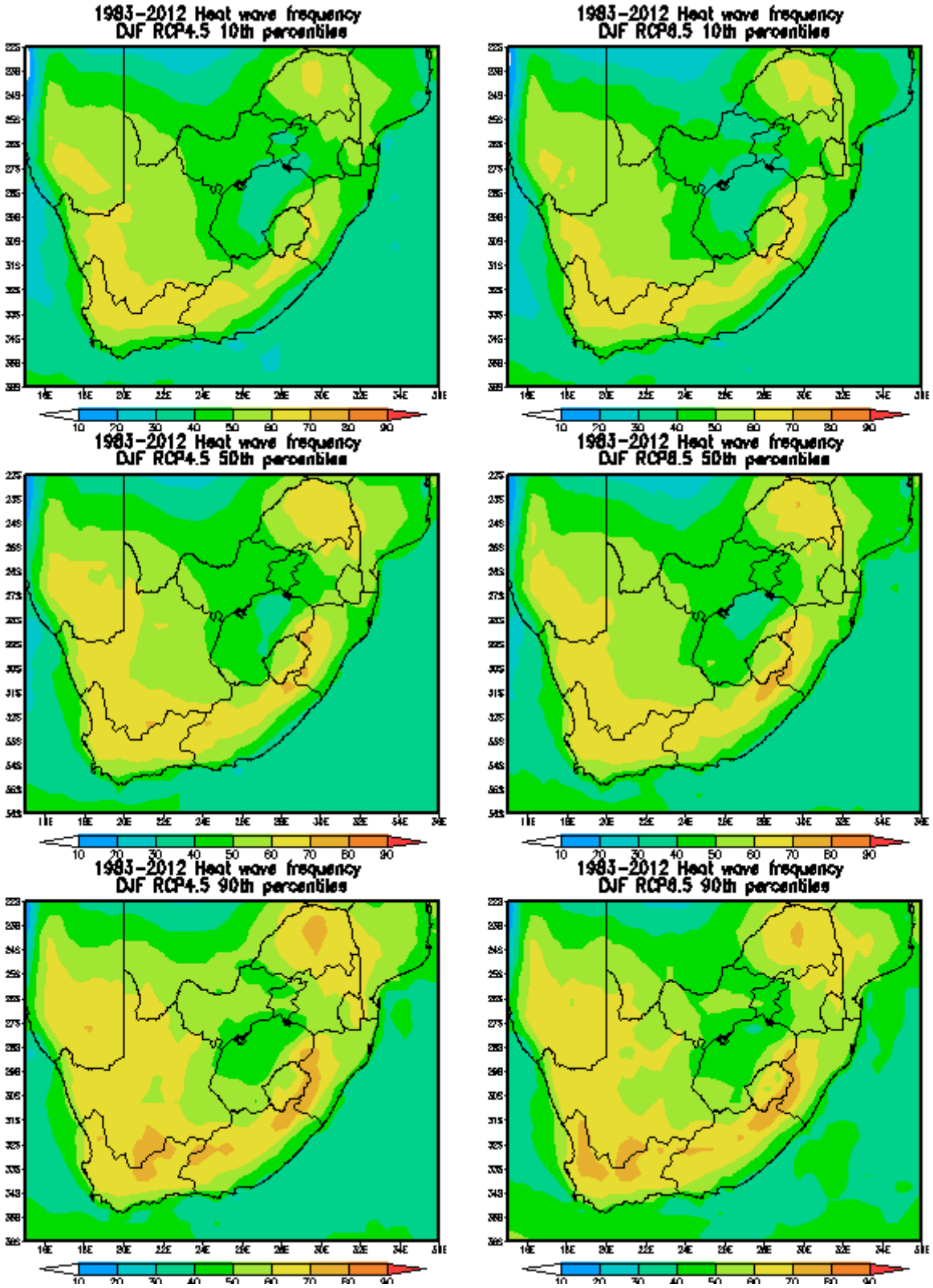

Figure 6.10: Comparisons between RCP4.5 and RCP 8.5 10th, 50th and 90th percentiles of DJF heat wave frequency during 1983-2012.

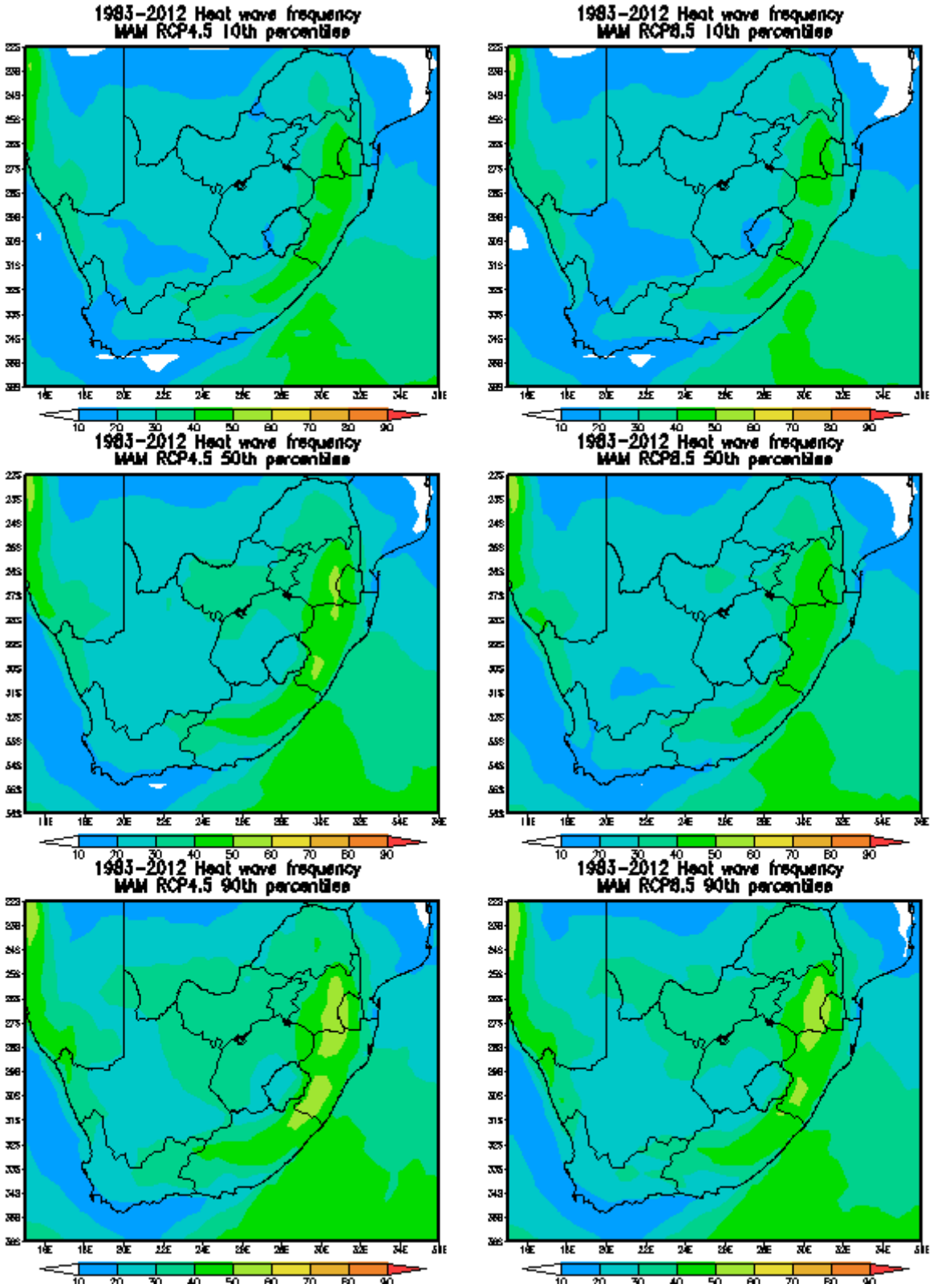

Figure 6.11: Comparisons between RCP4.5 and RCP 8.5 10th, 50th and 90th percentiles of MAM heat wave frequency during 1983-2012.

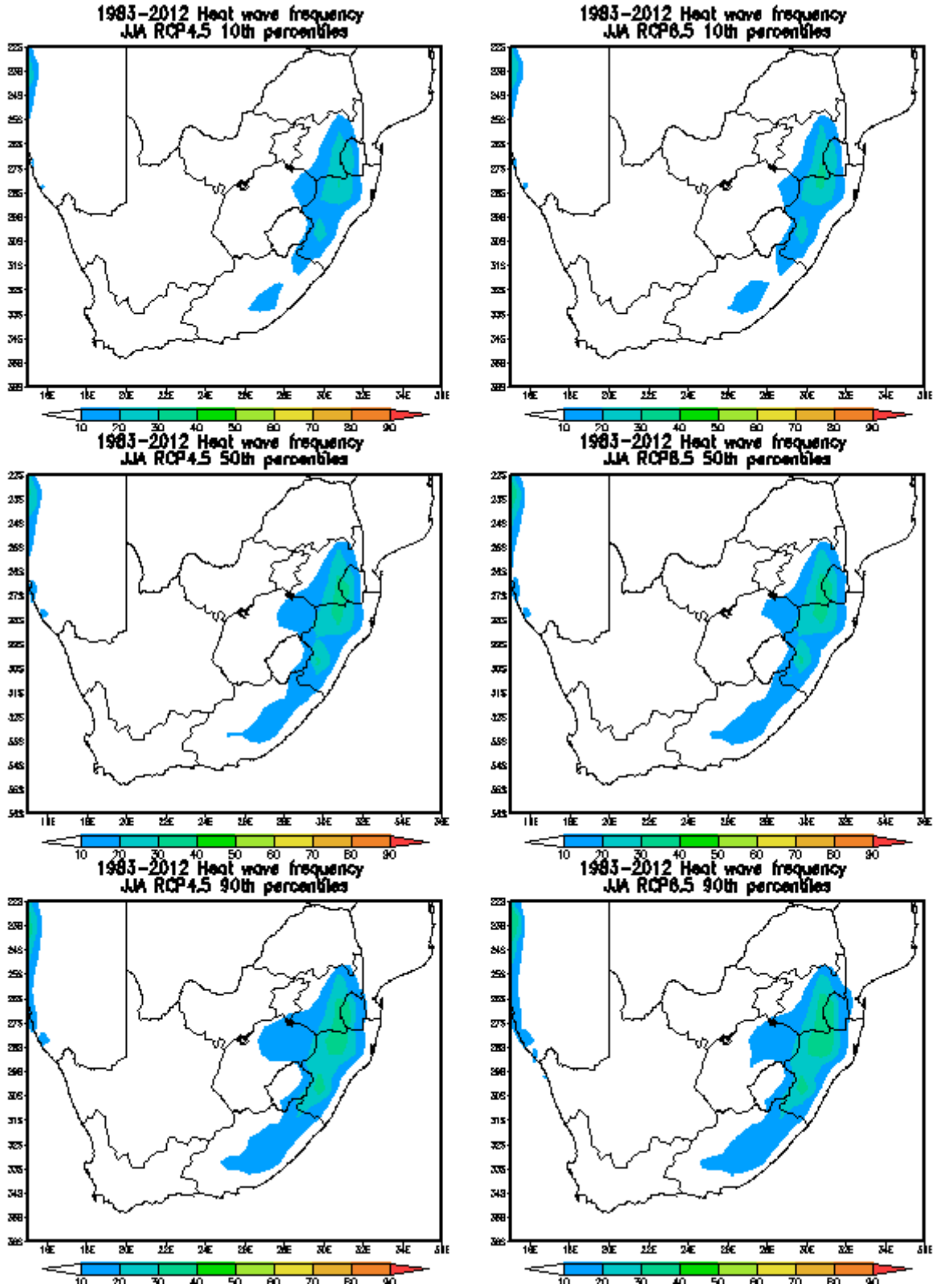

Figure 6.12: Comparisons between RCP4.5 and RCP 8.5 10th, 50th and 90th percentiles of JJA heat wave frequency during 1983-2012.

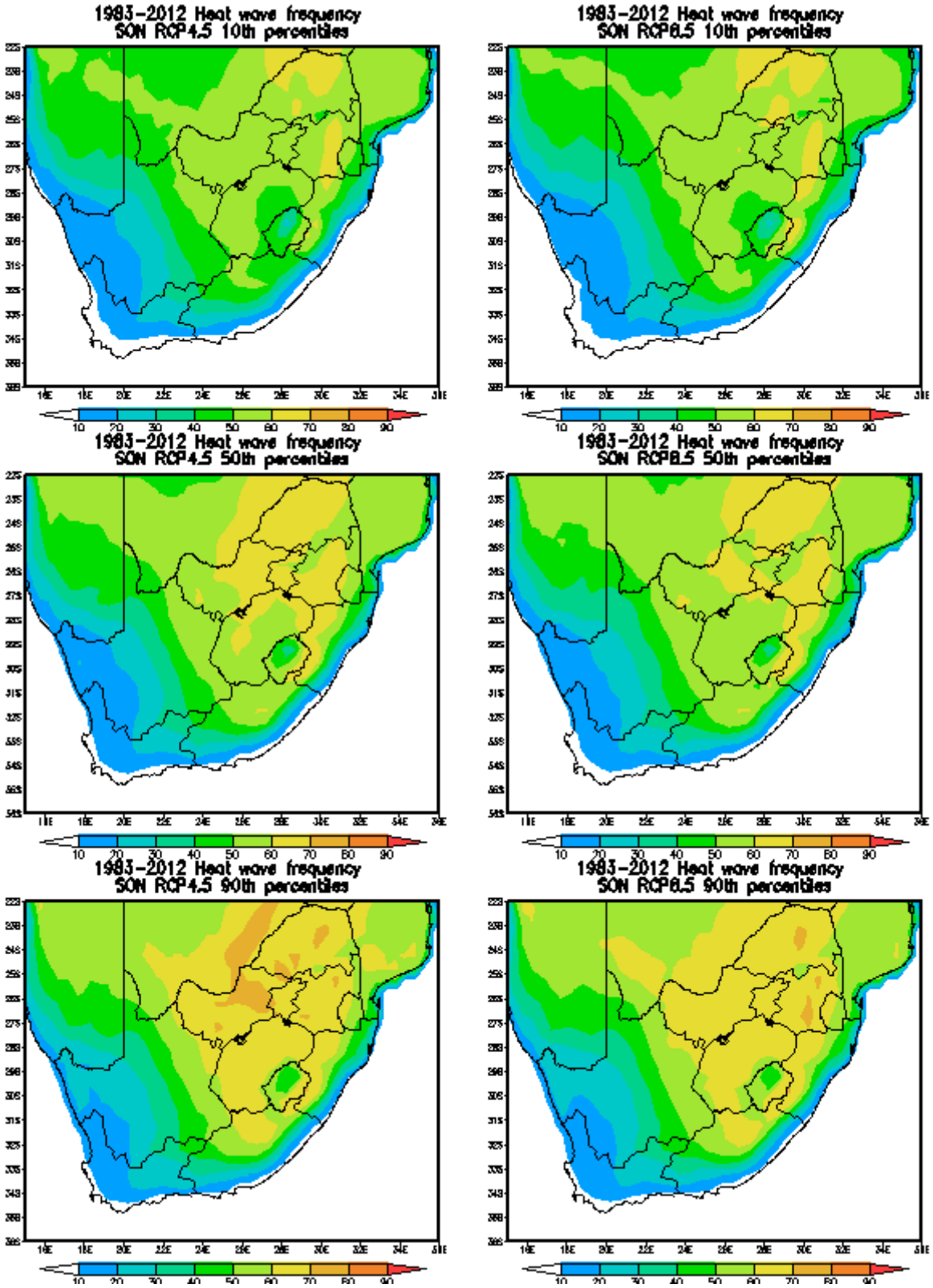

Figure 6.13: Comparisons between RCP4.5 and RCP 8.5 10th, 50th and 90th percentiles of SON heat wave frequency during 1983-2012.

Comparing the CCAM duration output with observations, there is also an agreement that heat waves last longer in the central interior and north-east lowveld regions compared to coastal regions. Both modelled outputs and observations indicate that coastal regions are experiencing shorter lasting heat waves compared to interior regions. The simulated spatiality of heat wave intensity in the present day climate is also consistent with that of observed heat wave frequency during the same period, verifying the suitability of using CCAM to project future heat wave intensity.

With a warming globe the expectation is that the heat wave characteristics may not be the same in future climate as compared to those occurring in current climate. This is largely the average temperatures are increasing, and hence the present day thresholds for defining a heatwave may be exceeded easily. We however still analyse the projected heatwaves using the present day definition, because that is the definition that we experience in our current climate. Very long lasting heatwaves in the future climate may simply mean the average temperature has gotten higher, and perhaps what is considered as a heatwave in the current will not be considered as a heatwave in the future climate using future averages. The subsequent sections provide expected heat wave frequency, duration and intensity in South Africa during the present-day climate and in the future climates, i.e. 2010 to 2039, 2040 to 2069 and 2070 to 2099 periods.

6.4 Heat waves in future climates

6.4.1 Period 2010 to 2039

The number of heatwaves in the immediate future period of 2012 to 2039 is higher than the heatwave frequency in 1983-2012. As expected, the number of heat wave occurrences are higher during the SON and DJF seasons (Figure 6.14-6.16), with areas in the east and northern parts of South Africa projected to experience over 80 events over the 30-year period. The simulations for 2010-3039 indicate is slight increase in the number of heat wave frequency in South Africa, particularly over the eastern parts of the country during the JJA season. Simulated heatwaves of RCP 4.5 and RCP 8.5 scenarios are in agreement with both showing an increase in the events in the future climate. The spatial pattern between the two scenarios is almost similar. Western parts of South Africa are simulated to experience least number of heat waves (less than 10 events in other areas) over this 30-year period during the austral autumn, winter and spring. These are the parts influenced the most by passing cold fronts which are responsible for the winter rainfall.

The average duration of heat waves over South Africa during the 2010-2039 period is projected to increase throughout the year. Regions in the central interior are expected to experience heat waves lasting for over a week during SON and DJF. Just like in the present

day-climate, heat waves occurring in winter will continue to last for few days, i.e. 3-4 days (Figure 6.16). This is thought to be as a results of the cooling effect by adjacent oceans. Heat wave intensity during this period slightly increases throughout the year than during the 1983-2012 period. This increase is more evident on both the 90th percentile of RCP 4.5 and 8.5 in winter with an average increase of about 6°C/30-year period over the Highveld of Mpumalanga and KwaZulu-Natal (Figure 6.17). Simulation also indicate that heat waves are more intense over the Karoo during DJF with a seasonal average ranging from 41-44°C during this period.

6.4.2 Period 2040 to 2069

Heatwave events are projected to be significantly higher during this period than during the present day climate. Some regions, such as the Free State and the Highveld of KwaZulu-Natal, that were simulated as not experiencing heat waves during present-day climate are beginning to experience few events over the 30-year with a dramatic increase in the winter season. Over 20 events are projected to occur over those areas during austral winter.

Dramatic increases in DJF heat wave frequency are expected during the 2040-2069 period (Figure 6.18) when compared to the present climate, particularly along the south and eastern coasts. These regions are expected to experience up to 100 events during summer over the 30-year period; which averages to slightly over three events per summer season per year. However, it has to be noted that these heat waves will last for less than a week along the coasts but the number of days per event increases inland. Increase in the number of heat waves is also more evident over the Karoo during both summer and autumn and the simulations also indicate 2040-2069 heat waves will last the longest, between 9 and 10 days, over this region in summer. This may be associated with the dry conditions over the Karoo, as the region experience little or no rainfall throughout the year. Drier regions heat up quickly because the heating that reaches the surfaces does not start by evaporating water on the surface, which can also result in cooling by latent heat absorption.

There is a continual pattern of heat waves becoming more intense simulated over most parts of the eastern half of South Africa. These increases are more evident in late summer and early winter over the northern parts of the country (Figure 6.19-6.20) where maximum temperatures are higher, as indicated in Chapter 4.

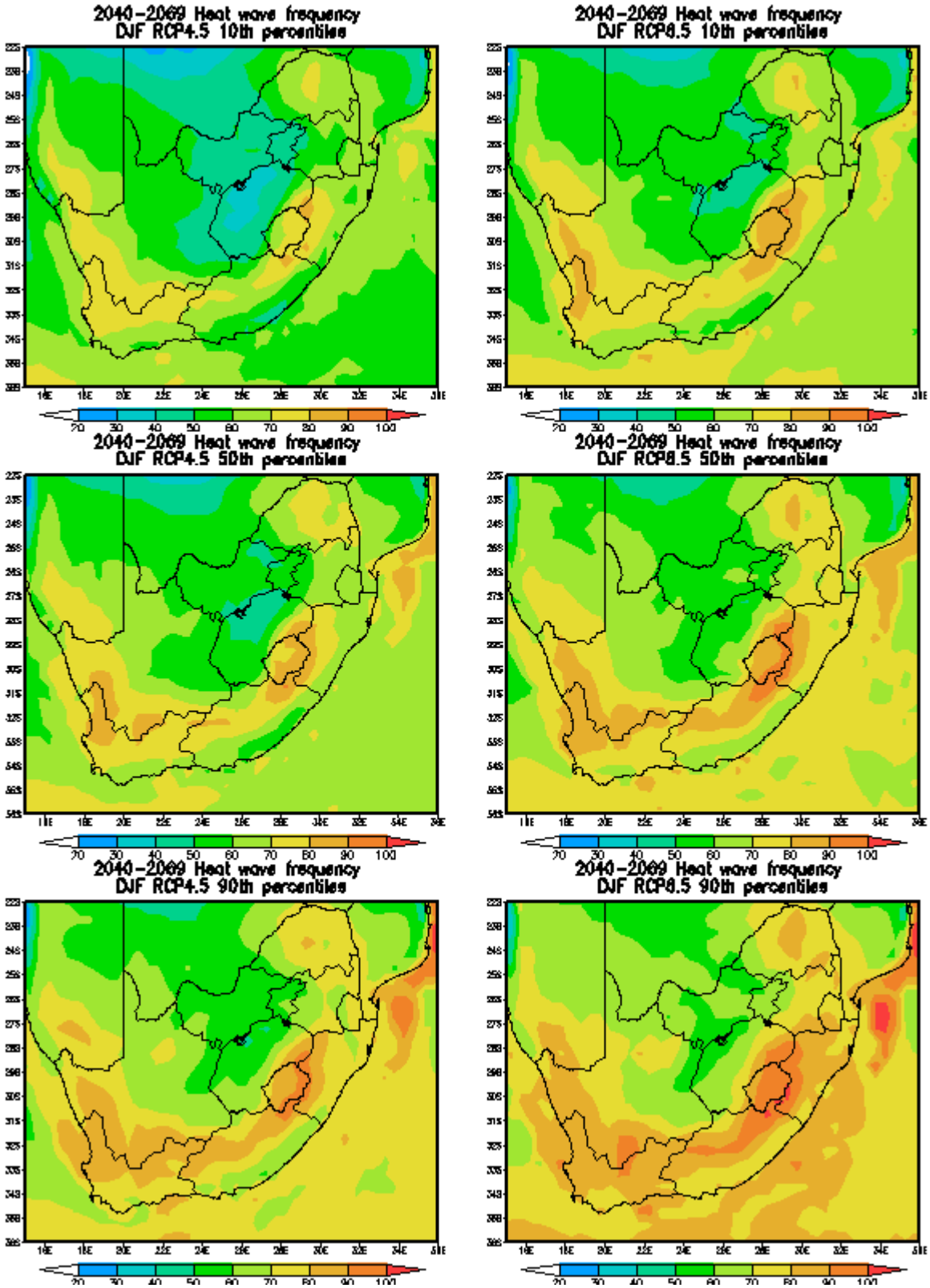

Figure 6.14: Comparisons between RCP4.5 and RCP 8.5 10th, 50th and 90th percentiles of DJF heat wave frequency during 2010-2039.

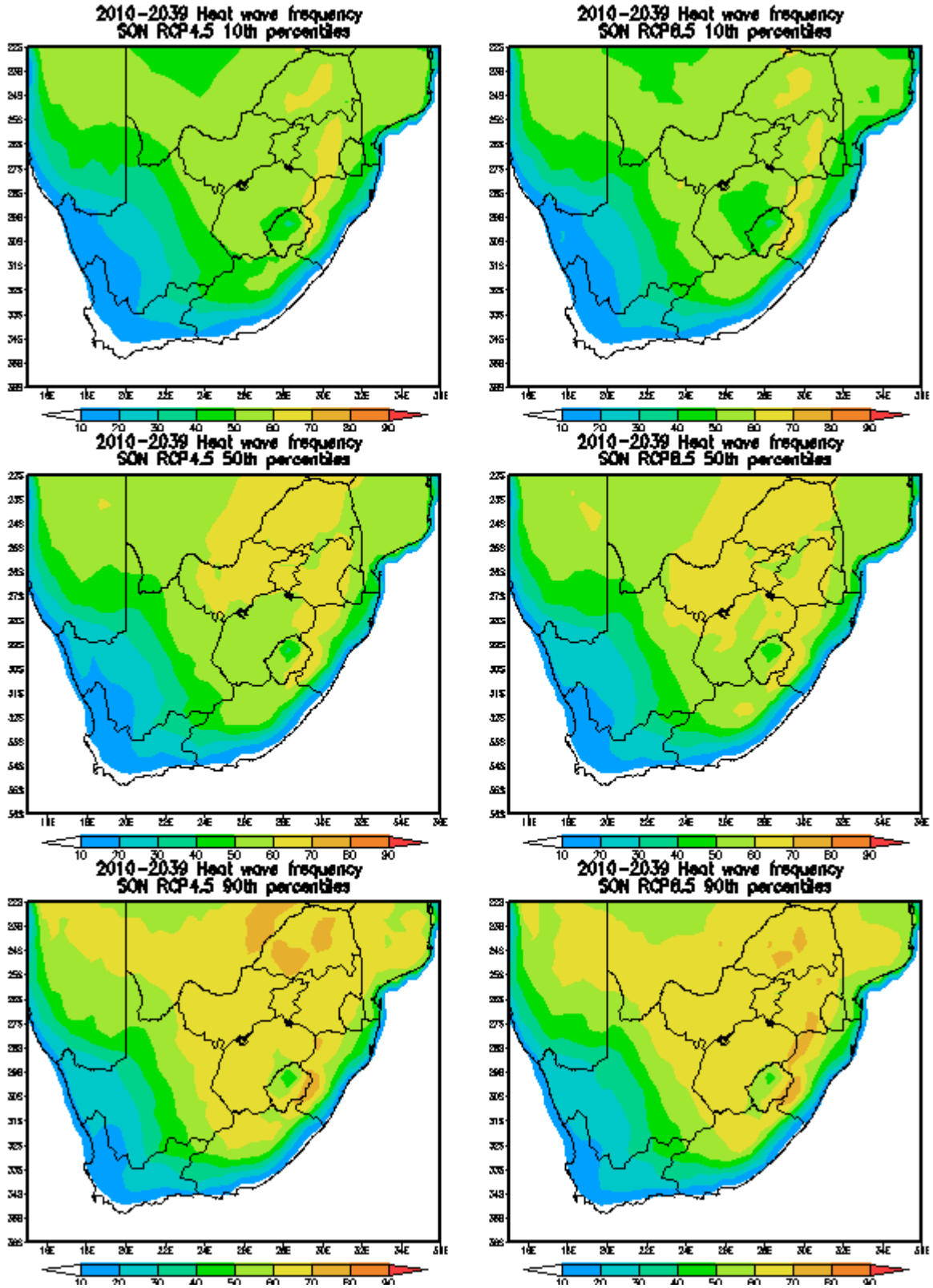

Figure 6.15: Comparisons between RCP4.5 and RCP 8.5 10th, 50th and 90th percentiles of SON heat wave frequency during 2010-2039.

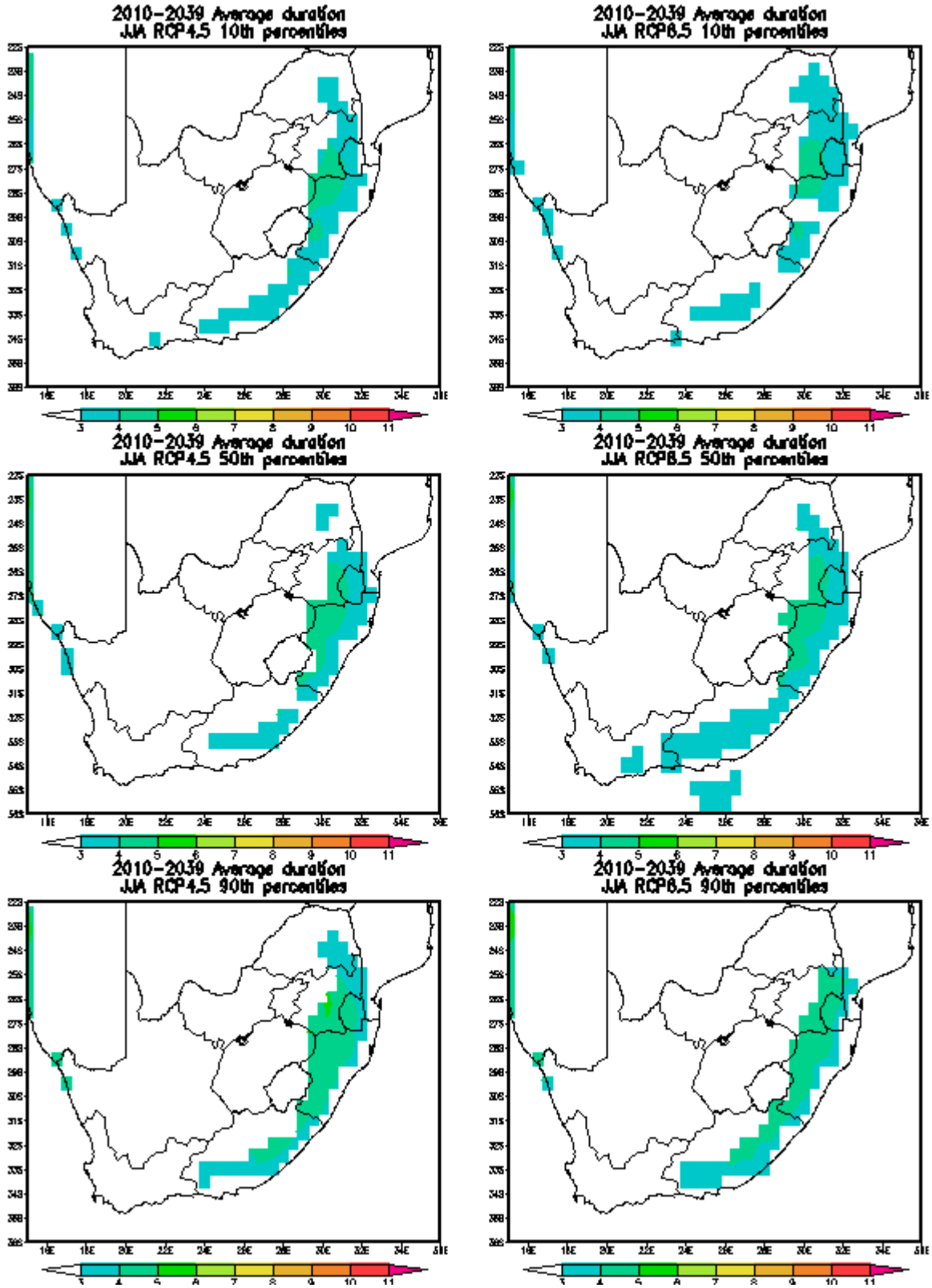

Figure 6.16: Comparisons between RCP4.5 and RCP 8.5 10th, 50th and 90th percentiles of JJA average duration (days) during 2010-2039.

6.4.3 Period 2070 to 2099

Heat wave frequency are expected to increase per season per year towards the end of the 21st century. RCP 8.5 indicates higher increases when compared to RCP 4.5, and the 90th percentile of RCP 8.5 also indicate that the eastern half of South Africa will experience up to 60 events in the 2070-2099 30-year period in all seasons; which averages to 2 heat waves per three month season per year. This increase is most evident during the SON (Figure 6.21) season.

Increases during the 2070-2099 period are slightly more than for the period 2040-2069. However, major differences in these two periods are observed in the average duration. Heat wave events over coastal and eastern regions of the country are expected to last for about a week. Heat waves are projected to be usual events over South Africa and much of the country will experience heat waves lasting for over 10 days, particularly during summer (Figure 6.22). In as much as simulations indicate that coastal regions will experience most heat waves in summer during this 30 year period, the heat waves over the coasts will continue to be the least lasting heat waves in the country.

The heatwaves intensity is projected to dramatically increase from the present day climate towards the end of the 21st century, 2070-2099. It is believed that climate change signal will be stronger during this period than the two other future periods. The eastern parts of South Africa are expected to experience heat waves of low intensity than the west during summer seasons of the same period. This may be linked to convective activities in the east during SON-DJF, which may bring rainfall and relief to high atmospheric temperatures. However, it is projected that heat waves will be more intense on the east during the MAM-JJA compared to the dry western parts of the country (Figure 6.23-6.26).

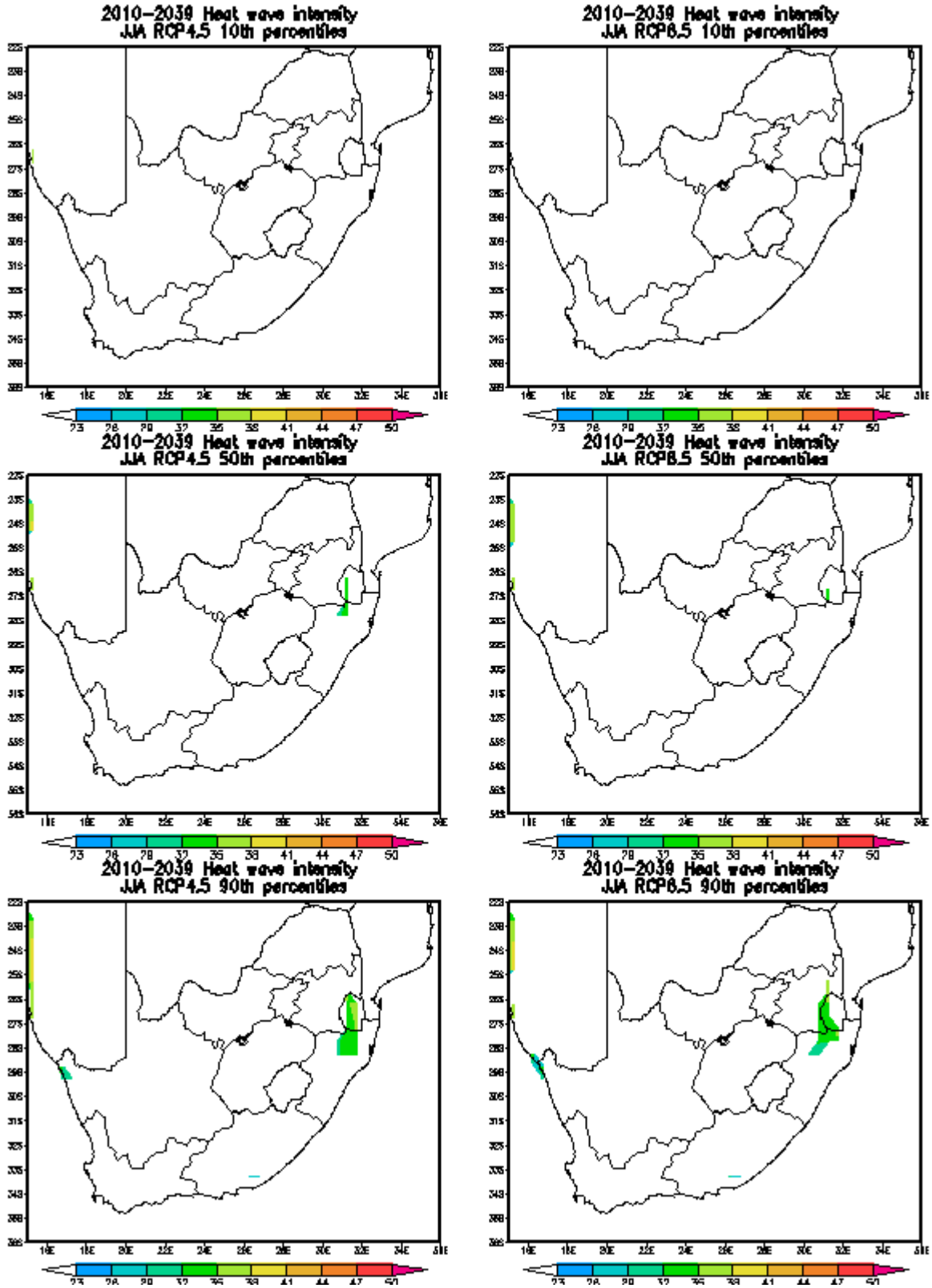

Figure 6.17: Comparisons between RCP4.5 and RCP 8.5 10th, 50th and 90th percentiles of JJA Intensity (°C) during 2010-2039.

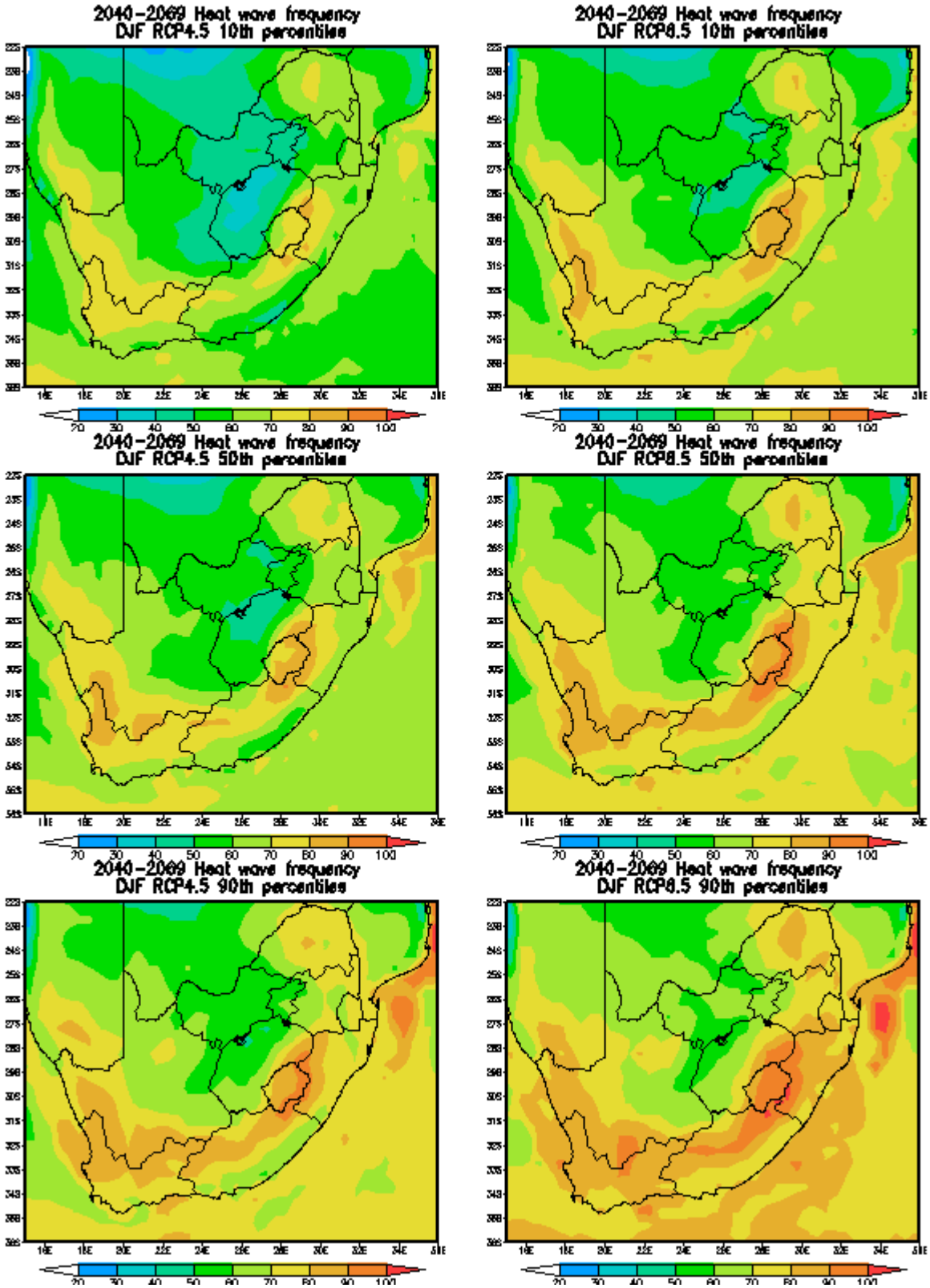

Figure 6.18: Comparisons between RCP4.5 and RCP 8.5 10th, 50th and 90th percentiles of DJF heat wave frequency during 2040-2069.

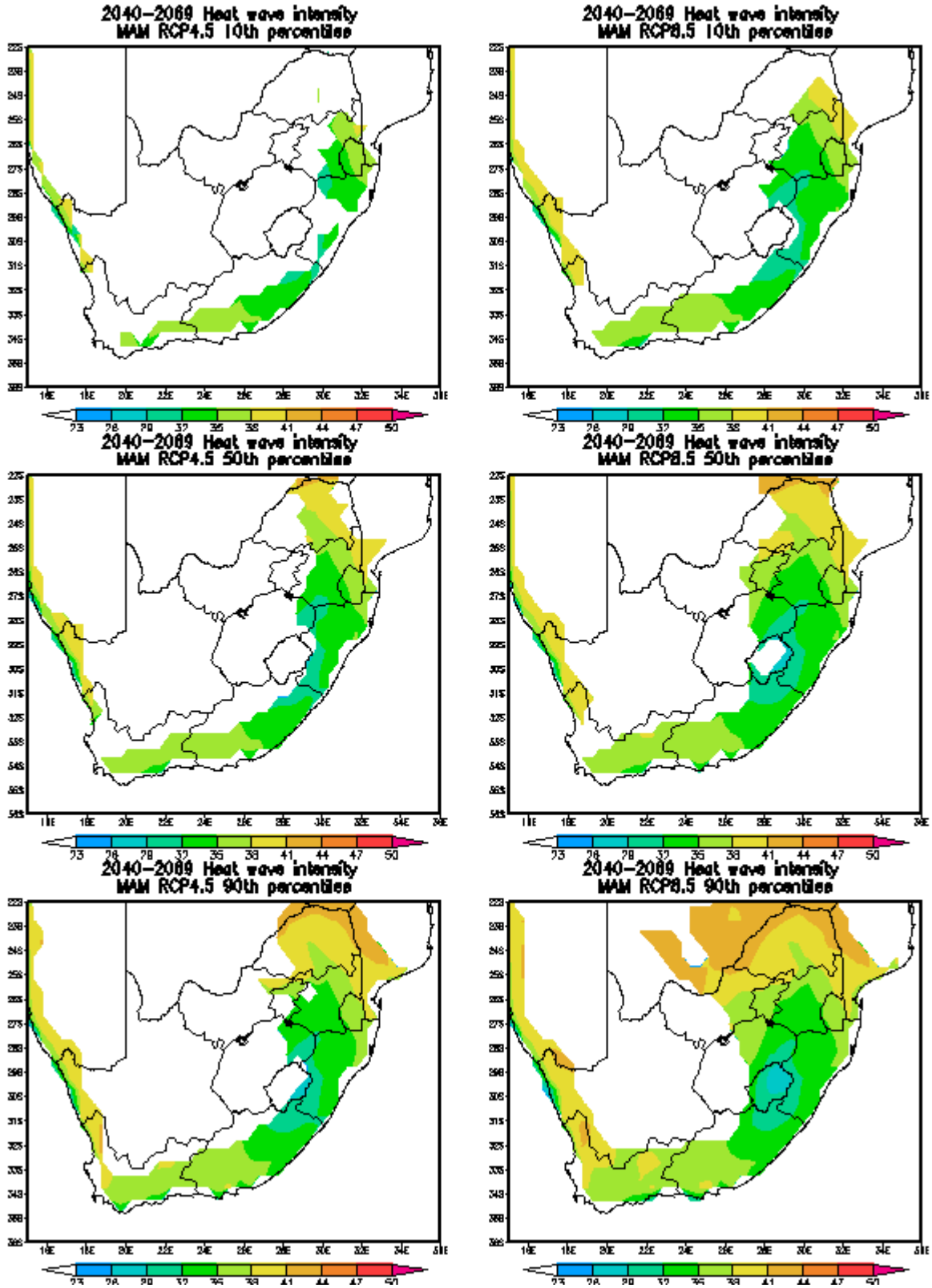

Figure 6.19: Comparisons between RCP4.5 and RCP 8.5 10th, 50th and 90th percentiles of MAM Intensity (°C) during 2010-2039.

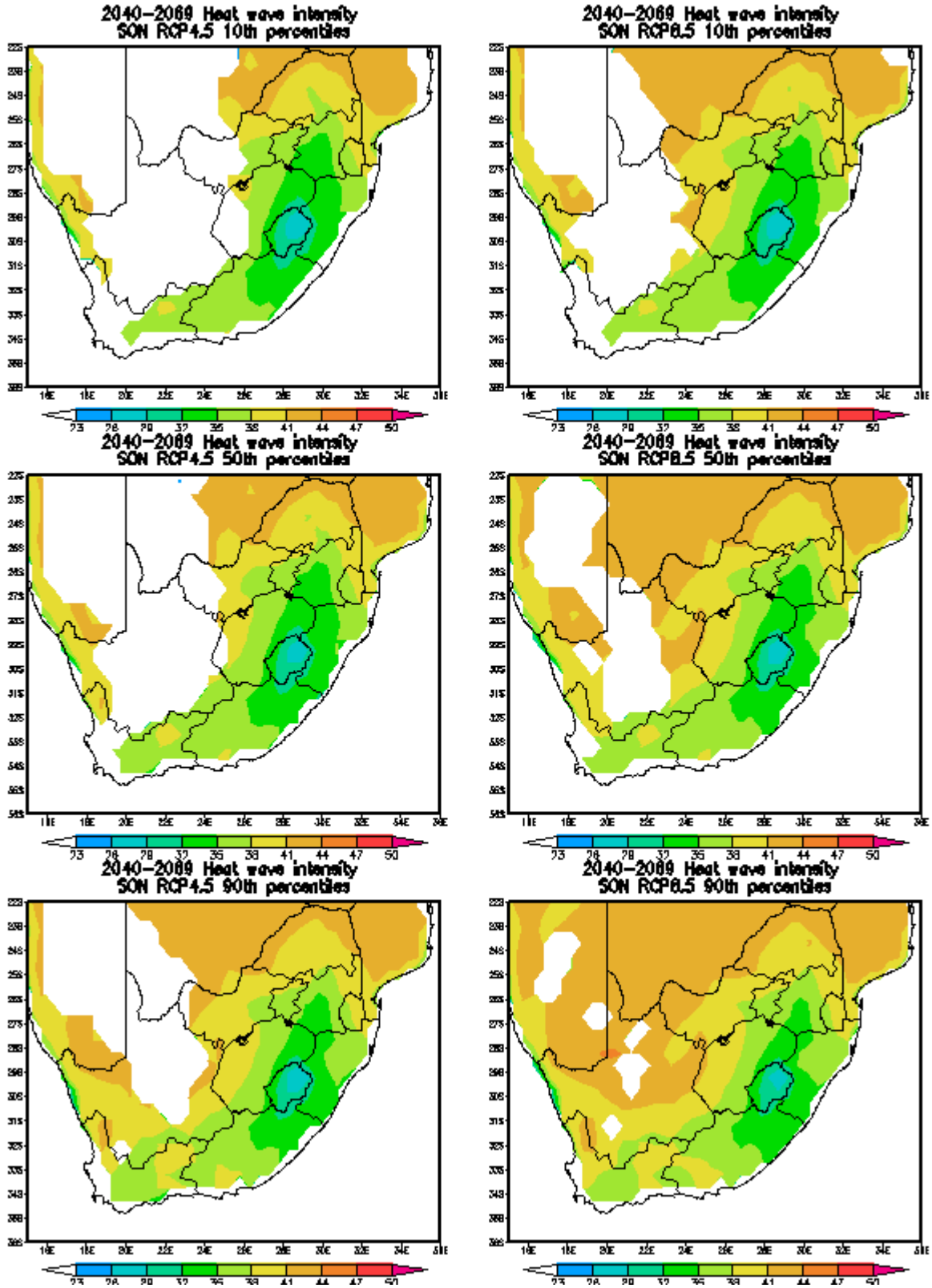

Figure 6.20: Comparisons between RCP4.5 and RCP 8.5 10th, 50th and 90th percentiles of SON Intensity (°C) during 2010-2039.

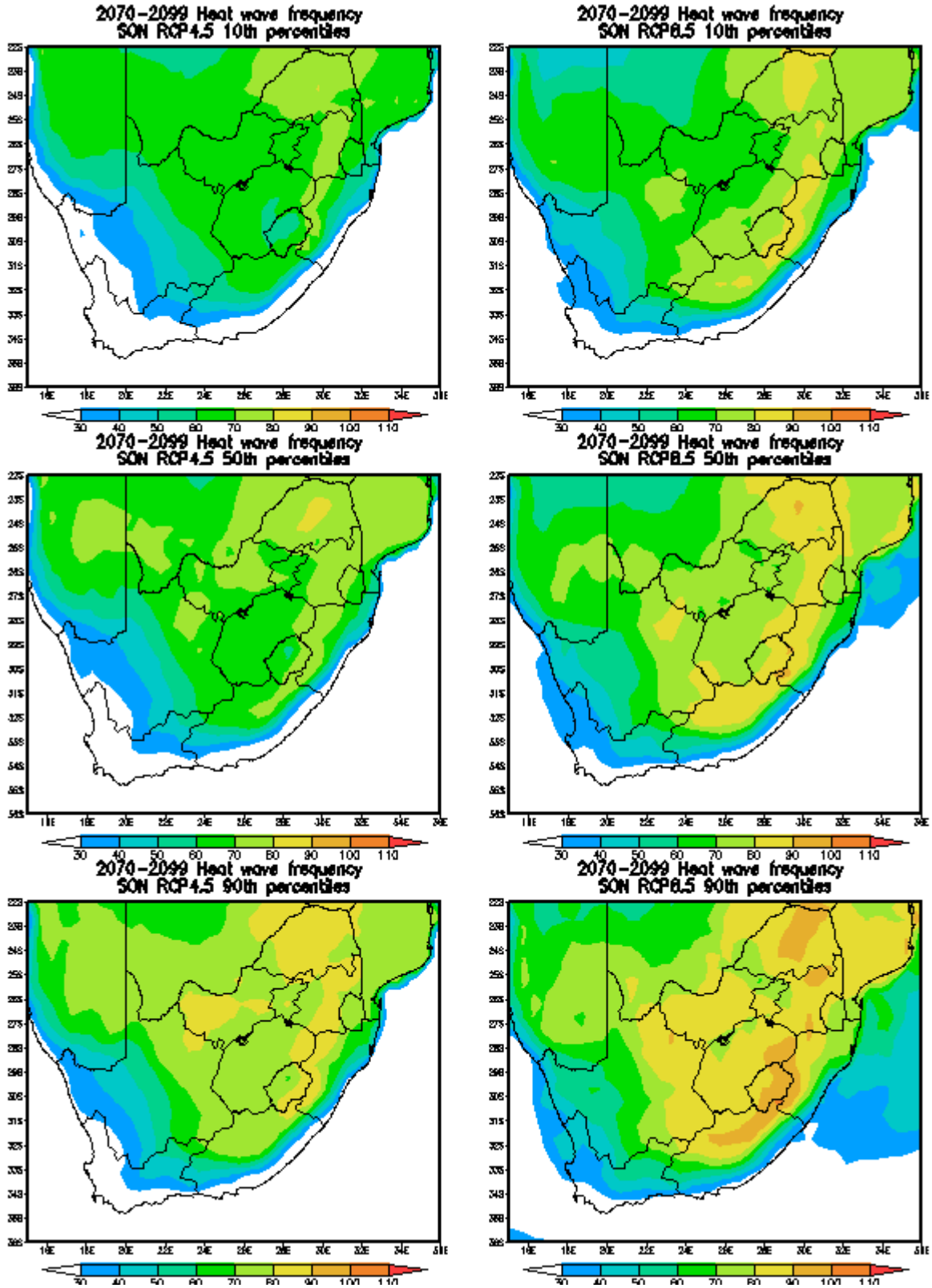

Figure 6.21: Comparisons between RCP4.5 and RCP 8.5 10th, 50th and 90th percentiles of SON heat wave frequency during 2070-2099.

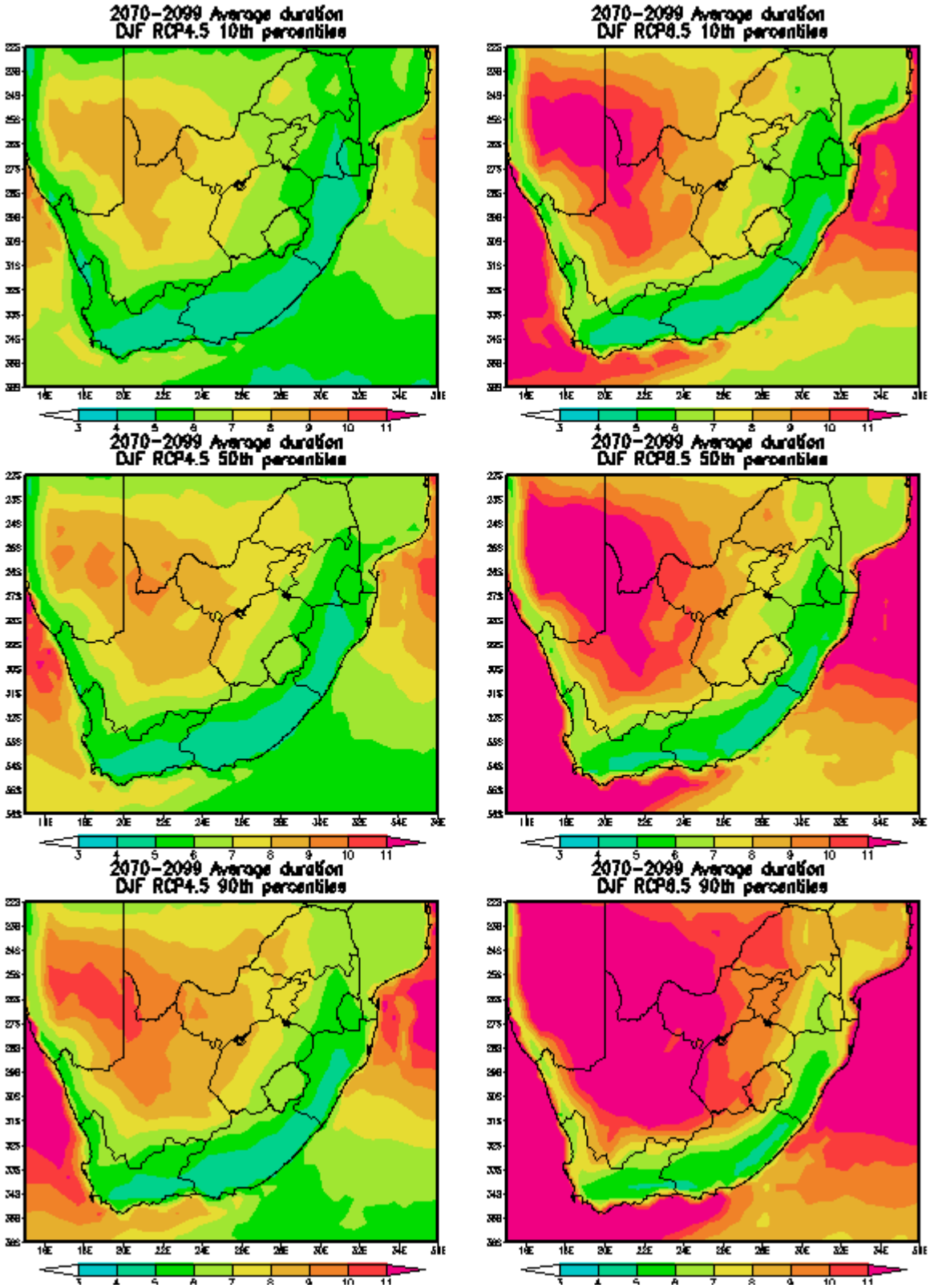

Figure 6.22: Comparisons between RCP4.5 and RCP 8.5 10th, 50th and 90th percentiles of JJA average duration (days) during 2070-2099.

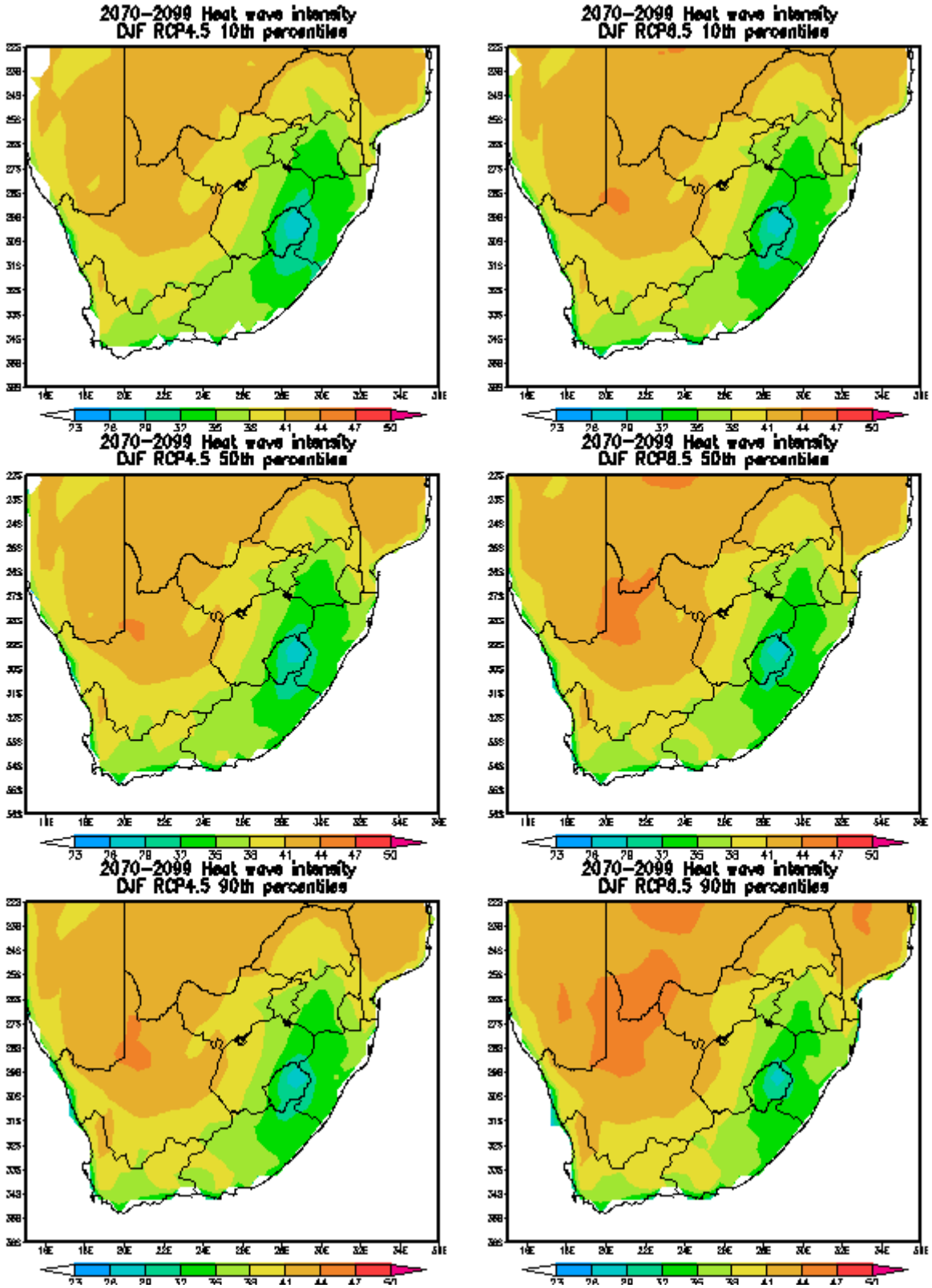

Figure 6.23: Comparisons between RCP4.5 and RCP 8.5 10th, 50th and 90th percentiles of DJF Intensity (°C) during 2010-2039.

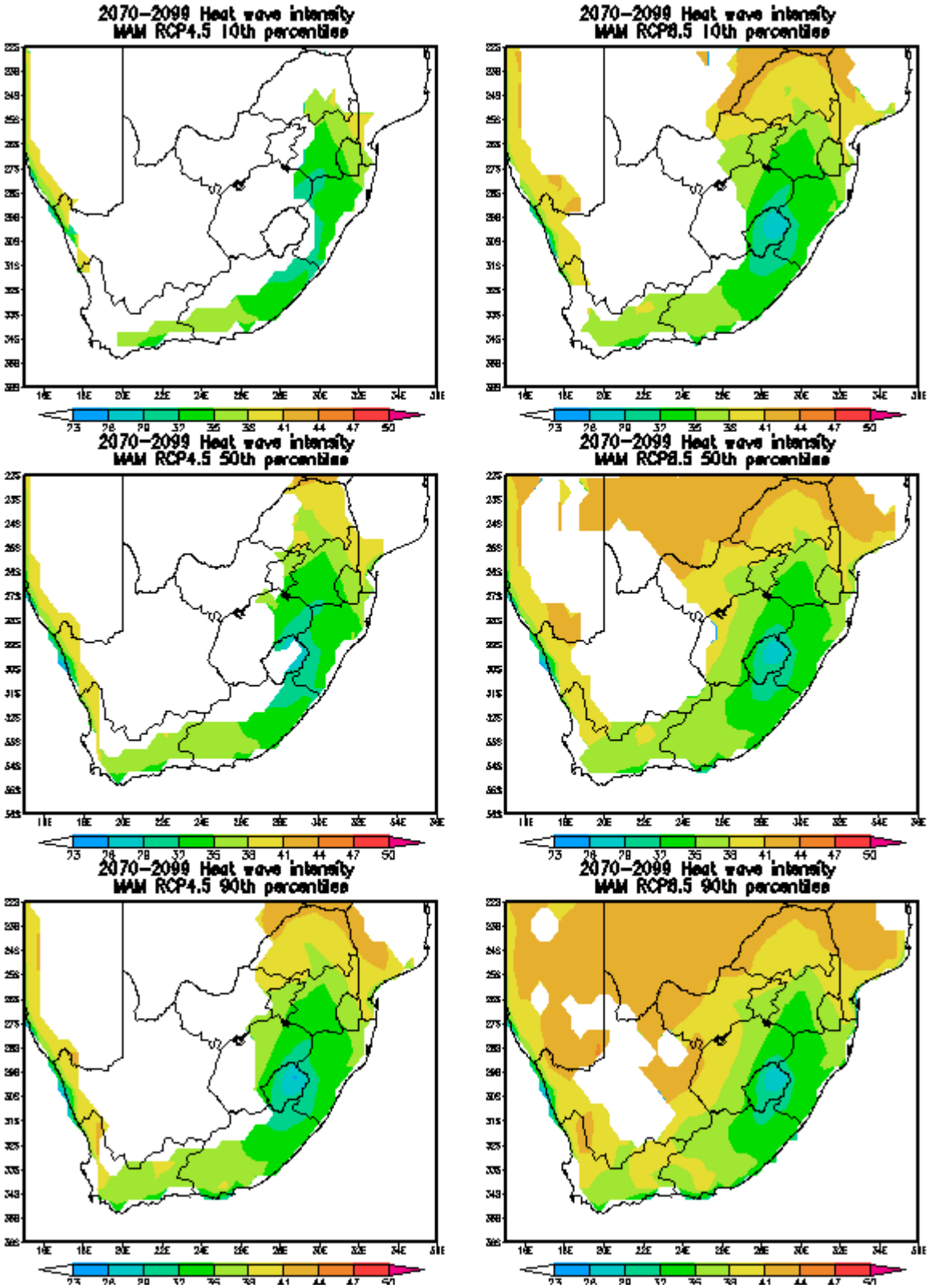

Figure 6.24: Comparisons between RCP4.5 and RCP 8.5 10th, 50th and 90th percentiles of MAM Intensity (°C) during 2010-2039.

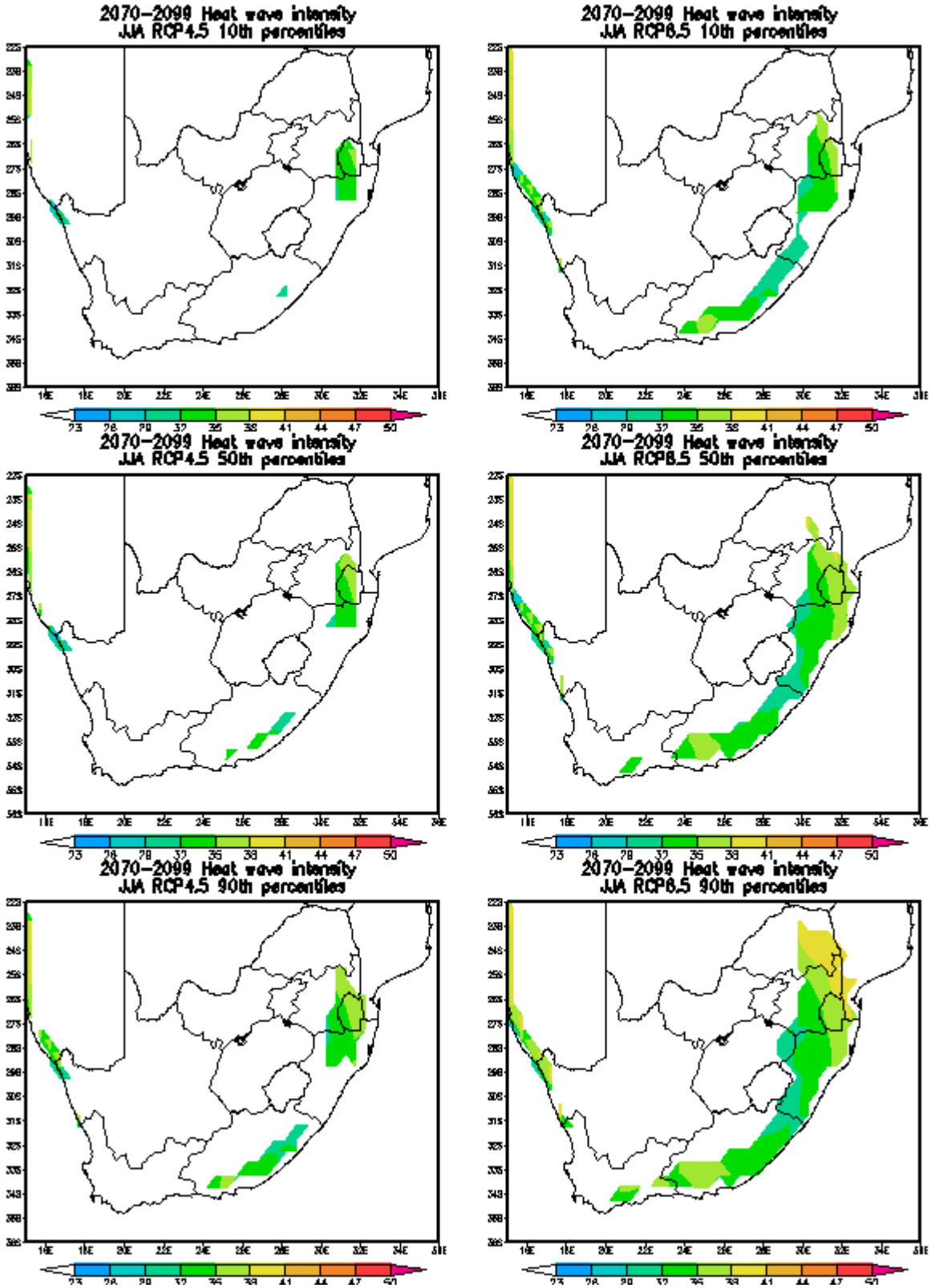

Figure 6.25: Comparisons between RCP4.5 and RCP 8.5 10th, 50th and 90th percentiles of JJA Intensity (°C) during 2010-2039.

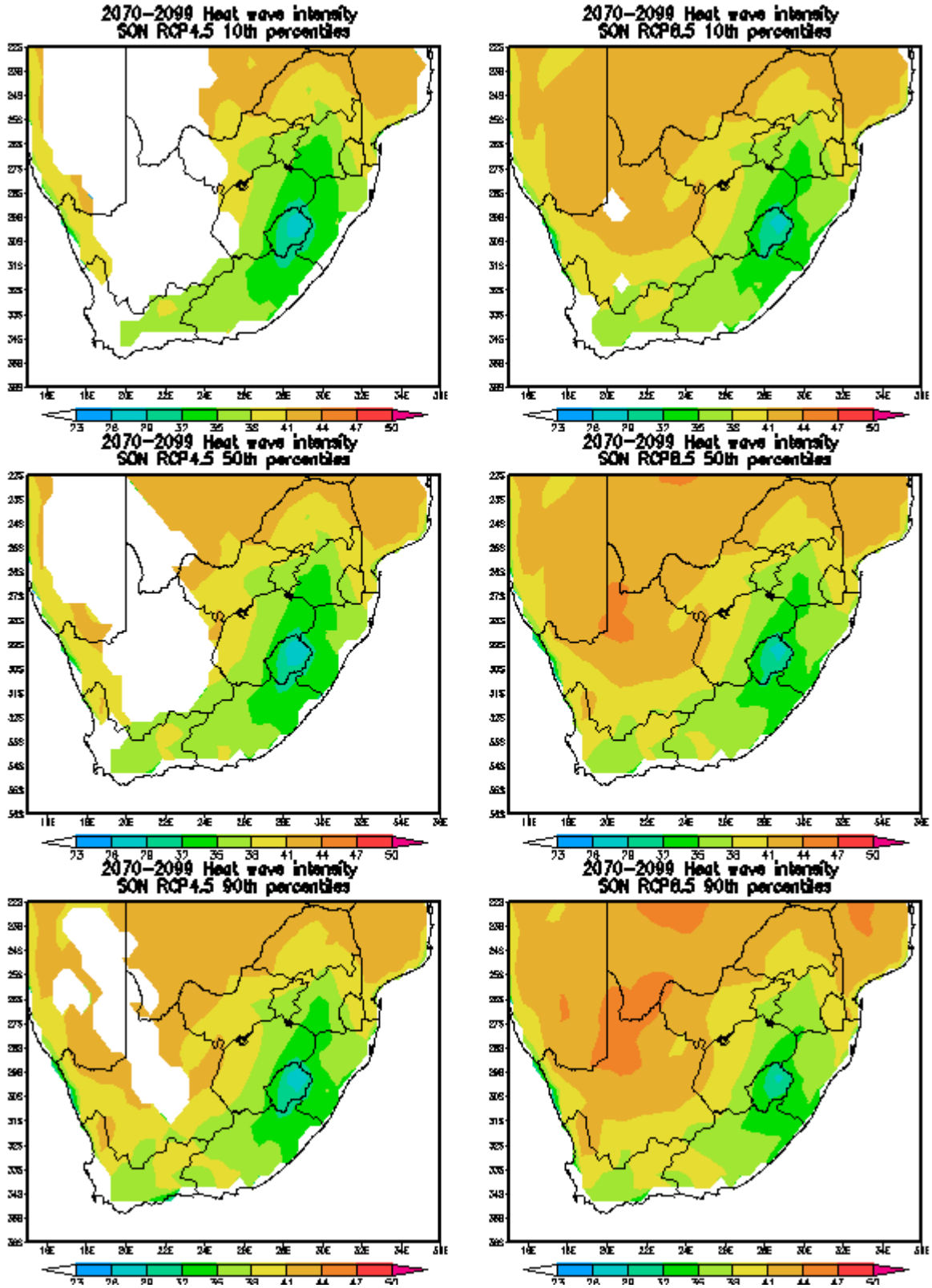

Figure 6.26: Comparisons between RCP4.5 and RCP 8.5 10th, 50th and 90th percentiles of SON Intensity (°C) during 2010-2039.

6.5 Summary

This study has found that heat wave are unusual in the present day climate but are expected to occur more frequently in the future warmer climate when using both RCP 4.5 and RCP 8.5 emission scenarios. It is also indicated that heat waves are also expected to last longer, particularly over the interior and become more intense. CCAM outputs also indicated the following things:-

a) Simulations indicated that maximum temperatures will continue to rise, reaching above 7°C over much of the interior throughout the year during the 2070-2099 period.
b) Simulated heat wave thresholds are consistent with observed heat wave threshold.
c) RCP 4.5 estimates lower number of heat waves and average duration in future warmer climates when compared to RCP 8.5. It also estimates higher maximum temperatures over the country than RCP 8.5.
d) Short lasting heat waves (average of 3-4 days) along the coasts are expected to increase in future climate, however the coasts will continue to have the least lasting heat waves in the country.
e) Least increase is expected for heat waves lasting for longer durations.
f) Karoo is expected to have the most dramatic increase of heat waves than most inland parts of the country.
g) Central interior is not projected to have the most dramatic increase in heat wave frequency, however heat waves over this region are expected to last longer in future climates.
h) Simulations are also in agreement with observations (Figure 1.1) that the southern tip of the country experiences the most warming, as indicated by the higher number of heat wave occurrences.
i) Model is struggling to simulate heat waves along the coasts.

The next chapter discusses key findings and provides fundamental conclusions of the study. It also presents recommendations for future work relevant to this study.

CHAPTER 7

DISCUSSIONS, CONCLUSIONS AND RECOMMENDATIONS

7.1 Introduction

The aim of this study was to analyse the variability, meteorological structure and trends of heat waves over South Africa in the present and future climates. Several studies investigated extreme weather events over South Africa (e.g. Tebaldi *et al*. 2006; Shongwe *et al*. 2009; Galarneau *et al*. 2012; Peterson *et al*. 2012) with more attention on floods and droughts and less attention to heat waves despite the negative impacts on livelihoods these events have in many regions across the country. Folland *et al*. (2001) have established that a global average increment of 0.6°C was observed during the late 20th century but the warming was not temporally and spatially uniform across the world.

Owing to the global continual warming of the atmosphere, weather and climate extremes such as droughts, floods and heat waves are occurring more frequent and becoming even more intense (e.g. Clark *et al*. 2006; Fischer and Schär 2010). This can not only lead to weather-related diseases such as malaria and heat stoke but can also negatively impact the economic status of a country. IPCC (2012) suggest that poor communities are likely to be affected the most by weather and climate extremes. While climate extremes such as droughts and floods received rigorous research attention in recent years in South Africa, less research attention has been given to heat waves.

This study addressed structure of heat waves in the context of South Africa as it is a country that warming is at a higher rate over the whole of southern Africa. The study also investigated the influence of El Niño Southern Oscillation (ENSO) on heat wave frequency and duration. Most heat waves studies have been done in the northern hemisphere (NH) (e.g. Beniston 2004; Cassou *et al.* 2005) because of continentality, while a handful of recent heat wave studies in the SH are based in Australia (e.g. Perkins *et al*. 2013; Nairn and Fawcett 2013; Boschat *et al*. 2014). This may be due to inadequate temperature data in most of the SH, however South Africa is a country that has a good network of temperature stations (New *et al.* 2006) than much of the southern hemisphere (SH).

The aim of this chapter is to provide general conclusions of the study. This chapter discusses how results of this study compares to what is already known in other parts of the world. It also provide recommendations on what can be done on future studies to further analyse and improve the understanding of heat wave characteristics. It is believed that this study will contribute to knowledge about weather extremes and temperature trends over the

country as previously there were contradictions [e.g. Muhlenbruch (1992) and Karl *et al.* (1993)]. The subsequent sections summarises findings of this study.

7.2 Discussion of key findings

7.2.1 Temperature trends over South Africa

Monthly means of maximum and minimum temperatures in inland regions of South Africa have general trends. Minimum and maximum temperatures are consistent. Lowest temperatures are observed between June and August (JJA) while the highest temperatures are observed during the DJF season when most heat waves during the study period were observed. However, the behaviour of temperatures in coastal regions does not have a steep summer-winter gradient like the interior. The interior is fairly warmer than coastal regions throughout the year. Richards Bay and Mount Edgecombe are the only coastal regions with December to February (DJF) minimum temperature exceeding 20°C throughout the year. Northern interior and north-east lowveld experiences hot temperatures in austral summer than most other parts of South Africa.

South Africa is showing positive trends of maximum temperatures in 21 of the 24 selected stations indicating warming of the atmosphere over time, however trends of minimum temperatures in the central plateau is negative. This is because of the extreme lowest minimum temperatures in winter, hence widening the annual diurnal temperature range (DTR) trend. These findings are in agreement with studies by Karl *et al.* (1993), Kruger and Shongwe (2004), New *et al*. (2006), and Kruger and Sekele (2013) who also indicated warming in most parts of the country. Overall, only 3 stations had a negative trend of annual DTR from 1983 to 2013. DTR is usually stronger in winter when heat waves are less frequent in most parts of the country. This confirms earlier findings by Easterling *et al*. (1997) who also found increasing trends of DTR in much of South Africa.

As a result of the observed warming of the atmosphere, the number of warm nights and hot days are increasing while cold nights and cool days are decreasing. This was also found to be the case on a global scale by Gutowski *et al*. (2008). The eastern coast of South Africa experiences stronger negative trends of cold nights. Only one of the 24 selected stations showed a positive trend of cool days and only one station had a negative trend of hot days during the study period.

7.2.2 Heat waves and ENSO

Heat waves are a common feature of South Africa's climate, but are more frequent and last for longer periods during El Niño seasons, particularly over the northern parts where there is also a strong October to March correlation of Southern Oscillation Index (SOI) and maximum temperature during the period investigated. The Niño 3.4 sea surface temperature

correlation with maximum temperature over South Africa is positive, particularly over cluster C. This is in agreement with a more recent study by Engelbrecht *et al*. (2015) over the whole of Africa which suggests that the northern and north-east lowveld of South Africa (Figure 7.1) experiences higher heat wave days.

7.2.3 Heat wave variability over South Africa

Heat waves in much of South Africa are mainly summer occurring events but dominate between December and January in most parts of the country with an exception of the subtropical western coast which usually experience most heat waves per season between March and August. Port Nolloth recorded 71 heat waves between 1983 and 2012, 66 were Divided in March-May (MAM) and JJA.

There was no uniform recurrence pattern of heat wave occurrences during the study period. Some seasons had high heat wave frequency, while no heat waves were observed during other seasons. More than one heat wave can be observed by a station in a season, however other stations (Mount Edgecombe and Cape Agulhas) did not record heat waves between 1983 and 2012. On average, it was observed that most stations (20 of the selected 24 stations) experienced less that heat wave per season during the study period.

Heat wave duration vary across the county. Heat waves in South Africa can last for more than 10 days over inland regions while the longest lasting heat wave during the study period in coastal regions was 7 days, recorded in Richards' bay, KwaZulu-Natal. Marico in the North-West province recorded the longest lasting heat waves (11 days) in South Africa and it was during the strong El Niño season of 1982/1983. This support the finding by Yulaeva and Wallace (1994) that warm phase of ENSO is characterized by warming of the troposphere.

On average, the majority of heat waves during this period last for 4.5 - 6 days in the north-east lowveld, northern and southern interior while an average of less than 4.5 days are observed in the subtropical western and south-east regions. It is good to note that regions such as the subtropical western coast of South Africa experienced high heat wave frequency which are short-lived while much of the interior experienced low frequency over the study period, however lasted for a longer duration.

7.2.4 Structure of heat waves

This study confirmed earlier findings by Tyson and Preston-Whyte (2000) that almost all prolonged heat waves in southern Africa are caused by anticyclonic circulations. All longest lasting heat waves per thermal region were associated with high pressure systems in the middle levels that propagate south-eastward. Descending nature of air in the middle of high pressure systems over South Africa and advection of hot near surface air towards a certain

region usually trigger heat wave occurrences. It was extensively indicated in other studies that heat waves in other parts of the world are associated with anticyclonic circulations (e.g. Kunkel *et al.* 1996; Palecki *et al.* 2001; Fischer *et al.* 2007).

This study also found that heat waves are associated with 850 hPa circulations that are conducive for warm and moist onshore winds in the subtropical western coast which result in the occurrence of berg winds. Kysely (2000) also suggested that cyclonic air circulations are not favourable for Heat wave occurrences. The near-surface winds in the interior are mainly northerly and transport warm and dry air towards the center of South Africa. The 850 hPa winds also transport moisture towards the east of the country during heat waves in cluster B, hence resulting in positive RH anomalies and increasing thermal discomfort over the region. Months when heat waves are recorded experiences soil moisture deficits in much of the country, and this may increase radiation reflectance since dry soils have high albedo compared to moist soils as indicated by Twomey *et al*. (1986).

Convective activities are unlikely to occur during heat waves as positive 200 hPa OLR anomalies are observed during all the longest lasting heat waves per thermal regions, hence it can be said that these events are associated with period of little or no rainfall. The observed negative omega in the middle levels also support that there is usually a subsidence of wind during heat waves. Atmospheric conditions over South Africa during a heat wave can vary considerably. Parts of the country can experience a heat wave while other regions are experiencing cool conditions. Such was observed during the weak La Niña season of 2000/01 when there was a low pressure system associated with low average temperatures between 4 and 9 June.

Eastern part of South Africa then experience higher thermal discomfort because of the above normal RH compared to the western part of the country. This is because of the positive RH anomalies over the east, while regions in the western interior are usually drier. Over 50% of the population in both the eastern lowveld and east coast of the country experiences discomfort with a DI of 92 during the longest lasting heat waves in the respective thermal regions. Less than 50% of the population in the interior feels discomfort during heat waves, while the drier subtropical regions in areas such as Port Nolloth experience less discomfort.

7.2.5 Heat waves in future climates

It has been indicated that on the global scale the magnitudes of the probability of climate extremes occurrences are expected to change in both mean and variance (Figure 7.2) in the future. IPCC (2001) suggested that on average, the world is expected to experience more hot weather events. However, that may not be the case on regional basis. Several studies

investigated temperature projections over Africa (e.g. Garland *et al*. 2015; Engelbrecht *et al*. 2015), with less emphasis on the structure and circulations of warm temperature extreme events such as heat waves in South Africa. In addition to the nature of heat waves in the present climate, this study also investigated the characteristics of heat waves in South Africa in a future warmer climate. Average maximum Simulations indicated that maximum temperatures will continue to rise, reaching over 7°C much of the interior throughout the year during the 2070-2099 period. This increases the likelihood of having intense and frequent heat wave occurrences.

Simulated heat wave thresholds are consistent with observed heat wave threshold. It was established in this study that heat waves will occur more frequent in future climates, especially during DJF season. The simulations also indicate that heat wave frequency increases with time and last longer, particularly in the interior of South Africa. Regions that are not prone to heat wave occurrences in the present-day climate are expected to experience heat waves in the future warmer climate.

Western coast experiences much of its heat wave events in mid-winter, and that is also expected to continue in future climates. Winter heat wave events are expected to extend to the eastern interior and also increasing in intensity. Heat waves in South Africa are not only increasing in frequency, but are also expected to last longer and become more intense. The increasing intensity is more evident with RCP 8.5 than 4.5. As in the present-day climate, it is also expected that in future climates heat waves will last longer, over 2 weeks in rare circumstances, over the interior of the country compared to coastal regions. In conclusion, heat waves in much of South Africa are expected to occur more frequently, last longer and become more intense.

7.3 Future work

Analysis and interpretations are provided from chapter 4 to chapter 6 in achieving the aim and objectives of this study outlined in chapter 1. While other results confirms what is already known about heat waves in other regions across the world, this study also contribute new scientific knowledge about the characteristics of heat waves with respect to South Africa during both the present and future climates.

It was mentioned earlier that heat waves have not received rigorous research attention over South Africa, as a result the impacts of heat waves on human health over the country are not well documented. However, some findings about the structure and circulations confirmed what is already known about heat waves in different parts of the world. Therefore a study

about the impacts of heat waves in the context of South Africa is recommended in order to observe whether the impacts are consistent worldwide.

This study indicated that both surface temperature over a certain region and circulation patterns transporting warm air towards that region can jointly lead to the occurrence of heat waves. When studying the occurrence of heat waves, it will also be good to quantify the contributions of warm air advection and land surface temperature in warming the atmosphere. This can also enhance the predictability of these events in the future warmer climate and benefit potential users (such as farmers and health facilities) of this information in taking informed decisions.

By far, the vast majority of South Africa depends on rain-fed agriculture. This therefore necessitate the need to investigate the relationship between heat wave impacts on agricultural yields as earlier studies (e.g. Change and Wallace 1987; Lyon 2009; Gershunov *et al*. 2009; Albright *et al.* 2010) have established a relationship between heat waves and droughts in other countries. In addition, heat waves and droughts last for different time scales and this study indicated that much of South Africa experiences dry conditions during warm temperature extremes. It is therefore recommended that links between heat waves and dry spells should be developed which can assist in formulating mitigation and/or adaptation strategies of heat waves on agricultural impacts.

The understanding of heat waves should be accompanied by precautionary measures to the hot conditions by the public. Weather and climate information should be utilized in a manner that seeks to save lives and property. Hence, it is of utmost importance to develop a project which aims to issue early warnings about heat wave occurrences and improve responses of the public and other parties affected in different parts of South Africa to extreme events such as heat wave occurrences.

It is established in this study that heat waves in South Africa tends to be more frequent during droughts seasons, hence impacts of heat waves and droughts should not be studied separately. The following questions remained unsolved:-

a) To what extent does the co-occurrence of heat waves and droughts affect agricultural yields?
b) Is there a direct correlation between heat wave occurrence and mortality rate in South Africa?
c) To what extent does the ocean-atmosphere interaction influence the occurrence and intensity of heat waves in the perspective of South Africa?

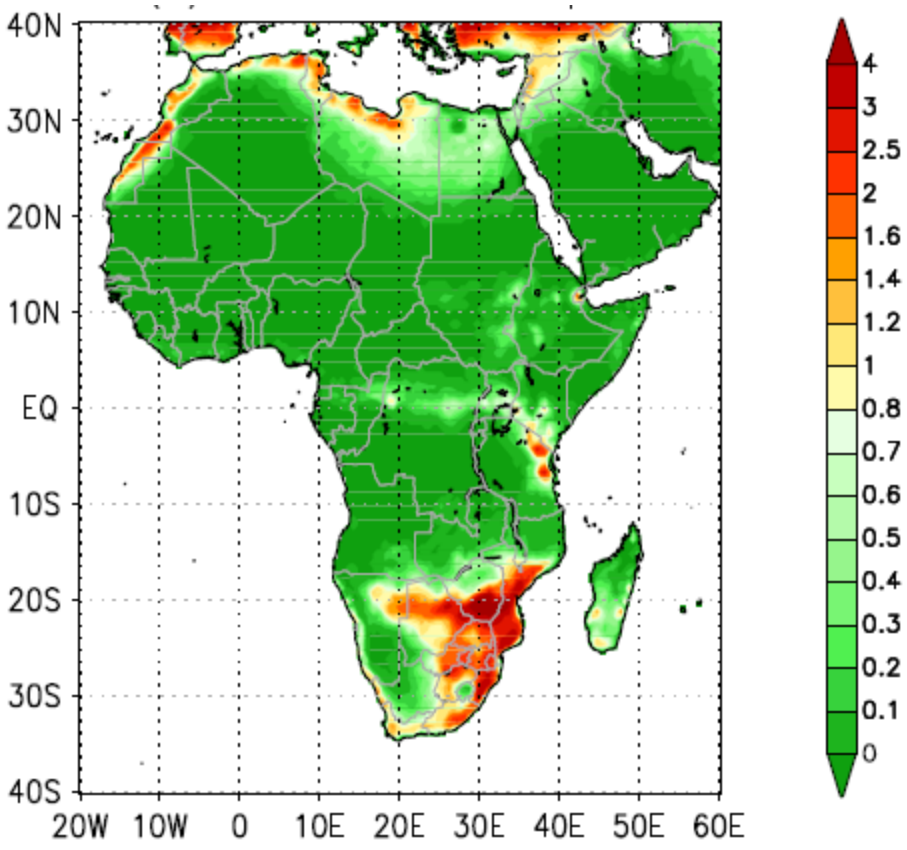

Figure 7.1: Annual average number of heat wave days between 1961 and 1990 over Africa (Source: Engelbrecht *et al*. 2015).

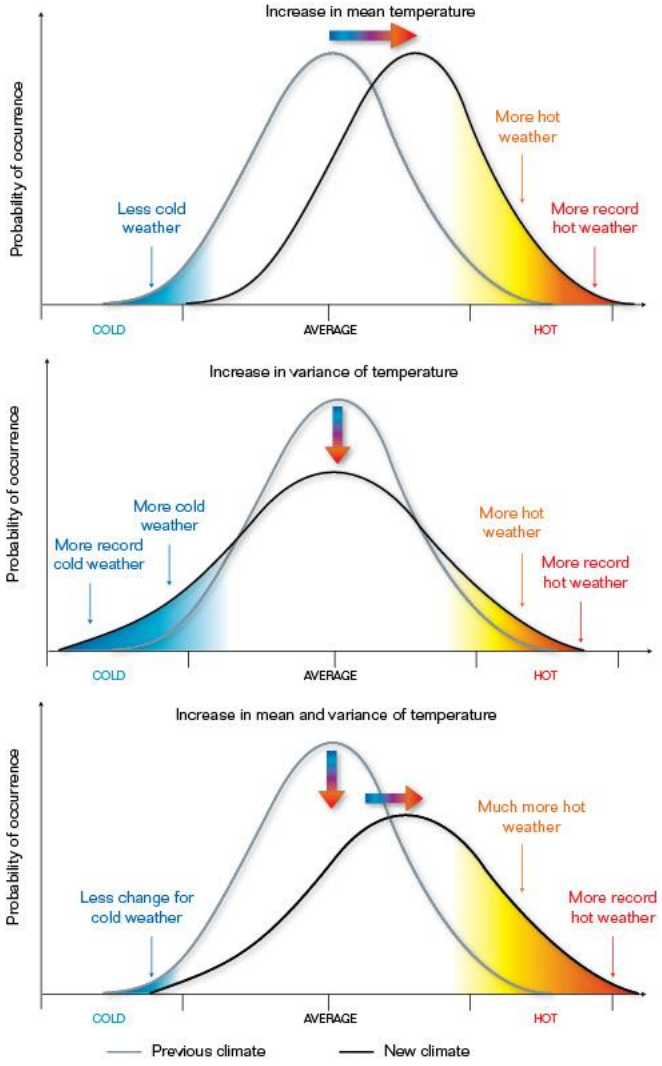

Figure 7.2: Theoretical changes in climate variable: the sequence indicates change of temperature extremes when the mean, variance, and both mean and variance of temperature increases in the future warmer climate (Source: IPCC 2001).

REFERENCES

Acock, M.C. and Pachepsky, Y.A.A. 2000. Estimating missing weather data for agricultural simulations using group method of data handling. *J. Appl. Meteor*., 39, 1176–1184.

Adams, R.M., Hurd, B., Lenhart, S. and Leary, N. 1998. The Effects of Global Warming on Agriculture: An Interpretative Review. *J. Clim. Res,* 11, 19–30.

Albright, T.P., Pidgeon, A.M., Rittenhouse, C.D., Clayton, M.K., Wardlow, B.D., Flather, C.H., *et al*. 2010. Combined effects of heat waves and droughts on avian communities across the conterminous United States. *Ecosphere,* 15, 1–22.

Albright, T.P., Pidgeon, A.M., Rittenhouse, C.D., Clayton, M.K., Flather, C.H., Culbert, P.D., *et al*. 2011. Heat waves measured with MODIS land surface temperature data predict changes in avian community structure, *Remote Sens. Environ.*, 115,245–254.

Allen, R.J. and De Gaetano, A.T. 2001. Estimating missing daily temperature extremes using an optimized regression approach. *Int. J. Climatol*., 21, 1305–1319. *And Remote Sensing*, 35, 980−996.

Alley, R.B., Bernetsen, T., Bindoff, N.L., Chen, Z., Chidthaisong, A., Friedlingstein, P., *et al*. 2007. Summary for Policymakers. Climate Change 2007. The Physical Science Basis. S. Solomon et al., Eds., Cambridge University Press, 1–18.

Anderson, B.G. and Bell, M.L. 2009. Weather-related mortality: how heat, cold, and heat waves affect mortality in the United States. *Epidemiology*, 20, 205–213.

Archer, E., Engelbrecht, F., Landman, W., Le Roux, A., van Huyssteen, E., Fatti, C., *et al*. 2010. *South African Risk and Vulnerability Atlas*, CSIR and DST, Pretoria.

Aydinalp, C. and Cresser, M.S. 2008. The effect of global climate change on agriculture. *American-Eurasian J. Agric. Environ. Sci*. 3, 672–676.

Barnston, A. 2015. Why are there so many ENSO indexes, instead of just one? *NOAA Climate.gov*. Available online at https://www.climate.gov/news-features/blogs/enso/why-are-there-so-many-enso-indexes-instead-just-one (Accessed on 7 March 2016).

Bartzokas, A., Lolis, C.J., Kassomenos, P.A. and McGregor, G.R. 2013. Climatic characteristics of summer human thermal discomfort in Athens and its connection to atmospheric circulation. *Nat. Hazards Earth Syst. Sci*., 13, 3271–3279.

Basara, J.B., Basara, H.G., Illston, B.G. and Crawford, K.C. 2010. The Impact of the urban heat island during an intense heat wave in Oklahoma City, *Adv. Meteorol.*, 230365, doi: 10.1155/2010/230365

Benhin, J.K.A. 2006. Climate change and South African agriculture: Impacts and adaptation options. CEEPA Discussion Paper No. 21. Centre for Environmental Economics and Policy in Africa, University of Pretoria.

Beniston, M. 2004. The 2003 heat wave in Europe: A shape of things to come? An analysis based on Swiss climatological data and model simulations. *Geophys. Res. Lett.*, 31, L02202.

Beniston, M. and Stephenson, D.B. 2004. Extreme climatic events and their evolution under changing climatic conditions. *Global and Planetary Change*, 44, 1–9.

Bhavika B. 2007. The influence of terrain elevation on lightning density in South Africa. *Master's thesis*, University of Johannesburg

Bi, P., Williams, S., Loughnan, M., Lloyd, G., Hansen, A., Kjellstrom, T., *et al*. 2011. The effects of extreme heat on human mortality and morbidity in Australia: implications for public health. *Asia Pac J Public Health*, 23, 27S–36S.

Bolund, P. and Hunhammae, S. 1999. Ecosystem services in urban areas. *Ecological economics*, 29, 293–301.

Boschat, G., Pezza, A.B., Simmonds, I., Perkins, S.E., Cowan, T. and Purich, A. 2014. Large scale and sub-regional connections in the lead up to summer heat wave and extreme rainfall events in eastern Australia. *Clim. Dyn.,* doi: 10.1007/ s00382-014-2214-5, in press.

Brabson, B.B., Lister, D.H., Jones, P.D. and Palutikof, J.P. 2005. Soil moisture and predicted spells of extreme temperatures. *J. Geophys. Res.,* 110, D05104, doi: 10.1029/2004JD005156.

Bureau of Meteorology, 2013. A prolonged autumn heat wave for southeast Australia. Special Climate Statement 45, Australian Bureau of Meteorology, 11 pp. Available online at http:// www.emknowledge.gov.au/resource/?id53569 (Accessed on 16 March 2015).

Cassou, L., Terray, L., Phillips, A. 2005. Tropical Atlantic influence on European heat waves. *J Climate*, 18, 2805–2811.

Cerne, S.B., Vera, C.S. and Liebmann, B. 2007. The nature of a heat wave in eastern Argentina occurring during SALLJEX. *Mon Wea Rev*, 135, 1165–1174.

Chai, H., Cheng, W., Zhou, C., Chen, X. Ma, X. and Zhao, S. 2011. Analysis and Comparison of Spatial Interpolation Methods for Temperature Data in Xinjiang Uygur Autonomous Region, China. *Natural Science*, 3, 999–1010.

Chang, F.C. and Wallace, J.M. 1987. Meteorological conditions during heat waves and droughts in the United States Great Plains. *Mon. Wea. Rev.*115, 1253–1269. Emissivity and temperature from EOS/MODIS data. *IEEE Transactions on Geoscience.*

Chikoore, H. 2005. Vegetation feedback on the boundary layer climate of southern Africa. *Master's thesis*, University of Zululand.

Christy, J. R., W. B. Norris, and McNider, R.T. 2009. Surface temperature variations in East Africa and possible causes. *J. Clim*ate., 22, 3342–3356.

Clark, R.T., Brown, S.J. and Murphy, J.M. 2006. Modelling Northern Hemisphere summer heat extreme changes and their uncertainties using a physics ensemble of climate sensitivity experiments. *J. Climate*, 19, 4418–4435.

Cleveland, W.S. 1979. Robust locally weighted regression and smoothing scatterplots. *J. Am. Stat. Assoc.,* 74**,** 829–836.

Cook, J., Nuccitelli, D., Green, S.A., Richardson, M., Winkler, B., Painting, R., et al. 2013. Quantifying the consensus on anthropogenic global warming in the scientific literature. *Environ. Res. Lett*., 8, 024024.

Coumou, D and Rahmstorf, S. 2012. A decade of weather extremes, *Nat. Clim. Change*, 2, 491–496.

Cowan, T., van Rensch, P., Purich, A. and Cai, W. 2013. The association of tropical and extra-tropical climate modes to atmospheric blocking across south-eastern Australia. *J. Climate*, 26, 7555–7569, doi:10.1175/JCLI-D-12-00781.1.

Cowan, T., A. Purich, S. Perkins, A. Pezza, G. Boschat, and Sadler, K. 2014. More frequent, longer, and hotter heat waves for Australia in the twenty-first century. *J. Climate*, 27**,** 5851–5871, doi: 10.1175/JCLI-D-14-00092.

CPC NOAA, 2015. ENSO: Recent Evolution, Current Status and Predictions. Available at http://www.cpc.ncep.noaa.gov/ (Accessed on 23 September 2015).

Crichton, M. 2003. Aliens Cause Global Warming. The Caltech Michelin Lecture, January 17, 2003. Available at www.crichton-official.com/speeches/speeches_quote04.html (Accessed: 11 May 2015).

Cubasch, U., Wuebbles, D., Chen, D., Facchini, M.C., Frame, D., Mahowald, N., *et al*. 2013. Introduction. In: Climate Change 2013. The Physical Science Basis. Contribution of Working Group I to the Fifth Assessment Report of the Intergovernmental Panel on Climate Change [Stocker, T.F., Qin, D., Plattner, G.K., Tignor, M., Allen, S.K., Boschung, J., *et al.* (Eds.)]. Cambridge University Press, Cambridge, United Kingdom and New York, NY, USA.

D'Amato, G., Cecchi, L., D'Amato, M. and Annesi-Maesano, I. 2014. Climate change and respiratory diseases. *Eur Respir Rev*, 23,161–9.

Davis, C.L. 2011. Climate risk and vulnerability. *A handbook for southern Africa. Pretoria*: Council for Scientific and Industrial Research.

Doty, B. 1995. The Grid Analysis and Display System (GrADS) version 1.5.1.12. Manual (Fairfax, VA: Center for Ocean-Land-Atmosphere Studies).

Du Plessis, J. 2003. Maize production, Department Agriculture, Republic of South Africa, Pretoria.

Easterling, D.R. 1997. Maximum and minimum temperature trends for the globe. *Science*, 277, 364–367.

Easterling, D.R., Karl, T.R., Gallo K.P., Robinson, D.A., Trenberth, K.E. and Dai, A. 2000. Observed climate variability and change of relevance to the biosphere. *J. Geophys. Res.,* 105, 20101- 20114.

Easterling, W.E. and Aggarwal, P.K. 2007. Food, Fibre and Forest Products. Climate change 2007. Impacts, adaptation and vulnerability. Contribution of Working Group II to the Fourth Assessment Report of the Intergovernmental Panel on Climate Change. Eds: Parry, M.L., Canziani, O.F., Palutikof,

Engelbrecht F. A., McGregor J.L. and Engelbrecht C. 2009. Dynamics of the Conformal-Cubic Atmospheric Model projected climate change signal over southern Africa. *Int. J. Climatol*., 29, 1013–1033.

Engelbrecht F.A. 2005. Simulations of climate and climate change over southern and tropical Africa with the conformal-cubic atmospheric model. In: Schulze, R.E. (Ed) Climate Change and Water Resources in Southern Africa: Studies on Scenarios, Impacts, Vulnerabilities and Adaptation. Chap. 4. Water Research Commission Report 1430/1/05

Engelbrecht F.A., Landman, W.A., Engelbrecht, C.J., Landman, S., Roux, B., Bopape, M.J., *et al*. 2011. Multi-scale climate modelling over southern Africa using a variable-resolution global model. *Water SA,* 37,647–658.

Engelbrecht, F.A., Adegoke, J., Bopape, M.J., Naidoo, M., Garland, R.M., Thatcher, M., *et al*. 2015.Preojections of rapidly rising surface temperatures over Africa under low mitigation. *Environ. Res. Lett*.,.doi:10.1088/1748-9326/10/8/085004

Epstein, Y. and Moran, D.S. 2006. Thermal comfort and the heat stress indices, *Ind. Health*, 44, 388–398.

FAO, 2007. Adaptation to climate change in agriculture, forestry, and fisheries: perspective, framework and priorities. FAO, Rome.

Ferranti, L. and Viterbo, P. 2006. The European summer of 2003: sensitivity to soil water initial conditions. *J. Climate*, 19, 3659–3680.

Feudale, L. 2006. Large scale extreme events in surface temperature during 1950–2003: An observational and modelling study, *Ph.D. Thesis*, George Mason University.

Feudale, L. and Shukla, J. 2007. Role of Mediterranean SST in enhancing the European heat wave of summer 2003. *Geophys. Res. Lett.,* 34, doi: 10.1029/2006GL027, 991

Feudale, L. and Shukla, J. 2010. Influence of sea surface temperature on the European heat wave of 2003 summer. Part II: a modelling study. *Clim. Dyn.,* doi: 10.1007/s00382-010-0789-z

Fink, A.H., Brucher, T. Kruger, A., Lackebusch, G.C., Pinto, J.G. and Ulbrich, U. 2004. The 2003 European summer heat waves and drought—Synoptic diagnosis and impacts. *Weather*, 59, 209–216.

Finley, J. and Raphael, M. 2007. The relationship between El Niño and the duration and frequency of the Santa Ana winds of Southern California. *Professional Geographer*, 59,184–192.

Fischer, E.M. 2007. The role of land–atmosphere interactions for European summer heat waves: Past, present and future. *PhD dissertation*, University of Bern, Switzerland.

Fischer, E.M. and Schär, C. 2010. Consistent geographical patterns of changes in high-impact European heat waves. *Nat. Geosci*., 3, 398–403.

Fischer, E.M., Seneviratne, S.I., Lüthi, D. and Schär, C. 2007. The contribution of land–atmosphere coupling to recent European summer heat waves. *Geophys. Res. Lett.* 34, L06707. Doi: 10.1029/2006GL029068.

Folland, C.K., Karl, T.R., Christy, J.R., Clarke, R.A., Gruza, G.V., Jouzel, J., *et al.* 2001. Observed Climate Variability and Change, in: Climate Change .2001. The Scientific Basis. Contribution of Working Group I to the Third Assessment Report of the Intergovernmental Panel on Climate Change, edited by: Houghton, J. T., Ding, Y., Griggs, D. J., Noguer, M., van der Linden, P. J., Dai, X., *et al.*

Fontana, G., Toreti, A., Ceglar, A. and De Sanctis, G. 2015. Early heat waves over Italy and their impacts on durum wheat yields. *Nat. Hazards Earth Syst. Sci*., 15, 1631–1637.

Forsyth, G., Kruger, F.G., and Le Montre, C.G. 2010. *National Veldfire Risk Assessment: Analysis of exposure of social, economic and environmental assets of veldfire hazards in South Africa*: CSIR. National Resources and the Environment CSIR, Fred Kruger Consulting cc.

Fowler, C.T. 2003. Human health impacts of forest fires in the Southern United States: a literature review. *J. Ecol Anthropol*., 7, 39–63.

Galarnean, T.J., Hamill, T.M., Dole, R.M. and Perlwitz, J. 2012. A multiscale analysis of the extreme weather events over Western Russia and Northern Pakistan during July 2010. *Mon. Wea. Rev*., 140, 1639–1664

Gale, P., Brouwer, A., Ramnial, V., Kelly, L., Kosmider, R., Fooks, A.R. and Snary, E.L. 2010. Assessing the impact of climate change on vector-borne viruses in the EU through the elicitation of expert opinion. *Epidemiol. Infect*. 138, 214–125.

Garland, R., Matoaane, M., Engelbrecht, E., Bopape, M.M., Landman, W.A., Naidoo, M., *et al.* 2015. Regional projections of extreme apparent temperature days in Africa and the related potential risk to human health. *Int. J Environ Res Public Health* 2015, 12, 10, 12577–12604.

Gershunov, A., Cayan, D. and Iacobellis, S. 2009. The great 2006 heat wave over California and Nevada: Signal of an increasing trend. *J. Climate*, 22, 6181–6203, doi:10.1175/2009JCLI2465.1.

Gornall, J., Betts, R., Burke, E., Clark, R., Camp, J., Willet, K., *et al*. 2010. Implications of climate change for agricultural productivity in the early twenty-first century. *Phil. Trans. R. Soc*. B, 365, 2973–2989.doi:10.1098/rstb.2010.0158

Guo, Z., Dirmeyer, P.A. and DelSole, T. 2011. Land surface impacts on subseasonal and seasonal predictability, *Geophys. Res. Lett.*, 38, L24812. Doi: 10.1029/2011GL049945.

Gutowski, W.J., Hegerl, G.C., Holland, G.J., Knutson, T.R., Mearns, L.O., Stouffer, R.J., *et al.* 2008. Causes of Observed Changes in Extremes and Projections of Future Changes in *Weather and Climate Extremes in a Changing Climate. Regions of Focus: North America, Hawaii, Caribbean, and U.S. Pacific Islands*. Karl, T.R., Meehl, G.A., Miller, C.D., Hassol, S.J., Waple, A.M. and Murray, W.L. (eds.). A Report by the U.S. Climate Change Science Program and the Subcommittee on Global Change Research, Washington, DC.

Guttman, N.B., 1999. Accepting the Standardized Precipitation Index: A calculation algorithm. *J. Amer. Water Resour. Assoc.*, 35, 311–322.

Hajat, S., Armstrong, B., Baccini, M., Biggeri, A., Bisanti, L., Russo, A., *et al*. 2006. Impact of high temperature on mortality: is there an added heat wave effect? *Epidemiology*, 17, 632-638.

Hayes, M.J., Svoboda, M.D., Wilhite, D.A. and Vanyarkho, O.V. 1999. Monitoring the 1996 drought using the standardized precipitation index. *Bull. Amer. Met. Soc*., 80, 429–438.

Hartmann, D.L., Klein Tank, A.M.G., Rusticucci, M., Alexander, L.V., Brönnimann, C.S., *et al*. 2013. Observations: Atmosphere and Surface. In: Climate Change 2013. The Physical Science Basis. Contribution of Working Group I to the Fifth Assessment Report of the Intergovernmental Panel on Climate Change [Stocker, T.F., Qin, D., Plattner, G.K., Tignor, M., Allen, S.K., Boschung, J., *et al.* (Eds.)]. Cambridge University Press, Cambridge, United Kingdom and New York, NY, USA.

HIG. 2005. Heat Island Group world-wide web: http://HeatIsland.LBL.gov. Lawrence Berkeley National Laboratory, Berkeley, CA.

Holben, B.N. 1986. Characteristics of maximum-value composite images from temporal AVHRR data. *Int. J. Rem. Sens.*, 7, 1417–1434.

Hollander, M. and Wolfe, D.A. 1973. Nonparametric Statistical Inference, John Wiley, Hoboken, N. J.

Houghton, J.T., Ding, Y., Griggs, D.J., Noguer, M. van der Linden, P.J., Dai, X., *et al.* 2001. *Climate Change 2001. The Scientific Basis*. Cambridge University press, 944 pp.

Howe, A.S. and Boden, B.P. 2007. Heat-related illness in athletes. *Am. J. Sports. Med.,* 35, 1384–1395.

Hulme, M., Doherty, R., Ngara. T., New. M. and Lister. D. 2001. African climate change 1900– 2100. *Clim Res*., 17, 145–168.

Hunt, B.G. 2007. A climatology of heat waves from a multi-millenial simulation. *J Climate,* 20, 3802–3821.

Hussein, K., Calvosa C., Roy, R. and the Global Environmental Facility Unit/IFAD, 2008. The effects of climate change on small holder farmers in West and Central Africa. Published for the 10th Meeting of the Africa Partnership Forum, April 2008, Tokyo, Japan.

Huth, R., Kysely, J. and Pokorna, L. 2000. A GCM simulation of heat waves, dry spells, and their relationship to circulation. *Climatic Change,* 46, 29–60.

IPCC. 2001. Climate Change. The Scientific Basis. Contribution of Working Group I to the Third Assessment Report of the Intergovernmental Panel on Climate Change. Cambridge University Press, Cambridge, United Kingdom and New York.

IPCC. 2007. Summary for Policymakers. In: Climate change 2007: Impacts, adaptation and vulnerability. Contribution of Working Group II to the Fourth Assessment Report of the Intergovernmental Panel on Climate Change: Parry, M.L., Canziani, O.F., Palutikof, J.P., Van der Linden, P.J. and Hanson, C.E., Cambridge, Cambridge University Press**:** 1000.

IPCC. 2012. Summary for Policymakers. In: Managing the Risks of Extreme Events and Disasters to Advance Climate Change Adaptation. A Special Report of Working Groups I and II of the Intergovernmental Panel on Climate Change Eds. Field, C.B.,

Barros, V., Stocker, T.F., Qin, D., Dokken, D.J., Ebi, K.L., *et al.*, editors. (Cambridge: Cambridge University Press) 1–19

Jan, N. 2015. El Niño and La Niña Years and Intensities Based on Oceanic Niño Index (ONI). Golden gate weather services. Available at http://ggweather.com/enso/oni.htm (Accessed: 22 September 2015)

Jones, P.D. 1994. Hemispheric surface air temperature variations: a reanalysis and an update to 1993. *J. Climate*, 7, 1794–1802

Jury, M.R, Rouault, M., Weeks, S. and M. Schormann, 1997. Atmospheric boundary-layer fluxes and structure across a land-sea transition zone in south-eastern Africa. *Boundary-Layer Meteorology,* 83,311–330.

Jury, M.R., Pathack, B. and Sohn, B.J. 1992. Spatial structure and interannual variability of summer convection over southern Africa and the SW Indian Ocean. *S. Afri. J. Sc.*, 88, 275–280.

Kanamitsu, M., Ebisukazi, W., Woollen, J., Kengyang, S., Hnilo, J., Fiorino, M., *et al.* 2002. NCEO-DOE AMIP-II Reanalysis (R2): An updated NCEP/NCAR reanalysis covering 1971- present feature new physics and observed soil moisture forcing and also eliminates several previous errors. *Bull. Amer. Meteor. Soc.* DOI: 10.1175/BAMS-83-11-1631.

Karl, T.R. and Knight, R.W. 1997. The 1995 Chicago heat wave: How likely a recurrence? *Bull. Amer. Meteor. Soc.*, 78, 1107–1119.

Karl, T.R., Jones, P.D., Knight, R.W., Kukla, G., Plummer, N., Razuvayev, V., *et al.* 1993. Asymmetric trends of daily maximum and minimum temperature. *Bull. Amer. Met. Soc.*, 74, 1007. Doi: 10.1175/1520–477.

Karnieli, A., Agam, N., Pinker, R.T., Anderson, M., Imhoff, M.L. and Gutman, G.G. 2010. Use of NDVI and land surface temperature for drought assessment: Merits and limitations. *J. Climate*, 23, 618–633.

Kiem, A., Verdon-Kidd, D., Boulter, S. and Palutikof, J. 2010. Learning from experience: historical case studies and climate change adaptation. Report for National Climate Change Adaptation Research Facility: Gold Coast.

Koppe, C. and Jendritzky, G. 2004. Health effects of the heat wave in August 2003, Ministry of Social Affairs. Chapter 3.The effects of heat waves on mortality in 2003. *Baden-Wurttemberg*, 5–18.

Kovats, R.S., Hajat, S. and Wilkinson, P. 2004. Contrasting patterns of mortality and hospital admissions during hot weather and heat waves in Greater London, UK. *Occup Environ Med*, 61, 893–898.

Kowalczyk, E.A., Garratt, J.R. and Krummel, P.B. 1994. Implementation of a soil-canopy scheme into the CSIROGCM— Regional aspects of the model response. CSIRO Marine and Atmospheric Research Tech. Report. 32, 65 pp.

Kruger, A.C. 2008. Climate of South Africa. Surface Temperature. WS48. *South African Weather Service*, Pretoria, South Africa.

Kruger, A.C. and Sekele, S.S. 2013. Trends in extreme temperature indices in South Africa: 1962–2009. *Int. J. Climatol*., doi:10.1002/joc.3455.

Kruger, A.C. and Shongwe, M. 2004. Temperature trends in South Africa: 1960–2003. *Int. J. Climatol*., 24, 1929–1945.

Kunkel, K.E., Changnon, S.A., Reinke, B.C. and Arritt, R.W. 1996. The July 1995 heat wave in the Midwest: A climatic perspective and critical weather factors *Bull. Amer. Meteor. Soc.,* 77, 1507–1518.

Kysely, J. 2000. Changes in the occurrence of extreme temperature events. *PhD thesis*, Charles University.

Kysely, J. 2010. Recent severe heat waves in central Europe: how to view them in a long-term prospect? *Int. J. Climatol.* 30, 89–109.

Kysely, J. 2010. Recent severe heat waves in central Europe: how to view them in a long-term prospect? Int. J. Climatol., 30, 89–109.

Laken, B.A. and Calagavic, J. 2013. Composite analysis with Monte Carlo methods: an example with cosmic rays and clouds. *J. Space Weather Space Clim*. 3, A29

Larsen, J. 2003. Record heat wave in Europe takes 35,000 lives. Earth Policy Institute.

Le Quéré, C., Raupach, M.R., Canadell, J.G., Marland, G., Bopp, L., Ciais, P., *et al*. 2009. Trends in the sources and sinks of carbon dioxide. *Nat. Geosci*., 2, 831–6.

Le Roux, N. 2009. Seasonal Maize Yield Simulations for South Africa Using a Multi-Model Ensemble System. *Master's thesis*, University of Pretoria.

Li, D. and Bou-Zeid, E. 2013. Synergistic interactions between urban heat islands and heat waves: the impact in cities is larger than the sum of its parts. J. *Appl. Meteorol. Climatol.* 52, 2051–2064

Li, Z.L., Tang, B.H., Wu, W., Ren, H., Yan, G., Wan, Z., *et al*. 2013. Satellite-derived land surface temperature: Current status and perspectives. *Rem. Sens. Env.,* 131, 14–37.

Lillesand, T. and Kiefer, R.W. 1994. Remote sensing and image interpretation, 3nd edition, John Wiley & Sons, Inc., New York.

Luüs, C. 2005. The Absa residential property market database for South Africa_ key data trends and implications. *BIS Paper*, 21,149-170.

Lyon, B. 2009. Southern Africa summer drought and heat waves: observations and coupled model behaviour *J. Climate*, 22, 6033–6046.

MacKellar, N., New, M. and Jack, C. 2014. Observed and Modelled Trends for Rain and Temperature for South Africa: 1960 - 2010. *S. A. J. Sc.,* 110 (7/8), Art. #2013-0353, http://dx.doi.org/10.1590/sajs.2014/20130353.

Maida, C.A., Gordon, N.S., Steinberg, A. and Gordon, G. 1989. Psychosocial impact of disasters: victims of the Baldwin Hills fire. *J. Trauma Stress,* 2, 37–48.

Makowski, K., Wild, M. and Ohmura, A. 2008. Diurnal temperature range over Europe between 1950 and 2005. *Atmos. Chem. Phys*., 8, 6483–6498.

Maller, C.J. and Strengers, Y. 2011. Housing, heat stress and health in a changing climate: promoting the adaptive capacity of vulnerable households, a suggested way forward. *Health Promot. Int*. 26 4, 492–498.

Mazdiyasni, O. and AghaKouchak, A. 2015. Substantial increase in concurrent droughts and heat waves in the United States. *Proc. Natl. Acad. Sci*., 112, 11484–11489.

McDowell, R.E. 1972. Improvement of Livestock Production in Warm Climates. W.H. Freeman & Co, San Francisco, USA.

McGregor, J.L. 2005. C-CAM: Geometric aspects and dynamical formulation. *CSIRO Atmospheric Research Tech. Paper No*. 70. 43 pp.

McGregor, J.L. and Dix, M.R. 2008. An updated description of the conformal cubic atmospheric model. High-Resolution Simulation of the Atmosphere and Ocean, K. Hamilton and W. Ohfuchi, Eds., *Springe*r, 51–76.

McKee, T.B., Doesken, N.J and Kliest, J. 1993. The relationship of drought frequency and duration to time scales. In *Proceedings of the 8th Conference of Applied Climatology, 17–22 January, Anaheim, CA*. *American Meteorological Society*, Boston, MA. 179-184.

McKee, T.B., Doesken, N.J. and Kliest, J. 1993. The relationship of drought frequency and duration to time scales. *Conf. on Appl. Climat*., 179–184.

Meehl, G.A. and Tebaldi, C. 2004. More intense, more frequent, and longer-lasting heat waves in the 21st century. *Science*, 305 994–997.

Miller, N.L., Hayhoe, K., Auffhammer, M. 2008.Climate, Extreme Heat, and Electricity Demand in California. *J. Appl. Meteorol.*, 47, 1834–1844.

Min, S.-K., Zhang, X., Zwiers, F.W. and Hegerl, G.C. 2011. Human contribution to more-intense precipitation extremes. *Nature*, 470, 378–381.

Miralles, D.G., Teuling, A.J., van Heerwaarden, C.C. and VilaGuerau de Arellano, J. 2014. Mega-heat wave temperatures due to combined soil desiccation and atmospheric heat accumulation, *Nat. Geosci*., 7, 345–349

Moss, R.H., Edmonds, J.A., Hibbard, K.A, Manning, M.R., Rose, S.K., van Vuuren, D.P., *et al.* 2010. The next generation of scenarios for climate change research and assessment. *Nature 463*,747–756

Mudekwe, J. 2007. Management Practices for the Protection of Forest Reserves The Case of Kalahari Sand Teak Forest Reserves in Western Zimbabwe. *Rome*: FAO. Available at http://www.fao.org/docrep/010/j9533e/J9533E00.htm#TopOfPage (Accessed on 17 February 2016).

Muhlenbrunch-Tegen, A. 1992. Long-term surface temperature variations in South Africa. Climatology.

Mukheibir, P. and Sparks, D. 2006. Climate variability, climate change and water resource strategies for small municipalities. Report 1500/1/06, *Water Research Commission*, Pretoria, January.

Munich Re. 1999. Cold waves and winter damage. MRNatCatSERVICE (A. Wirtz, pers.comm) Munich Reinsurance company, Munich, Germany.

Myron, T.P. 2011. Late-summer heat waves and their impacts on hyperthermia-related deaths in football players. *Master's thesis*, University of Georgia.

Nairn, J. and Fawcett, R. 2013. Defining heat waves: heat wave defined as a heat impact event servicing all community and business sectors in Australia. CAWCR Technical Report No. 060.

New, M., Hewitson, B, Stephenson, D.B., Tsiga, A., Kruger, A., Manhique, A. *et al.* 2006. Evidence of trends in daily climate extremes over southern and West Africa, *J. Geophys. Res.*, 111, D14102, doi: 10.1029/2005JD006289.

Nicholls, N., and Katz, R.W. 1991. Teleconnections and their implications for long range forecasts. In: Teleconnections linking Worldwide Climate Anomalies; scientific basis and societal impact. Glantz, M.H., Katz, R.W. and Nicholls, N. (eds.), Cambridge University Press, UK. 525pp.

Nyamadzawo, G., Gwenzi, W., Kanda, A., Kundhlande, A. and Masona, C. 2013. Understanding the causes, social and environmental impacts, and management of wildland fires in tropical Zimbabwe. *Fire Science Reviews*, 2, 9–13.

Oke, T. R. 1982. 'The Energetic Basis of the Urban Heat Island', *Quart. J. Royal Meteorol. Soc*. 108, 1–24.

Ordonez, C., Mathis, H., Furger, M., Henne, S., H¨uglin, C. Staehelin, J. *et al.* 2005. Changes of daily surface ozone maxima in Switzerland in all seasons from 1992 to 2002 and discussion of summer 2003. *Atmos. Chem. Phys*, 5, 1187–1203.

Orssengo, G. Predictions of Global mean temperatures and IPCC projections. Icecap, April 2010. Available at http://wattsupwiththat.files.wordpress.com/2010/04/predictions-of-gmt.pdf (Accessed on 20 July 2015).

Palecki, M.A., Changnon, S.A. and Kunkel, K.E. 2001. The nature and impacts of the July 1999 heat wave in the Midwestern United States: Learning from the lessons of 1995. *Bull. Amer. Met. Soc.,* 82, 1353–1367.

Palutikof, P., Subak, S. and Agnew, M.D. 1996. Impacts of the exceptionally hot weather in 1995 in the UK. *Climate Monitor,* 25, 884–887.

Parker, T.J. Berry, G.S. and Reeder, M.J. 2014. The Structure and Evolution of Heat Waves in Southeastern Australia. *J. Clim*, 27, 5768, 5785.

Peng, R.D., Bobb, J.F., Tebaldi, C., McDaniel, L., Bell, M.L., Dominici, F. 2011. Toward a quantitative estimate of future heat wave mortality under global climate change. *Environ Health Perspect*., 119,701–706.

Perkins, S.E., Pitman, A.J. and Sisson, S.A. 2013. Systematic differences in 20-year temperature extremes in AR4 model projections over Australia as a function of model skill. *Int. J. Climatol*., 33, 1153–1167, doi:10.1002/joc.3500.

Peterson, T.C., Heim, R.R., Hirsch, R., Kaiser, D.P., Brooks, H., Diffenbaugh, N.S., *et al*. 2013. Monitoring and understanding changes in heat waves, cold waves, floods and droughts in the United States: State of Knowledge, *Bull. Amer. Met. Soc. (in press).*

Peterson, T.C., Stott, P.A. and Herring, S. 2012. Explaining extreme events of 2011 from a climate perspective. *Bull. Amer. Met. Soc.,* 93**,** 1041–1067.

Pezza, A.B., van Rensch, P. and Cai, W. 2012. Severe heat waves in southern Australia: Synoptic climatology and large scale connections. *Clim. Dyn*. 38, 209–224, doi: 10. 1007/s00382-011-1016-2.

Potgieter C.J. 2006. Accuracy and skill of the Conformal-Cubic Atmospheric Model in short range weather forecasting in South Africa. *Master's Thesis*, University of Pretoria.

Purich, A., Cowan, T., Cai, W. and van Rensch, P. 2014. Atmospheric and oceanic conditions associated with Southern Australian heat waves: A CMIP5 Analysis. *J. Climate*, 27, 7808–7829.

Randriamahefasoa, T.M.S. 2011. Circulation of the Indian Ocean and its climate variability with their impacts on northern Madagascar rainfall. Postgraduate diploma, African Institute for Mathematical Sciences.

Rautenbach C.J. deW., Engelbrecht F.A., Engelbrecht C.J. Ndarana T. and McGregor J.L. 2005. Regional model development for simulating atmospheric behaviour and rainfall over southern Africa. Water Research Commission Report 1261/1/05, 121 pp.*Water Research Commission, Pretoria.*

Reeder, M.J. and Smith, R.K. 1987. A study of frontal dynamics with application to the Australian summertime ‘‘cool change.’’ *J. Atmos. Sci*., 44, 687–705.

Robinson, P.J. 2001. On the definition of a heat wave. *J Appl Meteorol*., 40,762–775

Rothfusz, L.P. 1990. The Heat Index "Equation" (or, More Than You Ever Wanted to Know About Heat Index). Available online at http://www.srh.noaa.gov/images/ffc/pdf/ta_htindx.PDF

Rotstayn, L.D. 1997: A physically based scheme for the treatment of stratiform clouds and precipitation in large-scale models. I: Description and evaluation of the microphysical processes. *Quart. J. Roy. Meteor. Soc*., 123, 1227–1282.

Rouault, M. and Richard, Y. 2003. Intensity and spatial extension of drought in South Africa at different time scales. *Water SA*, 29, 489-500.

Rouault, M. and Richard, Y. 2005. Intensity and spatial extent of droughts in southern Africa. *Geophy. Res. Lett*., 32, L15702, 4pp. 2005 doi: 10.1029/2005GL022436

Roux, B. 2009. Ultra high-resolution climate simulations over the Stellenbosch wine producing region using a variable-resolution model. *Master's thesis*, University of Pretoria.

Rowell, D.P. 2005. A scenario of European climate change for the late twenty-first century: seasonal means and interannual variability. *Clim. Dyn*., 25, 837–849.

Rowless, R. 2012. Managing hazards: Fire management in Cape Peninsula. *Master's thesis*, University of Cape Town.

Russell, J.B., O'Connor, J.D., Fox, D.G., Van Soest, P.J. and Sniffen, C.J. 1992. A net carbohydrate and protein system for evaluating cattle diets I. Ruminal fermentation. *J. Anim. Sci*., 70, 355–*367*.

Rust, J.M. and Rust, T. 2013. Climate change and livestock production: A review with emphasis on Africa. *S. Afr. J. Anim. Sci.*, 43, 255–267.

Sapra, R., Dhaka, S.K., Panwar, V., Bhatnagar, R., Praveen Kumar, K., Shibagaki, Y., *et al.* 2011. Long-term variations in outgoing long-wave radiation (OLR), convective available potential energy (CAPE) and temperature in the tropopause region over India. *J. Earth Syst. Sci*., 120, 807–823.

Scholtz, M.M., Furstenburg, D., Maiwashe, A., Makgahlela, M.L., Theron, H.E. and van der Westhuizen, J. 2010. Environmental-genotype responses in livestock to global warming: A Southern African perspective. *S.A. J. Animal Science*, 40, 408–413.

Semenza, J.C. and Menne, B. 2009. Climate change and infectious diseases in Europe. *Lancet ID*, 9, 365–375.

Seneviratne, S.I., Luthi, D., Litshi, M. and Schar, C. 2006. Land-atmosphere coupling and climate change in Europe. *Nature*, 443, 205–209.

Shongwe, M.E., van Oldenborgh, G.J., van den Hurk, B.J.J.M., de Boer, B., Coelho, C.A.S. and van Aalst, M.K. 2009. Projected changes in mean and extreme precipitation in Africa under global warming. Part I: Southern Africa. *J. Climate*, 22, 3819–3837.

Sinclair, M.R. 1996. A climatology of anticyclones and blocking for the Southern Hemisphere. *Mon. Wea. Rev*., 124, 245–264.

Smith, B., McNabb, D. and Smithers, J. 1996. Agricultural adaptation to climatic variation. *Climate change,* 43, 7–29.

Solomon, S. Qin, D., Manning, M., Alley, R.B., Berntsen, T. Bindoff, N.L., *et al*. 2007. Technical Summary. In: Climate Change 2007. The Physical Science Basis. Contribution of Working Group I to the Fourth Assessment Report of the Intergovernmental Panel on Climate Change [Solomon, S., Qin, D., Manning, M., Chen, Z., Marquis, M., Averyt, K.B., Tignor, M. and Miller, H.L. (eds.)]. Cambridge University Press, Cambridge, United Kingdom and New York, NY, USA.

Son, S.W., Gerber, E.P., Perlwitz, J., Polvani, L.M., Gillett, N.P., Seo, K.H., *et al.* 2010. Impact of stratospheric ozone on Southern Hemisphere circulation change: a multi-model assessment. *J. Geophys. Res. Atm.,* 115:D00M07. Doi: 10.1029/2010JD014271.

Stefanon, M., D'Andrea, F. and Drobinski, P. 2012. Heat wave classification over Europe and the Mediterranean region. *Environ. Res. Lett.,* 7 doi: 10.1029/2010JD014271.

Stephenson. D.B. 2008. Definition, diagnosis, and origin of extreme weather and climate events. In Climate Extremes and Society, Diaz HF, Murnane RJ (Eds). Cambridge University Press: New York; 348.

Taljaard, J.J., and van Loon, H. 1963. Cyclogenesis, cyclones and anticyclones in the Southern Hemisphere during summer 1957–1958. *NOTOS*, 12, 37–50.

Tan, J., Zheng, Y., Tang, X., Guo, C., Li L. and Song, G. 2010. The urban heat island and its impact on heat waves and human health in Shanghai. *Int. J. Biometeorol*, 54, 75–84.

Tebaldi, C., Hayhoe, K., Arblaster, J. and Meehl, J. 2006. Going to the extremes: An inter-comparison of model-simulated historical and future changes in extreme events. *Climatic Change,* 79, 185–211.

Thom, E.C. 1959. The discomfort index. *Weatherwise*, 12, 57–60.

Thornton, P., Herrero, M., Freeman, A., Mwai, O., Rege, E., Jones, P., *et al.* 2007. Vulnerability, climate change and livestock – Research opportunities and challenges for poverty alleviation. *SAT eJournal* 4, 1–23.

Topp, C.F. and Doyle, C.J. 1996. Simulating the impacts of global warming on milk and forage production in Scotland. 1. The effects on dry matter yield of grass and grass-white clover stands. *Agr. Syst*. 52, 213–242.

Trenberth, K.E., Jones, P.D., Ambenje, P., Bojariu, R., Easterling, D., Klein Tank, A., *et al.* 2007. Observations: surface and atmospheric climate change. In *Climate Change 2007: The Physical Science Basis. Contribution of Working Group I to the Fourth Assessment Report of the Intergovernmental Panel on Climate Change 2001*, Solomon, S., Qin, D., Manning, M., Chen, Z., Marquis, M., Averyt, K.B., et al. (eds). Cambridge University Press: Cambridge, United Kingdom and New York, NY, USA.

Trenberth, K.E. and Shea, D.J. 2005. Relationships between precipitation and surface temperature. *Geophys Res Lett* 32:L14703.

Trouet, V. and van Oldenborgh, G.J. 2013. KNMI Climate Explorer: A web-based research tool for high-resolution paleoclimatology. *Tree-Ring Res.*, 69, 3–13.

Tshiala, M.F., Olwoch, J.M. and Engelbrecht, F.A. 2011. Analysis of temperature trends over Limpopo province, South Africa. *J. geog. geol,*, 3, 13–21.

Twomey, S.A., Bohren, C.F. and Mergenthaler, J.L. 1986. Soil reflectances and albedo differences between wet and dry surfaces. *Appl. Optics*, 25,431–437.

Tyson, P.D .1986. Climatic change and variability in southern Africa. Oxford University Press, Cape Town. 220pp

Tyson, P.D. and Preston-Whyte, R.A. 2000. The Weather and Climate of Southern Africa. *Oxford University Press*, Cape Town, 396pp.

Unkaševica, M. and Tošic, I. 2009. An analysis of heat waves in Serbia. Global and Planetary Change 65, 17–26.

Van Vuuren, D.P., Edmonds, J., Kainuma, M., Riahi, K., Thomson, A., Hibbard, K., *et al.* 2011. The concentration representative pathways: An overview. *Climate change*, 109, 5–31.

Vandentorren, S., Bretin, P., Zeghnoun, A.,Mandereau-Bruno, L., Croisier, C., Riberon, J., *et al.* 2006. August 2003 heat wave in France: risk factors for death of elderly people living at home. *Eur. J. Public Health*, 19, 583–591.

Vidale, P.L., Lüthi, D., Wegmann, R. and C. Schär, 2007: European summer climate variability in a heterogeneous multi-model ensemble. Climatic Change, 81, 209–232.

Voogt, J.A. 2004. Urban Heat Island. Hotter Cities. ActionBioscience: North Port, FL, USA. Available online: http://www.actionbioscience.org/environment/voogt.html (Accessed on 16 March 2015).

Vose, R.S. and Menne, M.J. 2004. A Method to Determine Station Density requirements for Climate Observing Networks. *J. Climate* 17, 2961–2971.

Waggoner, P.E .1983. Agriculture and a climate changed by more carbon dioxide. Changing climate. National Academy Press, Washington, DC, pp418.

Waggoner, P.E. 1983. Agriculture and a Climate Changed By More Carbon Dioxide. p. 383-418. In National Research Council, Changing Climate. Rep. of the Carbon Dioxide Committee, Board of Atmospheric Sciences and Climate. National Academy Press, Washington, DC.

Wallace, J.M. and Gutzler, D.S. 1981. Teleconnections in the geopotential height field during the Northern Hemisphere winter. *Mon. Wea. Rev*., 109, 784–812.

Wheeler, T.R., Craufurd, P.Q., Ellis, R.H., Porter, J.R. and Prasad, P.V.V. 2000. Temperature variability and the yield of annual crops. *Agric. Ecosyst. Environ.* 82, 159–167.

Williams, C.A. 2014. Heat and drought extremes likely to stress ecosystem productivity equally or more in a warmer, CO_2 rich future. *Environ. Res. Lett*, 9, 1–4.

WWF. 2001. World Wide Fund (WWF). Fire management manual. Wildlife magement series, Zimbabwe. WWF, Harare

Yousif, A. and Tahir, H. M. 2013. Application of Thom's Thermal Discomfort Index in Khartoum State, Sudan. *J. Forest.*, 2, 36–38.

Yulaeva, E. and Wallace, J.M. 1994. The signature of ENSO in global temperature and precipitation fields derived from the microwave sounding unit. *J. Climate,* 7, 1719–1736.

Zacharias, S., Koppe, C. and Mücke, H.G. 2014. Influence of heat waves on ischemic heart diseases in Germany. *Climate*, 133–152.

Zacharias, S., Koppe, C. and Mücke, H.G. 2015. Climate change effects on heat waves and future heat wave-associated IHD mortality in Germany. *Climate,* 3, 100–17.

Zanobetti, A., Luttmann-Gibson H., Horton, E.S., Cohen, A., Coull, B.A., Hoffmann, B., *et al*. 2014. Brachial artery responses to ambient pollution, temperature, and humidity in people with type 2 diabetes: a repeated-measures study. *Environ. Health Perspect*. 122, 242–248.

Zhang, X. and Yang, F. 2004. RClimDex (1.0), User Manual, Climate Research Branch, Environment Canada, Downsview, Ontario, Canada. Available online at http://cccma.seos.uvic.ca/ETCCDMI (Accessed on 5 November, 2015).

Zhou, Y.Q., and G.Y. Ren. 2011. Change in extreme temperature event frequency over mainland China, 1961–2008. *Clim. Res.*, 50, 125–139.

Zuo, J., Pullen, S., Palmer, J., Bennetts, H., Chileshe, N. and Ma, T. 2015. Impacts of heat waves and corresponding measures: a review. *J. Clear Production*, 92, 1–12

Zwiers, F.W., Alexander, L.V., Hegerl, G.C., Knuston, T.R., Kossin, J.P., Naveau, P., *et al*. 2011. Challenges in estimating and understanding recent changes in the frequency and intensity of extreme climate and weather events. *Proc. World Climate Research Programme Open Science Conf.,* Denver, CO, WCRP, 45 pp. Available online at http://library.wmo.int /pmb_ged/wcrp_2011-zwiers.pdf. (Accessed on 13 March 2016).